INFORMATION TO USERS

This manuscript has been reproduced from the microfilm master. UMI films the text directly from the original or copy submitted. Thus, some thesis and dissertation copies are in typewriter face, while others may be from any type of computer printer.

The quality of this reproduction is dependent upon the quality of the copy submitted. Broken or indistinct print, colored or poor quality illustrations and photographs, print bleedthrough, substandard margins, and improper alignment can adversely affect reproduction.

In the unlikely event that the author did not send UMI a complete manuscript and there are missing pages, these will be noted. Also, if unauthorized copyright material had to be removed, a note will indicate the deletion.

Oversize materials (e.g., maps, drawings, charts) are reproduced by sectioning the original, beginning at the upper left-hand corner and continuing from left to right in equal sections with small overlaps.

ProQuest Information and Learning
300 North Zeeb Road, Ann Arbor, MI 48106-1346 USA
800-521-0600

University of Alberta

Identification and characterization of molecular determinants of inhibitor interactions with equilibrative nucleoside transporters.

by

Frank Visser 

A thesis submitted to the Faculty of Graduate Studies and Research in partial fulfillment of the requirements for the degree of Doctor of Philosophy

Department of Oncology

Edmonton, Alberta

Spring 2005

"We must, however, acknowledge as it seems to me, that a man with all his noble qualities...still bears in his bodily frame the indelible stamp of his lowly origin."

Charles Darwin (1809-1882)

To Andrea and Calum for all your support

Abstract

Nucleoside transporters are required for cellular uptake, release and trafficking of nucleosides and anticancer and antiviral nucleoside analogs. The human equilibrative nucleoside transporters (ENTs), hENT1 and hENT2, are functionally distinguished as equilibraitive sensitive (*es*) or equilibrative insensitive (*ei*), respectively, based on their sensitivity to inhibition by nitrobenzylmercaptopurine ribonucleoside (NBMPR). The cardioprotective drugs dipyridamole, dilazep, draflazine and soluflazine are also inhibitors of hENT1 and hENT2 for which they have nanomolar and micromolar affinities, respectively. Many pharmacological studies have suggested that inhibitor binding is either competitive for, or allosterically linked to, the permeant binding site. The molecular cloning of mammalian ENTs has provided a new avenue for study of the molecular determinants and the mechanisms of high affinity interactions of these inhibitors. Random mutagenesis of ENT cDNAs and phenotypic complementation screening in yeast identified six amino acid residues that were involved in inhibitor interactions. The first of these, M33 in hENT1, was a determinant of the functional differences and the dipyridamole- and dilazep-sensitivity differences between hENT1 and hENT2 and a common component of both the permeant and dipyridamole binding sites. L442 of hENT1 was a critical residue for transporter function, permeant selectivity and high-affinity interactions with dipyridamole and dilazep. W29 was critical for hENT1 function and altered sensitivity to all of the inhibitors. F80 mutations induced modest changes in transporter function and inhibitor sensitivities whereas F334 markedly increased catalytic activities of hENT1 and rENT1 when mutated to Tyr and was critical for dipyridamole and dilazep sensitivity. Although N338 mutations altered all inhibitor

sensitivities (draflazine in particular), effects on transporter function were generally minor. A helical wheel projection involving the four TMs containing these six residues was constructed. All of the identified residues except N338 were functionally important and appeared to be located on extracellular aspects of the transmembrane segments (TMs) in which they are found. It is concluded that the inhibitors competed with permeants for binding by the transporter.

Preface

Dipyridamole, dilazep, draflazine and soluflazine are routinely used as cardioprotective agents because they potentiate the protective effects of extracellular adenosine in insulted tissues by blocking its cellular uptake via equilibrative nucleoside transporters (ENTs). Results of pharmacological studies of the mechanisms of inhibitor interactions with mammalian ENTs have led to intensive debate in the published literature for the past two decades, with the central argument being whether they bind competitively or allosterically to the transporters. The molecular cloning of human ENTs has provided an opportunity to address these questions using recombinant proteins. Chimeric approaches aimed at exploiting the difference in sensitivity between hENT1 and the rat isoform rENT1 have revealed regions that may be important for inhibitor binding but the individual amino acid residues responsible for these effects have not been identified. The experiments described within this thesis used an alternative approach, random mutagenesis and screening by phenotypic complementation in yeast, to identify six amino acid residues of hENT1 as important for inhibitor sensitivity and permeant transport activity. The results represent a major contribution to the understanding of the molecular determinants of inhibitor interactions and provide evidence in support of the competitive binding model.

Acknowledgements

Completion of my degree could not have been made possible without the kind and loving support of my wife, Andrea and my son Calum. I would also like to extend my gratitude to my parents, Kees Visser and Nieke de Boer and my sister, Marjolein Visser, for their unending support throughout my life and in pursuit of my Ph.D. degree, especially when times got tough. Carol was the perfect supervisor for me, providing me with the freedom to pursue whatever avenues of science I wanted to, which helped to foster my independence as a researcher, but she always included me as a top priority in providing wisdom and guidance. I would also like to thank Carol's collaborators, Jim Young and Steve Baldwin for guidance with my research projects, manuscript writing and great fun at the conferences in Barcelona and Munich. I am also especially grateful that Susan Cole agreed to travel from Kingston to be my external examiner for my thesis defence. My supervisory committee members including Joe Casey and Michael Weinfeld have been instrumental in providing constructive criticism and useful guidance. The great administrative and academic people in the department of oncology and the membrane protein research group, especially Bernie Lemire, have been incredibly helpful over the years. The Cass lab was absolutely the most enjoyable place anybody could ever want to work, where I had the chance to meet so many people over the years, and my thesis is as much a credit to them as it is to me. These excellent people included Jing Zhang, Doug Hogue, Mark Vickers, Miguel Cabrita, Thack Lang, Karen King, Robert Paproski, Adam Elwi, Alan Doucette, Lori Jennings, Elizabeth Silver, Nancy Zhang, Taylor Raborn, Nicole Lutic, Delores Mowles, Pat Carpenter, Kathryn Graham, Vijaya Damaraju, Rajam Mani, Xuejun Sun, Cheryl Santos, Tracey Tackaberry, Gerry Barron, Michelle Kuzma, Lily Zombor, Milada Selner, Dawn Fang, Haide Razavy, Sherry Perdue, John Mackey and Michael Sawyer. The University of Alberta is a first-class institution that makes you believe anything is possible and I wouldn't miss the opportunity to come back some day.

Table of Contents

List of Tables

List of Figures

List of Abbreviations, Symbols and Nomenclature

A_1AR	adenosine receptor A_1
A_{2A}AR	adenosine receptor A_{2A}
A_{2B}AR	adenosine receptor A_{2B}
A_3AR	adenosine receptor A_3
Ab	antibody
ABA	N^6-(*p*-azidobenzyl) adenosine
ALL	acute lymphocytic leukemia
AtENT	*Arabidopsis thaliana* equilibrative nucleoside transporter
CeENT	*Caenorhabditis elegans* equilibrative nucleoside transporter
CeENT1	*Caenorhabditis elegans* equilibrative nucleoside transporter 1 (dipyridamole-sensitive)
cENT1	canine equilibrative nucleoside transporter (NBMPR-sensitive)
CLL	chronic lymphocytic leukemia
CMM	complete minimal media
CNT	concentrative nucleoside transporter
DmENT	*Drosophila melanogaster* equilibrative nucleoside transporter
hCNT1	human concentrative nucleoside transporter 1 (sodium-dependent, pyrimidine nucleoside selective)
hCNT2	human concentrative nucleoside transporter 2 (sodium-dependent, purine nucleoside selective)
hCNT3	human concentrative nucleoside transporter 3 (sodium-dependent, broadly selective for pyrimidine and purine nucleosides)
CfNT	*Crithidia fasciculata* nucleoside transporter
cladribine	2-chloro-2'-deoxyadenosine
DIC	differential interference contrast
didanosine	2', 3'-dideoxyinosine, ddI
dilazep	*N,N'-bis*-[3-(3,4,5-trimethoxybenzoyloxy)propyl]-homopiperazine
dipyridamole	2,2',2",2"'-[(4,8-Dipiperidinylpyrimido[5,4-d]pyrimidine-2,6-diyl)dinitrilo]tetraethanol

draflazine	2-aminocarbonyl)-*N*-(4-amino-2,6-dichlorophenyl)-4-[5,5-*bis*(4-fluorophenyl)pentyl]-1-piperazineacetamide)
ei	equilibrative insensitive; insensitive to inhibition by NBMPR
EhENT1	*Entamoeba histolytica* equilibrative nucleoside transporter
ENT	equilibrative nucleoside/nucleobase transporter
es	equilibrative sensitive; sensitive to inhibition by NBMPR
fludarabine	2-fluoro-2'-deoxyadenosine
FUI1	uridine permease from *Saccharomyces cerevisiae*
FUN26	function unknown now 26; an intracellular equilibrative nucleoside transporter from *Saccharomyces cerevisiae*
FUR4	uracil/uridine permease from *Saccharomyces cerevisiae*
gemcitabine	2', 2'-difluoro-2'-deoxycytidine
GLU	glucose
GLUT1	glucose transporter 1; erythrocyte glucose transporter
hENT1	human equilibrative nucleoside transporter 1 (NBMPR-sensitive)
hENT2	human equilibrative nucleoside/nucleobase transporter 2 (NBMPR-insensitive)
hENT3	human equilibrative nucleoside transporter 3 (function unknown)
hENT4	human equilibrative nucleoside transporter 4 (function unknown)
hexobendine	structural analog of dilazep
HIV	human immunodeficiency virus
LdNT	*Leishmania donovani* nucleoside transporter
lidoflazine	4-[4,4-Bis(4-fluorophenyl)butyl]-N-(2,6-dimethylphenyl)-1-piperazineacetamide
mENT1	mouse equilibrative nucleoside transporter 1 (NBMPR-sensitive)
mENT2	mouse equilibrative nucleoside/nucleobase transporter 2 (NBMPR-insensitive)
mENT3	mouse equilibrative nucleoside transporter 3 (function unknown)
mENT4	mouse equilibrative nucleoside transporter 4 (function unknown)
mioflazine	4-[4,4-Bis(p-fluorophenyl)butyl]-3-carbamoyl-2,6-dichloro-1-piperazineacetamide

MTX	methotrexate
NBMPR	nitrobenzylmercaptopurine ribobuncleoside, 6-[(4-nitrobenzyl)thio]-9-(β-D-ribofuranosyl)purine
nimodipine	Isopropyl 2-methoxyethyl 1,4-dihydro-2,6-dimethyl-4-(m-nitrophenyl)-3,5-pyridinedicarboxylate, Ca^{2+} blocker
pCMBS	p-chloromercuribenzyl sulphonate
PfENT1	*Plasmodium falciparum* equilibrative nucleoside transporter (also known as PfNT1)
PKC	protein kinase C
rCNT1	rat concentrative nucleoside transporter 1 (sodium-dependent, pyrimidine nucleoside selective)
R75231	negative enantiomer of draflazine
rbENT2	rabbit equilibrative nucleoside transporter 2
rENT1	rat equilibrative nucleoside transporter 1 (NBMPR-sensitive)
rENT2	rat equilibrative nucleoside transporter 2 (NBMPR-insensitive)
Ro 31-6045	2,3-*bis*(1H-Indol-3-yl)-N-methylmaleimide
SAA	sulfanilamide
SAENTA	5'-S-(2-aminoethyl)-N^6-(4-nitrobenzyl)-5'-thioadenosine
SB203580	4-(4-fluorophenyl)-2-(4-methylsulfinylphenyl)-5-(4-pyridyl)1H-imidazole
SCAM	substituted cysteine accessibility method
SLC28	solute carrier family 28; concentrative nucleoside transporter family
SLC29	solute carrier family 29; equilibrative nucleoside transporter family
soluflazine	3-(aminocarbonyl)-4-[4, 4-(fluorophenyl-3-pyridinyl)butyl]-*N*-(2,6-dichlorophenyl)-1-piperazineacetamide
ST7092	structural analog of dilazep
TbAT1	*Trypanosoma brucei* adenosine transporter, also known as TbNT1
TbNT	*Trypanosoma brucei* nucleoside transporter
TgAT1	*Toxoplasma gondii* adenosine transporter
TM(s)	transmembrane segments(s)
X. laevis	*Xenopus laevis*
zalcitabine	2', 3'-dideoxycytidine, ddC

zidovudine 3'-azido-2', 3'-dideoxythymidine, AZT

Chapter 1: General introduction to inhibitors of nucleoside transport

Introduction to nucleoside transporters

Nucleosides

Nucleosides are the metabolic precursors of many fundamental biological molecules including DNA, RNA and ATP. . Adenosine (Fig. 1-1) is a ubiquitous signaling molecule, regulating many physiological processes in a broad variety of cells and tissues (1). In pig erythrocytes, which lack glucose transport systems, inosine acts as the primary source of energy (2,3). Although many cell types are capable of *de novo* synthesis, nucleoside salvage is energetically favored and some are exclusively dependent on salvaging nucleosides from their environment. In multicellular organisms these include, enterocytes and hemopoietic cells, and in unicellular organisms, parasitic protozoa (4,5).

Nucleosides are hydrophilic molecules and their passive diffusion across biological membranes is minimal. Therefore, specialized integral membrane nucleoside transporters (NTs) are required to mediate the movement of nucleosides across the plasma membrane or between intracellular compartments (6). Although many distinct integral membrane proteins in different organisms have been shown to transport nucleosides, the two major families of transporters that are active in most organisms are the concentrative (CNT) and equilibrative (ENT) nucleoside transporters, respectively (7,8).

Concentrative nucleoside transporters

In 1994, rCNT1 from rat tissues was identified by molecular cloning and functional characterization, as the first sodium-dependent NT (9). This discovery led to the molecular cloning of the transporters responsible for the three major CNT processes present in mammalian cells: CNT1, CNT2 and CNT3, which all accept uridine as a permeant, but differ functionally with respect to their selectivities for other permeants (10-16). In humans (as in other mammals), hCNT1 prefers pyrimidine nucleosides but also transports adenosine, whereas hCNT2, which is 72 % identical to hCNT1, prefers purine nucleosides but also transports uridine. hCNT3, which is 48 % identical to hCNT1 and hCNT2, transports both pyrimidine and purine nucleosides.

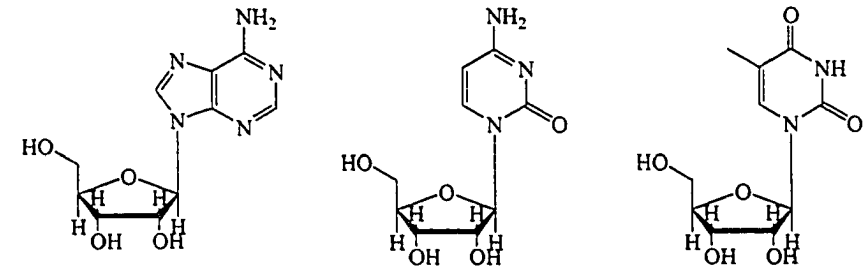

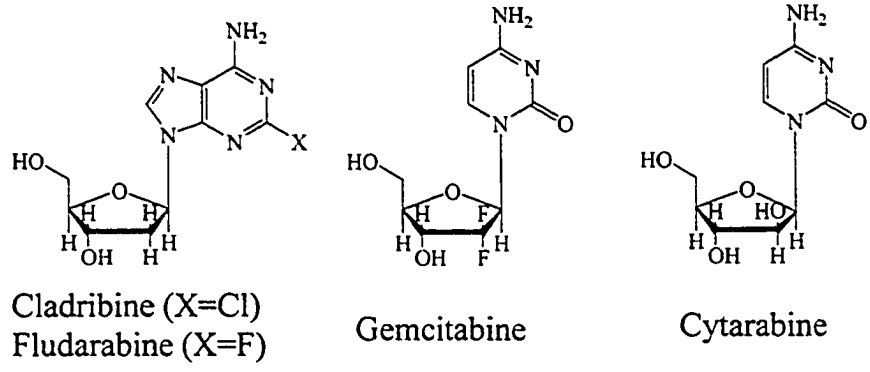

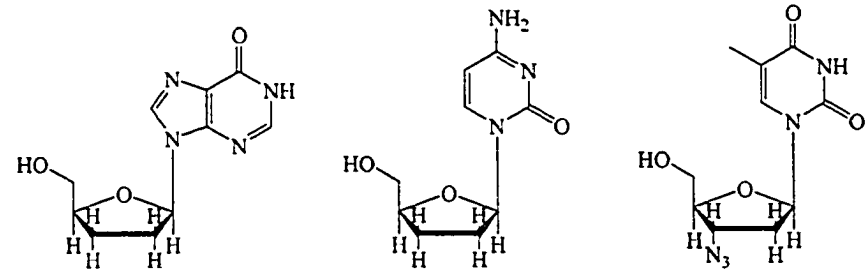

Figure 1-1. Chemical structures of nucleosides and nucleoside analogs.

The structures of adenosine, cytidine, thymidine, cladribine (2-chloro-2'-deoxyadenosine), fludarabine (2-fluoro-2'-deoxyadenosine), gemcitabine (2' ,2'-difluoro-2'-deoxycytidine), cytarabine (araC, cytosine-β-D-arabinofuranoside), didanosine (ddI, 2', 3'-dideoxyinsoine), zalcitabine (ddC, 2', 3'-dideoxycytidine) and zidovudine (AZT, 3'-azido-2', 3'-dideoxythymidine) were generated using ChemDraw Ultra version 6.0 software.

Human CNTs appear to share a common topology model consisting of 13 transmembrane segments (TMs) and a large glycosylated C-terminal tail (Fig. 1-2) (17). Chimeric and mutagenesis approaches have led to the identification of two pairs of adjacent residues in TMs 7 and 8 that are responsible for the permeant selectivity differences between mammalian CNTs (Fig. 1-2) (13,18-20). Furthermore, structure-activity relationship studies involving a series of uridine analogs indicated that hCNT1 forms hydrogen bonds with 3' and 5' hydroxyl groups on the sugar moiety and with the NH group at the 3 position of the base, whereas the 3' hydroxyl group is the only critical determinant for uridine binding with hCNT3 (21). Future research efforts that will reveal important information regarding the structure and function and CNTs will be provided by systematic substituted cysteine-accessibility methods (SCAM) on functional Cys-less CNT mutants.

Sequences with homology to human CNTs (several of which have been cloned and characterized) have been identified *in silico*, revealing that they are evolutionarily conserved in many prokaryotic and eukaryotic organisms, and have now been named the solute carrier family 28 (SLC28) (22-26). All of the members of the SLC28 that have been characterized couple transport with sodium and/or proton electrochemical gradients (24,26-30).

The tissue distribution and localization of human CNTs is beginning to reveal the physiological role of these transporters. hCNT1 and hCNT2 are predominantly found in specialized epithelial cells of tissues such as intestine, kidney and liver, in which they display apical localization and participate in transepithelial nucleoside movement (10,11,17,31-37). In contrast, hCNT3 is expressed in a wide variety of tissues, suggesting that this transporter plays multiple physiological roles in the body (12). The development of appropriate model cell culture systems and specific antibodies that recognize the three different CNT isoforms will allow for further elucidation of the physiological roles of CNTs, particularly hCNT3, in the context of specific cell and tissues types. Although efforts to discover specific, high-affinity inhibitors of CNTs are being made, none are currently available.

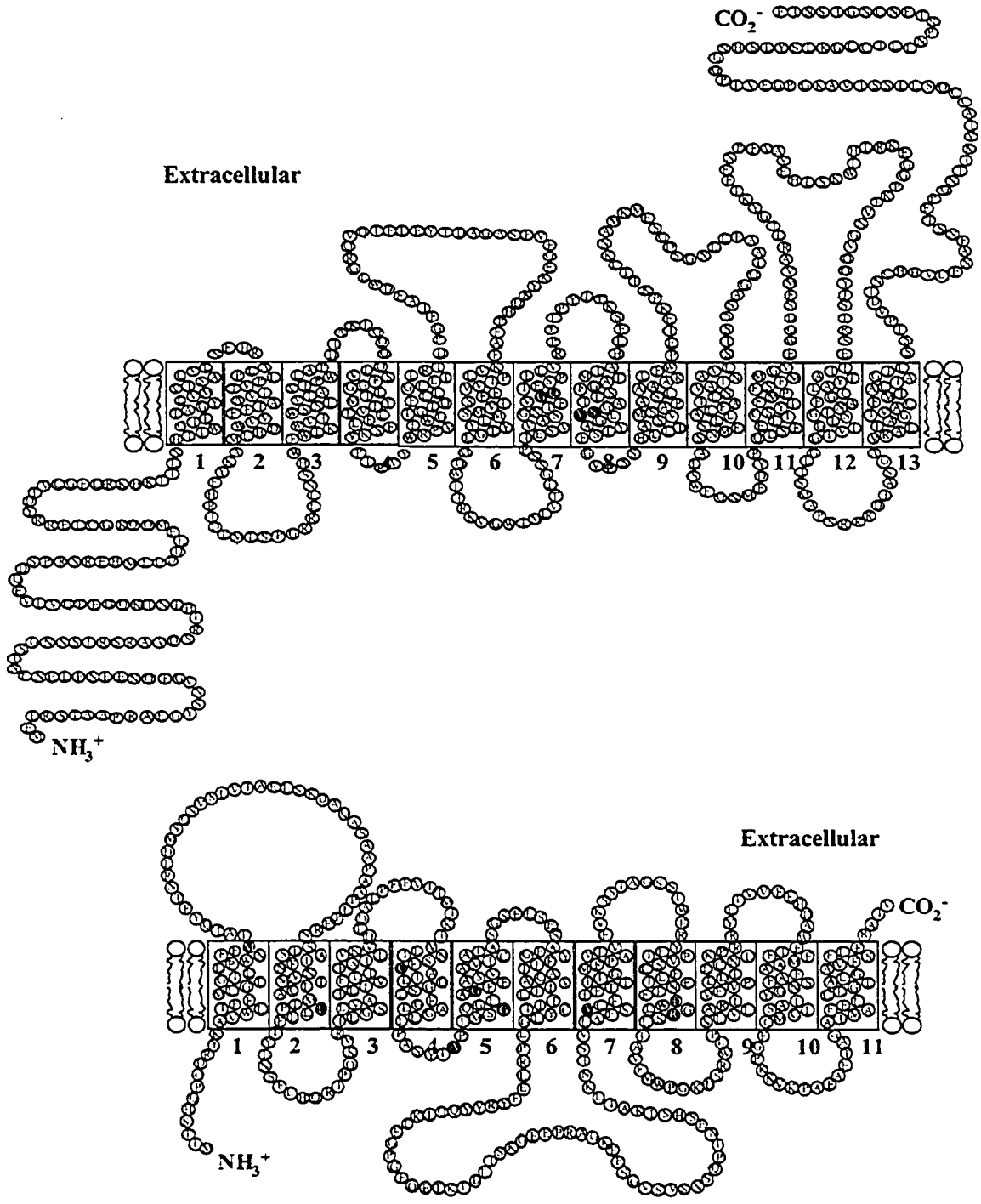

Figure 1-2. Topology models of hCNT3 and hENT1.

The topology models of hCNT3 (*upper*) and hENT1 (*lower*) contain 11 and 13 transmembrane segments, respectively. Amino acid residues that correspond to those which are functionally important in CNTs and ENTs, respectively, are indicated by the filled circles.

Equilibrative nucleoside transporters

In 1996, the first ENTs, hENT1 and hENT2 from humans, were identified by molecular cloning and functional characterization. Consistent with previously reported characteristics of equilibrative transport processes, hENT1 and hENT2 are functionally distinguished as being either equilibrative-sensitive or insensitive (*es* or *ei*), respectively, to inhibition by nM concentrations of nitrobenzylmercaptopurine ribonucleoside (NBMPR) (38-40). These discoveries led to the identification of many ENTs from eukaryotic organisms, which are now collectively known as the solute carrier family 29 (SLC29) (Fig. 1-3) (41) Amongst these, two additional human ENTs, hENT3 (an intracellular transporter) and hENT4, have been identified but the functional characteristics of these transporters have not been published (41,42). The term "equilibrative" was originally assigned to these transporters because most mediate the transport of permeants according to the concentration gradient in agreement with the simple carrier model of transport (43). However, some SLC29 members from kinetoplastid protozoa exhibit concentrative activity by coupling transport to protons (42,44). Furthermore, since many ENTs, including hENT2, are capable of transporting nucleobases, the term ENT now refers to equilibrative nucleoside/nucleobase transporter (5,42,45-48).

ENTs share a common topology model consisting of 11 TMs with a large glycosylated loop between TMs 1 and 2 and a large cytoplasmic loop between TMs 6 and 7 (Fig. 1-2) (49). Studies in which chimeric and mutagenesis approaches have been applied to human and parasitic ENTs have begun to reveal regions and amino acid residues that are important for the structure and function of these proteins. The ability of hENT2 to transport nucleobases, a function that hENT1 lacks, has been attributed to residues in TMs 5 and 6 (46). C140 in TM 4 of rENT2 was shown to line the exofacial permeant translocation pore, the corresponding residue of which in hENT1 (G154) can be mutated to Ser to render the transporter insensitive to NBMPR (50,51). Also, L92 in TM 2 and G179 in TM 5 of hENT1 have been shown to be important determinants of inosine and guanosine transport, and overall function and localization, respectively (52,53). Studies of ENTs from *Leishmania donovani*, have revealed that G183 in TM 5 of LdNT1.1 is critical for permeant selectivity, C337 in TM 7 is critical for transporter

function and TM 5 forms part of the nucleoside-binding site (53,54). In the closely related inosine-guanosine transporter, LdNT2, two highly conserved residues D389 and R393 in TM 8 were found to functionally interact with each other, and be critical for transporter function and plasma membrane targeting (55).

Structure-activity relationship studies that paralleled those involving CNTs indicated that hENT1 formed strong interactions with the 3' hydroxyl group and moderate interactions with the 2' and 5' hydroxyl groups whereas hENT2 formed strong interactions with the 3' hydroxyl group and only weak interactions with the 5' hydroxyl group (56,57). This study suggested that hENT2 was more tolerant of sugar modifications than hENT1, which is consistent with the observation that hENT2 and rENT2 accept 2', 3'dideoxynucleosides as permeants, a function that has been attributed to TMs 3-6 (58). To further the current knowledge of the structure and function of ENTs, future research efforts will focus on comprehensive SCAM studies of functional Cys-less mutants.

In humans, hENT1 appears to have a ubiquitous tissue distribution whereas the distribution of hENT2 is more limited, with relatively high expression levels in skeletal muscle (37-40). hENT1 and hENT2 differ functionally in that hENT2 generally displays lower affinities for nucleosides (59). Although hENT1 and hENT2 likely play many roles in nucleoside physiology depending on their cellular contexts, it is presently unclear why two major isoforms exist. It has been demonstrated that hENT1 and hENT2 are involved in the regulation of extracellular adenosine levels in brain and heart tissues whereas they also participate as basolateral transporters in the transepithelial movement of nucleosides in the intestines and kidney (32,34,36,60). Detailed analysis of these proteins in appropriate model systems, such as primary cultures, and the use of specific antibodies will aid in determining the role of ENTs in other tissues.

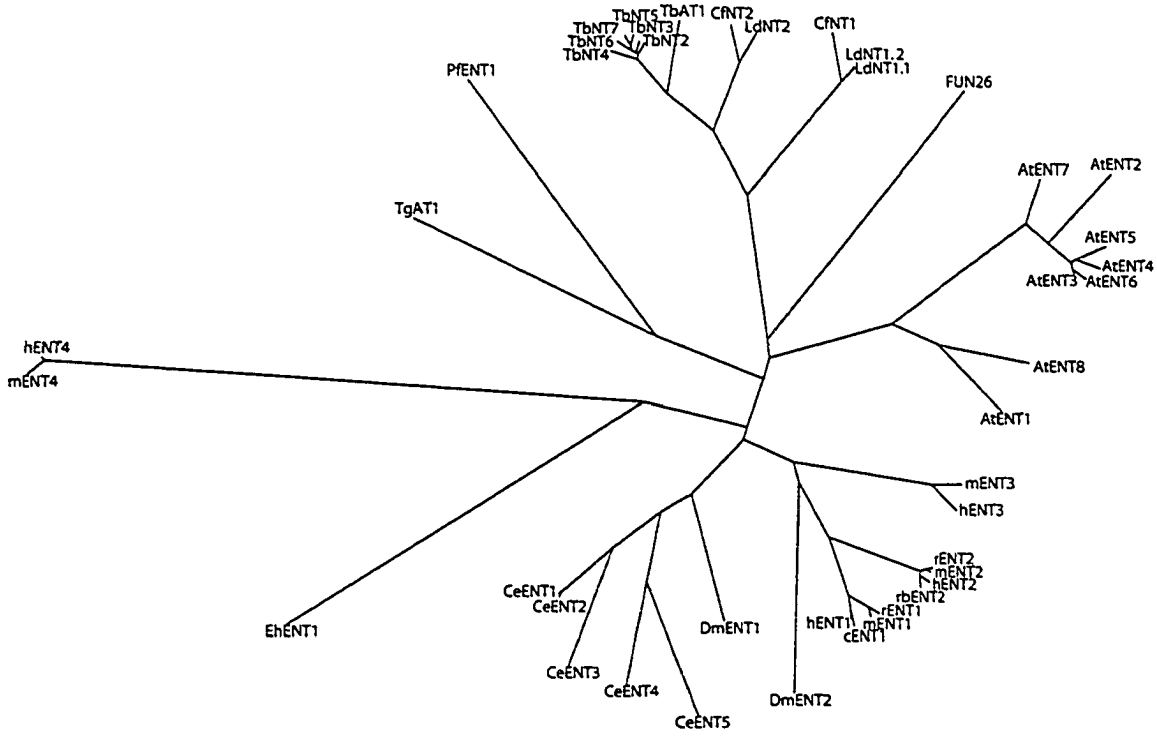

Figure 1-3. Phylogenetic tree of the ENT (SLC29) family.

The protein sequences of 43 ENT family members were obtained from GenBank™ using the accession numbers AAC51103 (human; hENT1), AAF78452 (mouse; mENT1), AAS99848 (canine; cENT1), AAB88049 (rat; rENT1), AAC39526 (hENT2), AAF78477 (mENT2), AAK11605 (rabbit; rbENT2), AAB88050 (rENT2), AF326987 (hENT3), AF326986 (mENT3), NP_694979 (hENT4), AAH25599 (mENT4), AAM46663 (*Caenorhabditis elegans*; CeENT1), CAB01882 (CeENT2), CAB01223 (CeENT3), CAB62793 (CeENT4), AAA98003 (CeENT5), AAF52405 (*Drosophila melanogaster*; DmENT1), AAL28809 (DmENT2), NP_564987 (*Arabidopsis thaliana*; AtENT1), AAL25095 (AtENT2), AAL25096 (AtENT3), AAL25097 (AtENT4), NP_192423 (AtENT5) AAL25098 (AtENT6), AAL25094 (AtENT7), AAO31974 (AtENT8), P31381 (*Saccharomyces cerevisiae*; FUN26), AAG09713 (*Plasmodium falciparum*, PfENT1), AAC32597 (*Leishmania donovani*; LdNT1.1), AAC32315 (LdNT1.2), AAF74264 (LdNT2), AAF03246 (*Toxoplasma gondii*; TgAT1), AAD45278 (*Trypanosoma brucei*; TbAT1), AAQ16072 (TbNT2), AAQ16077 (TbNT3), AAQ16079 (TbNT4), AAQ16081 (TbNT5), AAQ16089 (TbNT6), AAQ16085 (TbNT7), AAG22610 (*Crithidia fasciculata*; (CfNT1), AAG22611 (CfNT2) and S49592 (*Entamoeba histolytica*; EhENT1) and subjected phylogenetic analysis using the PHYLIP software package version 3.6, alpha 3.

Mechanism of transporter function

Nucleoside transporters belong to the major facilitator superfamily, the members of which are thought to share a common transport mechanism, as originally proposed by Widdas in 1952 (61). This "alternating access" mechanism involves a series of conformational changes that make the permeant binding site accessible from one side of the membrane or the other, but not both sides simultaneously (62). The *es* transporter has been studied most extensively in this regard, and has been shown to be capable of alternating between the inward-facing (endofacial) and outward-facing (exofacial) conformations in either the permeant-bound or unbound state, although the rate of conformational change is substantially faster when the *es* transporter is bound to the permeant (1). Therefore, the *es* transporter is in constant equilibrium between the inward and outward-facing conformations. Although it is not clear whether the *es* transporter can be locked in the inward-facing conformation, site-bound NBMPR is thought to lock the protein in the outward-facing conformation (63).

Nucleoside analogs

Nucleoside analogs form part of the antimetabolite class of drugs used in the treatment of cancer and viral diseases and are discussed in detail in several recent reviews (4,32,64,65). Nucleoside analogs exert toxicity by perturbing nucleotide pools, incorporating into DNA and RNA and inducing DNA strand breakage (66). Examples of routinely used nucleoside analogs for cancer treatment include cytarabine (araC, cytosine-β-D-arabinofuranoside), which is a curative agent in the treatment of acute lymphocytic leukemia (ALL), fludarabine (2-fluoro-2'-deoxyadenosine), which has activity in the treatment of chronic lymphocytic leukemia (CLL), cladribine (2-chloro-2'-deoxyadenosine), which has activity against hairy cell leukemia and CLL, and gemcitabine (2', 2'-difluoro-2'-deoxycytidine), which has activity against many types of solid tumors including breast, non-small cell lung, pancreatic, bladder, ovarian and head and neck cancers (Fig. 1-1) (64). Nucleoside analogs used in the treatment of viral diseases include zidovudine (AZT, 3'-azido-2', 3' dideoxythymidine), zalcitabine (ddC, 2', 3'-dideoxycytidine) and didanosine (ddI, 2', 3'-dideoxyinosine) used in the treatment

of human immunodeficiency virus (HIV) infections, and acyclovir (9-(2-hydroxyethoxymethyl) guanine) used in the treatment of *Herpes simplex* virus infections (Fig. 1-1) (32).

The obligatory first steps for many nucleoside drugs to exert cytoxicity are cellular uptake via nucleoside transporters followed by phosphorylation by intracellular kinases such as deoxycytidine kinase, thymidine kinase or deoxyguanosine kinase (4,67-71). Most of the anticancer nucleoside analogs are robust permeants for both CNTs and ENTs whereas the antiviral nucleosides, many of which lack the obligatory 3' hydroxyl group, are less efficiently transported (72-75). However, transport of AZT, ddC and ddI mediated by hENT2, hCNT1, hCNT2 and hCNT3 has been observed, suggesting that nucleoside transporters are involved in the cellular uptake of these drugs (12,58,76). The importance of nucleoside transport processes has been established by the observation that cells lacking transport processes often display resistance to nucleoside analogs (74,77,78). Clinical relevance of this observation has been demonstrated *in vivo* by studies that determined hENT1 abundance by immunohistochemical staining of tumors, which revealed large variations in staining intensities and even instances of hENT1 deficiency (79-81). Furthermore, patients with pancreatic adenocarcinoma lacking hENT1 have been shown to experience significantly decreased survival when treated with gemcitabine compared to patients whose tumors possess hENT1 (82). Single nucleotide polymorphisms affecting nucleoside transporter function were not detected for hENT1, hENT2, hCNT2 or hCNT3 whereas hCNT1 was found to be truncated and non-functional in 3 % of the African-American population (65,83-86).

Adenosine and tissue protection

Most of the research involving the protective effects of adenosine has been focused on heart and brain, tissues in which adenosine serves to protect insulted tissue by decreasing energy demands and increasing oxygen supply. In the heart, ischemia, hypoxia or injury to the myocardium results in rapid formation of adenosine (87,88). Cardiomyocytes are the primary cellular origin of adenosine, which is generated from ATP breakdown leading to dephosphorylation of 5'-AMP via intra- and extracellular 5'-nucleotidases and from S-adenosylhomocysteine (SAH) via SAH hydrolase. Under

baseline conditions, adenosine has a very short half-life with ~80 % being converted to AMP by adenosine kinase (AK) and the rest becoming protein-bound or deaminated by adenosine deaminase (ADA), which results in a net inward concentration gradient. However, during ischemia adenosine kinase and adenosine deaminase are inhibited, resulting in a net outward concentration gradient. In human cells adenosine exerts its effects by binding to one of the four subtypes of adenosine receptors that have been identified by pharmacological analysis and molecular cloning: A_1, A_{2A}, A_{2B} and A_3 receptors (A_1AR, A_{2A}AR, A_{2B}AR and A_3AR) (89-94). A_1ARs and A_3ARs have been shown to couple to G_i and G_o family proteins whereas A_{2A}ARs and A_{2B}ARs couple to G_q family proteins, giving adenosine receptors influence over a broad range of signaling pathways (88). Each receptor subtype has distinguishable ligand binding properties and controls distinct functions in tissues and cells of varying origin (88). In the ischemic, hypoxic, or injured myocardium, activated adenosine receptors exert many protective physiological processes such as (i) modulating cardiomyocyte metabolism (A_1AR and A_3AR) and vasodilation (A_{2A}AR), and (ii) inhibiting excitatory neurotransmitter release (A_1AR and A_{2A}AR), inflammation (A_{2B}AR) and platelet aggregation (A_{2A}AR) (87,95). The molecular basis of adenosine receptor signaling pathways has previously been reviewed (96) and is beyond the scope of this review.

Adenosine is normally present in the central nervous system at nanomolar concentrations but during events such as cerebral ischemia, hypoxia, sleep deprivation or epileptic seizures, the levels of adenosine increase to micromolar levels due to the breakdown of ATP (97,98). The mechanisms of neuroprotection, in addition to those involved in cardioprotection, involve activation of A_1ARs and A_{2A}ARs resulting in prevention of release of excitatory amino acid (EAA) neurotransmitters such as glutamate and stabilization of neuronal membrane potentials via activation of K^+ and Cl^- channels.

The primary means by which the protective influences of adenosine are terminated is cellular uptake via ENTs present in cardiomyocytes, vascular endothelial and smooth muscle cells and neurons in the CNS (99-104). Physiologically, the effects of adenosine are potentiated by down-regulation of ENT1 in response to reduced oxygen levels (105,106). However, one study that addressed the regional distribution of hENT1 and hENT2 in the human brain indicated a positive correlation between the abundances

of hENT1 and adenosine receptor A_1 (A_1AR) (107) and another subsequently reported that the mouse ortholog, mENT1, is upregulated in cultured cardiomyocytes upon A_1AR activation as a necessary prerequisite to reperfusion (108). Although recent research has indicated that CNTs are inhibited by some adenosine receptor ligands (75), the role of CNTs in adenosine homeostasis still represents a significant knowledge gap and is an important avenue for future research. Specific, high-affinity inhibitors of hENT1 and hENT2 have been developed as cardioprotective and antiplatelet agents, including dilazep, dipyridamole, draflazine and soluflazine, which potentiate the effects of extracellular adenosine (Fig. 1-4). This review summarizes the current state of knowledge regarding the pharmacological, molecular and structural basis of inhibitor interactions with ENTs.

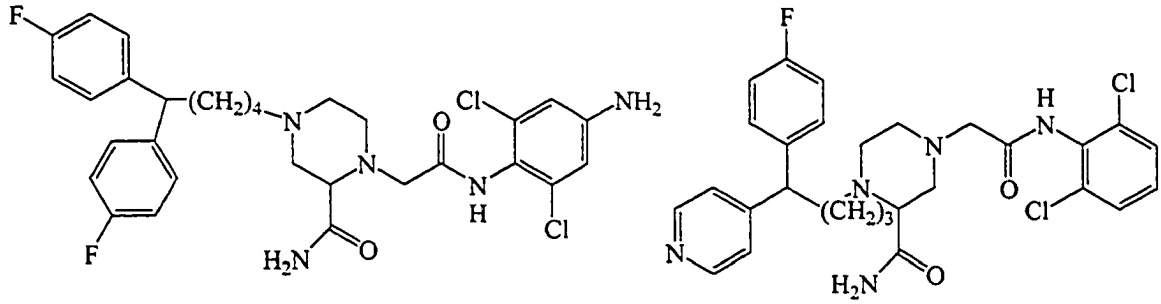

Draflazine

Soluflazine

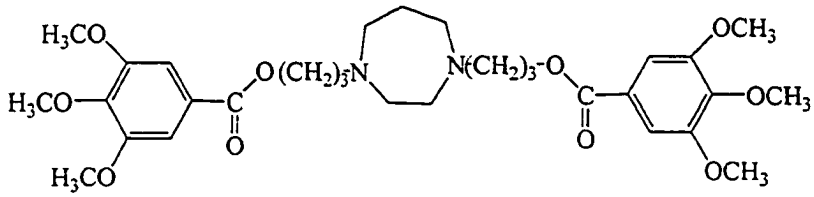

Dilazep

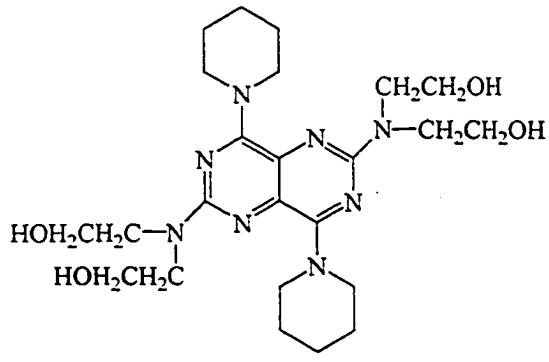

Dipyridamole

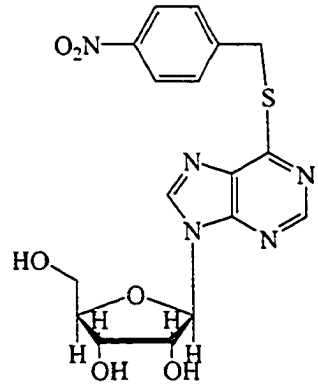

NBMPR

Figure 1-4. Chemical structures of ENT inhibitors.

The structures of draflazine (2-(aminocarbonyl)-*N*-(4-amino-2,6-dichlorophenyl)-4-[5,5-*bis*-(4-fluorophenyl)pentyl]-1-piperazineacetamide), soluflazine (3-(aminocarbonyl)-4-[4,4-(fluorophenyl-3-pyridinyl)butyl]-*N*-(2,6-dichlorophenyl)-1-piperazineacetamide 2HCl), dilazep (*N,N'-bis*[3-(3,4,5-trimethoxybenzoyloxy)propyl]-homopiperazine), dipyridamole (2,2',2",2"'-[(4,8-dipiperidinylpyrimido[5,4-d]pyrimidine-2,6-diyl)dinitrilo]tetraethanol) and NBMPR (6-[(4-nitrobenzyl)thio]-9-(β-D-ribofuranosyl)purine) were generated using ChemDraw Ultra version 6.0 software.

NBMPR

Pharmacological studies

NBMPR (Fig. 1-4) and its thioinosine analogs have been extensively studied because they are specific, reversible, tight-binding inhibitors of *es* transport processes of mammalian cells, binding with a K_d of (0.1 – 1 nM) in accordance with a simple single-site binding model (109-114). The structural basis for potency of thioinosine analog-mediated inhibition of *es* transporters was attributed to the hydrophobicity of the substituent at the 6-position on the purine base moiety (nitrobenzyl group on NBMPR) (115). NBMPR has since proven to be an extremely useful tool in radioligand binding analyses for quantitation of *es* transporter abundance (1,64,113,116). As a non-radioactive alternative, 5'-S-(2-aminoethyl)-N^6-(4-nitrobenzyl)-5'-thioadenosine-χ_n-fluorescein (SAENTA-fluorescein) analogs of NBMPR, with a fluorescent moiety at the 5' position of the sugar, have also been synthesized for purposes of *es* transporter/ENT1 quantitation (117-119).

Knowledge of the number of *es* transporters present on cell surfaces and maximum transport rates for nucleosides has allowed calculation of transporter turnover rates. Values for zero-*trans* uridine influx into erythrocytes from various species were remarkably similar, being on average ~150 molecules/transporter/s (113). A study involving recombinant hENT1 produced in stably transfected PK15 cells yielded a turnover number of 46 molecules/transporter/s (59). However, SAENTA-fluorescein bound to a single class of sites in cells in which NBMPR bound to two classes of sites. This raises the possibility that NBMPR can diffuse across the plasma membrane and access intracellular binding sites, which puts into question the accuracy of the turnover rates calculated by assuming that cellular NBMPR binding-sites directly reflect the number of transporters in plasma membranes (117).

Many studies addressing the kinetic mechanisms of NBMPR binding have been performed. NBMPR was shown to be a competitive inhibitor of uridine influx and a non-competitive inhibitor of zero-*trans* uridine efflux in sheep erythrocytes, a result that suggested binding of inhibitor and permeant to the same site, or to a site that overlapped with the outward-facing permeant binding site (1,120). This observation was later

confirmed in experiments that assessed NBMPR binding to inside-out and right-side out membrane vesicles from pig erythrocytes in which it was apparent that NBMPR binds to the extracellular aspect of the *es* transporter (63). The affinity of NBMPR for the *es* transporter was also shown to be unaffected by pH, suggesting that ionizable groups are not involved in binding (121).

The competitive nature of NBMPR inhibition of the *es* transport system was put into question by the observation that, in cultured hamster fibroblasts, high concentrations (20 to 40 mM) of uridine were able to accelerate the dissociation of site-bound NBMPR, which was suggestive of separate binding sites (122). A subsequent study reproduced these findings in human erythrocytes but noted that no significant changes in dissociation rates of NBMPR were observed when nucleosides were present at concentrations equal to the apparent K_i for inhibition of NBMPR binding (123). One determination of NBMPR association kinetics suggested a slow, first-order mechanism whereas a similar analysis of NBMPR binding to Ehrlich ascites cells, which are of mouse origin, indicated that NBMPR association consisted of two components (123-125). Measurements of dissociation rates in Ehrlich ascites cells revealed that nucleosides accelerated dissociation of site-bound NBMPR, suggesting the presence of distinct permeant and NBMPR-binding sites that are allosterically linked (125). The molecular cloning of the human, rat and mouse *es* transporter cDNAs has allowed for continued research aimed at resolving this long-standing contreversy (38-40,126,127).

Photoaffinity labeling

A study aimed at investigating the covalent attachment of a photoactive analog of NBMPR, N^6-(*p*-azidobenzyl) adenosine (ABA), to *es* transporters in human erythrocytes led to the discovery that NBMPR itself can be covalently cross-linked by exposure to ultraviolet light (128). The mechanism of the photoreactivity of NBMPR was determined by exposing the molecule to ultraviolet radiation, which results in the formation of a 6-thioinosine radical species that can subsequently react with the protein (129). When erythrocyte membranes labeled with either [^{3}H]-NBMPR or [^{3}H]-ABA were separated by sodium dodecylsulfate polyacrylamide gel electrophoresis (SDS-PAGE), the resulting gel distribution of the ^{3}H label indicated specific photoincorporation into proteins that

migrated with apparent molecular weights of 45,000 to 65,000 Da, which corresponded to band 4.5 polypeptides (128,130). It was subsequently shown that NBMPR selectively labeled nucleoside transporter polypeptides in many different kinds of mammalian cells of varying origins (130-135).

Using NBMPR as a covalent probe, some of the first insights into the structure and function of the *es* transporter were made. Enzymatic deglycosylation of photolabeled polypeptides reduced their mobility on SDS-PAGE to a sharp 46,000-Da peak, indicating that *es* transporters consisted of a group of hetergenously glycosylated polypeptides (136). A combination of tryptic digestion and enzymatic deglycosylation of the photolabeled polypeptides led to the conclusion that NBMPR bound to the *es* transporter within 12,000 Da of the glycosylation site (137). The specific site of covalent attachment of NBMPR to the *es* transporter remains an important unanswered question.

Biochemical studies

A major challenge to the study of ENTs has been the lack of a highly abundant source of transporter proteins for purification purposes. Several studies have addressed methods of solubilization and reconstitution, using NBMPR as a probe to detect the *es* transporter protein. Octylglucoside is the most effective detergent for extracting *es* transporters from cells of mammalian origin and a complex mixture of lipids including phosphatidylcholine, cholesterol, phosphatidylethanolamine and phosphatidylserine is the most favorable for *es* transporter reconstitution studies (138-143).

Although erythrocytes represent the least complex system from which purified nucleoside transporters can be obtained, the erythrocyte glucose transporter (now known as GLUT1) represents the vast majority of band 4.5 polypeptides (144-146), making purification of *es* transporters difficult. This problem was circumvented by purifying and functionally reconstituting *es* transporters from pig erythrocytes, which lack glucose transporters (147,148). Purification of human *es* transporters was subsequently achieved using specific anti-glucose transporter antibodies to remove contaminating glucose transporters from a preparation of band 4.5 polypeptides (149). The identity of the purified transporter was confirmed by NBMPR binding and photolabeling experiments (149). This preparation was subjected to gas-phase N-terminal sequencing of the first 21

amino acid residues, which allowed the synthesis of cDNA probes that were used to clone hENT1 from a human placental cDNA library (38,149). This breakthrough, in which NBMPR played an instrumental role as a specific, high-affinity probe for *es* transporters, represented the beginning of a new era in nucleoside transporter research.

Molecular studies

The molecular cloning of ENT1 and ENT2 from humans, rats and mice opened a new avenue of investigation into the molecular determinants of NBMPR interactions (38-40,126,127). It was demonstrated that recombinant hENT1 produced in yeast binds NBMPR with an apparent K_d of ~ 1 nM, providing strong evidence that it is the protein responsible for *es*-mediated in human cells (150). Although many ENTs from different organisms have been cloned and characterized, the only transporters with notable sensitivities to NBMPR are those responsible for *es*-type transport in mammalian cells.

Chimeric constructs involving swaps between rENT1 and rENT2 led to the identification of TMs 3-6 as a major determinant of NBMPR sensitivity (151). Chimeric studies also implicated TMs 3-6 as a region involved in nucleobase and antiviral nucleoside transport in rENT2, suggesting that NBMPR binds to the same, or overlapping, sites with permeants. It was subsequently shown that when G154 in TM 4 of hENT1 is mutated to Ser, the corresponding residue in hENT2, the mutant hENT1 is ~2500-fold less sensitive to inhibition by NBMPR (51). The corresponding residue in rENT2, C140, was shown to form a part of the exofacial nucleoside-binding site (50). Another study showed that when L92 of hENT1, is mutated to Gln, a >200-fold reduced sensitivity to NBMPR and reduced affinities for inosine and guanosine are observed (152). These studies have provided direct molecular evidence that NBMPR is a competitive inhibitor of nucleoside transport.

Dipyridamole

Pharmacological studies

Dipyridamole (Fig. 1-4), also known as persantine, is routinely used as a cardioprotective or antiplatelet agent (153). Dipyridamole inhibits both the *es* and *ei* transport systems, although with much higher affinity for the *es* system (154). Structure-activity relationship studies using ~90 dipyridamole analogs have indicated that a hydroxyl or alkoxy group is required at the 2 and 6 positions (those occupied by the diethanolamino groups in the parent compound) whereas the structural requirements of the 4, 8 positions (those occupied by the piperidino groups) remain unclear (154-156). These studies were aimed at identifying dipyridamole analogs that potently inhibit nucleoside transport but do not interact with the serum protein α_1-acid glycoprotein, which reduces the bioavailability of dipyridamole to nucleoside transporter sites. Therefore, a more systematic approach aimed at studying interactions with nucleoside transporters will be required to define the structure-activity relationships for dipyridamole binding.

Several early studies have suggested that dipyridamole, like NBMPR, is a competitive inhibitor of the *es* transport process (120,157,158). Dipyridamole associated slowly with its binding sites on guinea pig lung membranes, by a first-order mechanism, with a half-life of ~2 min and requiring ~15 min to reach full equilibrium (159). Dipyridamole binds to a single class of binding sites on *es* transporters of guinea pig lung membranes, human erythrocytes and HeLa cells, whereas it binds to both the *es* and *ei* transporters in the guinea pig and rabbit central nervous system (159-162). Nonetheless, dipyridamole was shown to reduce the rate of dissociation of site-bound NBMPR in human erythrocytes and Ehrlich ascites cells, suggesting that it may interact allosterically with *es* transporters (123,125). Therefore, the same debate regarding the mechanism of NBMPR binding also applies to the mechanism of dipyridamole binding, although, the allosteric properties of dipyridamole binding were only observed at high (i.e. micromolar) concentrations (123,158).

Rat lung membranes and cultured cells of rat origin lack high-affinity dipyridamole binding sites (159,161). These results are consistent with the findings of many studies involving rat cells and tissues of varying origins that rat *es* transporters are ~100-fold more resistant to dipyridamole inhibition than those of other species (112). These observations have led to interest in determining species differences in sensitivities to dipyridamole and other inhibitors (163). Many of the early studies reporting IC_{50} values for dipyridamole and various other inhibitors in different species are difficult to evaluate because it has become clear, since the molecular cloning of human and rodent ENTs, that direct comparisons of values obtained from cells and tissues of differing origins may be misleading. Furthermore, even experiments performed in the same model systems but by different research groups have yielded significantly different IC_{50} values. Therefore, the most valid species comparison data comes from a single study that involved analysis of erythrocytes from different species in parallel, and required the assumption that the membrane lipid compositions and extents of post-translation modifications are similar in different mammalian erythrocytes (163). The IC_{50} values reported in that study (161) for dipyridamole, dilazep and lidoflazine (a draflazine analog) are displayed in Table 1-1. These data indicated that the human, rabbit and pig *es* transporters were highly sensitive, mouse *es* transporters were of intermediate sensitivity and rat *es* transporters were relatively insensitive. This information would prove useful in structure-function studies of dipyridamole interactions with recombinant ENTs.

Table 1-1. IC_{50} values for dipyridamole, dilazep and lidoflazine inhibition of 500 μM [^{3}H]-uridine transport into erythrocytes of human, mouse, rat, rabbit and pig origin.

Adapted from Plagemann and Woffendin (1988) (163).

	IC_{50} (nM)		
Species	Dipyridamole	Dilazep	Lidoflazine
Human	40	7	12
Mouse	150	40	>10000
Rat	300	1000	>10000
Rabbit	50	30	12

Molecular studies

The molecular cloning and functional characterization of ENT1 and ENT2 from humans and rats have led to new insights into dipyridamole interactions with these transporters. Dipyridamole was shown to inhibit recombinant hENT1 produced in *Xenopus laevis* oocytes with an IC_{50} value of ~140 nM and a Hill coefficient of one, suggestive of a single class of binding sites, whereas rENT1 was insensitive to inhibition by this compound (38,126,164). It has also been shown, in parallel analyses of recombinant hENT1 and hENT2 produced in either cultured cells or yeast, that hENT1 was 71- and 130-fold, respectively, more sensitive than hENT2 to inhibition by dipyridamole (59,165). These results confirmed that the observed differences in dipyridamole sensitivities between human and rat *es* processes, and the human *es*- and *ei*-mediated processes, were exhibited by the recombinant transporters produced in model expression systems.

Other ENTs from non-mammalian species have been shown to display some degree of dipyridamole sensitivity. CeENT1 and 2 from *Caenorhabditis elegans*, which share, respectively, 94 % and 26 % sequence identity with hENT1, when produced in *X. laevis* oocytes, displayed an IC_{50} value of ~200 nM for dipyridamole, which was comparable to that obtained by the same research group for hENT1 in the same model system (38,166). Other non-mammalian ENTs that have been tested for dipyridamole sensitivity include AtENT3 from *Arabidopsis thaliana*, which was inhibited by micromolar concentrations (167), TgAT1 from *Toxoplasma gondii*, which has been shown to be completely inhibited by 1 μM dipyridamole (168), and FUN26, the intracellular ENT from *Saccharomyces cerevisiae*, which was insensitive to 1 μM dipyridamole (169). Ambiguity has arisen with respect to the ENT that was cloned and characterized from *Plasmodium falciparum*, which was reported to be inhibited by high (10 μM) dipyridamole concentrations by one group and to be insensitive by another group (170,171). There have not yet been enough recombinant ENTs tested for dipyridamole sensitivity to easily identify interacting residues from sequence alignments. The findings regarding dipyridamole interactions with recombinant ENTs, although

limited, are suggestive of a common, complex, dipyridamole-binding pocket in many of these transporters.

Studies of chimeric constructs, involving swaps between hENT1 and rENT1 have suggested that the region encompassing TMs 3-6 is responsible for the major sensitivity differences between these two proteins (164). This region has also been implicated in NBMPR binding and permeant interactions, providing evidence in favor of the competitive model of dipyridamole binding (46,76,151). However, the individual residues responsible for the effects observed in the chimera study have not been identified. Random mutagenesis and screening of hENT1 in yeast led to the identification M33 (I33 in hENT2 and rENT1) in TM 1, which is responsible for ~10 fold of the observed species differences in dipyridamole sensitivity (Chapter 3) (165). This study also demonstrated that when I33 of hENT2 was mutated to Met, the apparent K_m for uridine decreased ~8-fold. Although this study suggested that residue 33 was important for both dipyridamole and uridine interactions, its direct involvement in binding of inhibitor and permeant has not been shown. Therefore, the current level of knowledge with respect to the molecular nature of dipyridamole interactions with ENTs is still limited.

Dilazep

Pharmacological studies

Dilazep (Fig. 1-4), also known as cormelian, has similar clinical uses to dipyridamole as a cardioprotective and antiplatelet agent and inhibits *es* transporters with nanomolar affinities (1,112,172). Although dilazep inhibits both *es* and *ei* transporters, it is bound by *es* transporters with substantially higher affinities than by *ei* transporters (1,165). Two structural analogs of dilazep, hexobendine and ST7092, differ structurally with respect to the central 7-member ring of dilazep, which is 6-membered in ST7092 and open in hexobendine but otherwise share very similar properties with respect to transport inhibition (173). A unique feature of dilazep compared to dipyridamole and NBMPR is that it is positively charged at neutral pH and possess two ionizable groups

with pK_a values of ~5 and 8 (173). Furthermore, dilazep is highly water-soluble compared to NBMPR and dipyridamole, making it a useful "stopping" reagent in transport assays involving mammalian ENTs. Overall, less is known about the mechanism and structural requirements for interactions of dilazep with ENTs than for either NBMPR or dipyridamole.

The first study that systematically addressed the mechanism of dilazep interactions with *es* transporters (conducted with cultured hamster fibroblasts) yielded the observation that high concentrations (25 μM) of dilazep, like dipyridamole, reduced rates of dissocation of site-bound NBMPR for binding to the same transport-inhibitory sites (122). In another study (conducted with Ehrlich ascites cells), dilazep also reduced dissociation rates of site-bound NBMPR. These results were inconsistent with simple competition between dilazep and NBMPR. Analysis of [^{3}H]-dilazep binding in mouse S49 lymphoma cells revealed that dilazep required ~15 min to reach equilibrium with its binding sites and bound to two classes of sites with apparent K_d values of 0.25 and 13 nM, respectively (174). A study of pH dependence of dilazep binding revealed that the uncharged form has the highest affinity for *es* transporters and competes with NBMPR and nucleosides for binding (173,174). The charged forms of dilazep appeared to interact allosterically with the NBMPR and nucleoside-binding sites (174).

Many studies have suggested that dilazep follows a similar species sensitivity pattern as dipyridamole, with human, rabbit, mouse and pig *es* transporters being highly sensitive and rat *es* transporters being more resistant (Table 1-1) (1,112,163). Unlike the kinetic analyses, these studies provided evidence for a common, conserved structural basis for dilazep and dipyridamole binding to *es* transporters.

Molecular studies

Advances in the knowledge of dilazep interactions have been made with the molecular cloning of mammalian ENTs. None of the non-mammalian ENTs have been shown to exhibit dilazep sensitivity similar to that of hENT1, although AtENT6 and 7 have been shown to be sensitive to micromolar concentrations of dilazep. Also, systematic structure-activity relationship studies using analogs of dilazep have not been reported.

The same chimera study that identified TMs 3-6 as a region responsible for the difference in dipyridamole sensitivity between hENT1 and rENT1 also implicated this region in dilazep interactions (164). Interestingly, residue 33, which was a determinant of the difference in dipyridamole sensitivity of hENT1 and hENT2, was shown to also be a determinant of the difference in dilazep sensitivity (165), suggesting a common basis for high-affinity binding of dilazep and dipyridamole by hENT1. A separate study implicated the involvement of L92 in TM 2 of hENT1 in dilazep interactions, but the effects of mutating this residue on dilazep sensitivity were relatively small (152). Therefore, knowledge of the individual amino acid residues involved in dilazep interactions is limited.

Draflazine, soluflazine and analogs

Pharmacological studies

Lidoflazine and its analogs (which include mioflazine, soluflazine, draflazine (R88021) and the (-) enantiomer of draflazine, R75231) are all potent inhibitors of nucleoside transport in human erythrocytes (see Fig. 1-4 for structures of draflazine and soluflazine) (175). These drugs offer an attractive alternative to dipyridamole, which has limited bioavailability because it binds to plasma proteins (87,176) whereas, the oral bioavailability of draflazine and R75231 is excellent (87). Structure-activity relationship studies with various analogs indicated that an alkyl chain length of five carbons connecting the piperazine ring and the two fluorophenyl groups were required for high-affinity interactions with *es* transporters whereas an alkyl chain length of four carbons was preferred by *ei* transporters (177,178). The *ei* transporters of rat erythrocytes and Ehrlich ascites cells have been reported to have high affinities for soluflazine (178,179). For *es*-mediated transport processes, draflazine and R75231 are the most potent inhibitors of this inhibitor class (175,179,180). For example, extensive washing of site-bound [^{3}H]-R75231 did not remove the inhibitor, suggesting that it binds in a pseudo-irreversible fashion, since it was fully displaced by nucleosides, NBMPR and dipyridamole (180,181).

Several studies have suggested that R75231, draflazine and mioflazine are mixed-type inhibitors of *es* transporters from various species, based on the observations that (i) their presence causes increased K_d and decreased B_{max} values for NBMPR binding, and (ii) they inhibit NBMPR binding with Hill coefficients that are consistently greater than one (177,178,180,181). Other analogs in this inhibitor class, however, behave as purely competitive inhibitors of NBMPR binding (178). Consistent with the observations for dipyridamole and dilazep, rat *es*-mediated transport appears to be several orders of magnitude less sensitive to these agents than *es*-mediated transport in other mammals (163,179). The IC_{50} values obtained in erythrocytes for lidoflazine are presented in Table 1-1. These results suggest that some of the structural features involved in high-affinity binding of draflazine, soluflazine and their analogs are conserved and shared with those of NBMPR, dipyridamole and dilazep.

Molecular studies

The molecular cloning of ENTs has not yet led to advances in the understanding of interactions of draflazine, soluflazine or their analogs with *es* transporters at the molecular level. These compounds are not commercially available, although Janssen Pharmaceuticals, Beers, Belgium, will supply these compounds for research on the molecular biology of transporter proteins (178). The molecular basis of draflazine and soluflazine interactions with recombinant ENTs remains an open question for future research efforts.

Other inhibitors of nucleoside transport

Adenosine receptor ligands

Several studies have investigated the possibility of interactions between adenosine receptor agonists or antagonists and *es* transporters (182-188). In general, *es* transporters display affinities for these compounds that are several orders of magnitude lower than those of adenosine receptors (1). However, one study identified CV1808 (2-phenylaminoadenosine) and its derivatives CGS 23321 and CGS 23302 as potent

inhibitors of uridine transport in guinea pig erythrocytes, with IC_{50} values ranging from ~150 nM to ~370 nM (189). More recently, it was observed that N^6-(*p*-aminobenzyl)adenosine, caffeine and nicotine were non-permeant inhibitors of hCNT1 and hCNT2 stably transfected into a transport-deficient cell line (75). Although these studies did not identify many high-affinity inhibitors, they provide a starting point for the synthesis of new inhibitors, some of which may have high affinities for CNTs.

Ca^{2+} channel blockers

Several early studies also noted that Ca^{2+} channel blockers were capable of inhibiting nucleoside transport, although most required high micromolar concentrations to do so (190,191). The most notable of these was (+)nimodipine, which displaces NBMPR from human brain membranes and inhibits transport of nucleosides into human erythrocytes at nanomolar concentrations (191,192). Although it was demonstrated that (+)nimodipine is a competitive inhibitor of *es*-mediated transport, there has been little further interest in the interactions of this compound with nucleoside transporters (112).

Protein kinase inhibitors

It was recently reported that the p38 MAP kinase inhibitors SB203580 and SB203580-iodo inhibited uridine uptake in cultured human K562 erythroleukemia cells with apparent IC_{50} values of ~700 nM and ~100 nM, respectively (193). These two compounds were also shown to inhibit NBMPR binding to intact K562 cells and human erythrocyte membranes, confirming that they interacted with human *es* transporters. In a follow-up study, a large number of protein kinase inhibitors were tested for their ability to inhibit nucleoside transport into K562 cells, revealing that several of these compounds were capable of inhibiting transport (194). These included tyrosine kinase inhibitors (AG825, AG1517, AG1478, STI-571), protein kinase C (PKC) inhibitors (staurosporine, GF 109203X, RO 31-8220, arcyriarubin A), cyclin-dependent kinase inhibitors (roscovitine, olomoucine, indirubin-3'-monoxime) and rapamycin. Most of these compounds were bound by *es* transporters with modest affinities and IC_{50} values of ~ 1 μM. The most notable inhibition was observed for the PKC inhibitor analog, Ro 31-6045, which itself does not inhibit PKC; this compound displayed an IC_{50} of ~60 nM for

inhibition of *es*-mediated transport of K562 cells. These studies have contributed a starting point for the synthesis of novel nucleoside transport inhibitors, some of which could have selectivity for *ei* transporters or CNTs. A comprehensive analysis in a high-throughput model system to assess the inhibitory potential of these compounds on the individual transporters is warranted.

Summary and future directions

Nucleoside transporters are important pharmacological determinants of the efficacy of anticancer and antiviral therapy as well as cardio and neuroprotective transport inhibitors (195). This review has provided a historical perspective on the interactions of inhibitors with nucleoside transporters and has shown that the molecular cloning of the cDNAs encoding ENT proteins has provided a novel molecular avenue of investigation into mechanisms of high-affinity interactions. Several studies have suggested that NBMPR, dipyridamole and dilazep interact with regions and amino acid residues on recombinant ENTs that are also important for permeant interactions. Additionally, these studies strongly suggest that the inhibitors compete with permeants for binding to the exofacial aspect of the *es* transporters. However, since most of the more complex models of inhibitor binding are based on observations made when high (micromolar) concentrations of inhibitor were present, the possibility of a second low-affinity, broadly specific allosteric site exists, as proposed by Griffith and Jarvis in 1996 (1). Many different ENTs from different organisms appear to interact with these inhibitors with variable affinities, suggesting that the structural determinants for binding are complex, involving contributions from many residues on different parts of the protein.

Continued research using chimeric approaches to exploit inhibitor sensitivity differences between related transporters, random mutagenesis and phenotypic screening in yeast and comprehensive substituted cysteine accessibility methods (SCAM) will define the amino acid residues responsible for high-affinity inhibitor binding. These studies would also be especially interesting for draflazine, which appears to have unique binding characteristics but about which there is no knowledge from the molecular perspective. Systematic studies to define the structure-activity relationships for inhibitor interactions with the transporters would also provide useful information about the mechanisms of high-affinity interactions. Furthermore, with many ENTs having been identified and produced as recombinant proteins for functional characterization, it would be prudent to reassess the species differences in inhibitor sensitivity in parallel, by producing the transporters in identical genetic and proteomic backgrounds. The high-

throughput transport assay system developed using yeast as the model host system would be ideal for these purposes (21,57). The results of such studies should provide enough information to identify residues responsible for the sensitivity differences between different ENTs using a bioinformatics approach. These studies would also allow for structural modeling of the inhibitor binding sites.

The molecular cloning of ENTs and CNTs allows for comprehensive screening efforts of novel compounds to develop inhibitors selective for each transporter isoform, as has been done for many receptor subtypes. The study of the roles of nucleoside transporters in cells and tissues is normally complicated by the simultaneous presence of multiple subtypes, so the availability of specific inhibitors would faciliate dissection of these processes. Such studies would aid in elucidating the specific roles of nucleoside transporters in different cellular contexts. Furthermore, the availability of new inhibitors coupled with knowledge of the transporter subtypes present in specific tissues or organs could provide options for more targeted protective therapies against conditions such as ischemia or hypoxia. Also, as proposed by Baldwin et. al. (193), the identification of ENTs from parasitic protozoa, which are entirely dependent on the host system for purine salvage, suggests that parasite-specific inhibitors could be developed as potential anti-parasitic agents. Studies of inhibitors of nucleoside transport have led to the identification of therapeutically important drugs, providing insights into the mechanisms of transporter function, and led to the molecular cloning of hENT1 in 1996. Continued research of existing inhibitors and development of novel inhibitors is critical to further our understanding the roles of nucleoside transporters in physiology and nucleoside analog drug chemotherapy.

The objectives of the research of this thesis were to identify and functionally characterize the molecular determinants (amino acid residues) of equilibrative nucleoside transporters. The approaches used involved random mutagenesis of hENT1 and CeENT1 followed by screening for mutants with resistance to either dilazep, dipyridamole or draflazine, using a yeast-based phenotypic complementation assay. The resulting mutant clones, together with mutant clones of hENT1, hENT2, CeENT1 and rENT1 produced by site-directed mutagenesis, were produced in a nucleoside-transport deficient yeast strain for functional characterization and inhibitor sensitivity assays. The results of these

studies suggested the mechanisms and kinds of interactions involved in inhibitor and/or permeant binding and were used to generate a preliminary helical wheel projections of the inhibitor binding site(s).

References

1. Griffith, D. A., and Jarvis, S. M. (1996) *Biochim Biophys Acta* **1286**, 153-181
2. Young, J. D., Jarvis, S. M., Clanachan, A. S., Henderson, J. F., and Paterson, A. R. (1986) *Am J Physiol* **251**, C90-94
3. Young, J. D., Paterson, A. R., and Henderson, J. F. (1985) *Biochim Biophys Acta* **842**, 214-224
4. Cass, C. E. (1995) in *Drug Transport in Antimicrobial and Anticancer Chemotherapy* (Georgopapadakou, N. H., ed), pp. 403-451, Marcel Deker, New York, NY
5. Landfear, S. M., Ullman, B., Carter, N. S., and Sanchez, M. A. (2004) *Eukaryot Cell* **3**, 245-254
6. Cass, C. E., Young, J. D., Baldwin, S. A., Cabrita, M. A., Graham, K. A., Griffiths, M., Jennings, L. L., Mackey, J. R., Ng, A. M. L., Ritzel, M. W. L., Vickers, M. F., and Yao, S. Y. M. (1999) in *Membrane Transporters as Drug Targets* (Amidon, G. L., and Sadee, W., eds) Vol. 12, 1 Ed., 12 vols., Kluwer Academic/Plenum Publishers
7. Vickers, M. F., Young, J. D., Baldwin, S. A., and Cass, C. E. (2000) *Emerging Therapeutic Targets* **4**, 515-539
8. Cabrita, M. A., Baldwin, S. A., Young, J. D., and Cass, C. E. (2002) *Biochem Cell Biol* **80**, 623-638
9. Huang, Q. Q., Yao, S. Y., Ritzel, M. W., Paterson, A. R., Cass, C. E., and Young, J. D. (1994) *J Biol Chem* **269**, 17757-17760
10. Ritzel, M. W., Yao, S. Y., Huang, M. Y., Elliott, J. F., Cass, C. E., and Young, J. D. (1997) *Am J Physiol* **272**, C707-714
11. Ritzel, M. W., Yao, S. Y., Ng, A. M., Mackey, J. R., Cass, C. E., and Young, J. D. (1998) *Mol Membr Biol* **15**, 203-211
12. Ritzel, M. W. L., Ng, A. M., Yao, S. Y. M., Graham, K., Loewen, S. K., Smith, K. M., Ritzel, R. G., Mowles, D. A., Carpenter, P., Chen, X., Karpinski, E., Hyde, R. J., Baldwin, S. A., Cass, C. E., and Young, J. D. (2001) *J Biol Chem* **276**, 2914-2927

13. Wang, J., and Giacomini, K. M. (1997) *J Biol Chem* **272**, 28845-28848
14. Pajor, A. M. (1998) *Biochim Biophys Acta* **1415**, 266-269
15. Gerstin, K. M., Dresser, M. J., Wang, J., and Giacomini, K. M. (2000) *Pharm Res* **17**, 906-910
16. Che, M., Ortiz, D. F., and Arias, I. M. (1995) *J Biol Chem* **270**, 13596-13599
17. Hamilton, S. R., Yao, S. Y., Ingram, J. C., Hadden, D. A., Ritzel, M. W., Gallagher, M. P., Henderson, P. J., Cass, C. E., Young, J. D., and Baldwin, S. A. (2001) *J Biol Chem* **276**, 27981-27988.
18. Loewen, S. K., Ng, A. M., Yao, S. Y., Cass, C. E., Baldwin, S. A., and Young, J. D. (1999) *J Biol Chem* **274**, 24475-24484
19. Wang, J., and Giacomini, K. M. (1999) *Mol Pharmacol* **55**, 234-240
20. Wang, J., and Giacomini, K. M. (1999) *J Biol Chem* **274**, 2298-2302
21. Zhang, J., Visser, F., Vickers, M. F., Lang, T., Robins, M. J., Nielsen, L. P. C., Nowak, I., Baldwin, S. A., Young, J. D., and Cass, C. E. (2003) *Mol Pharm* **64**, 1512-1520
22. Gray, J. H., Owen, R. P., and Giacomini, K. M. (2004) *Pflugers Arch* **447**, 728-734
23. Xiao, G., Wang, J., Tangen, T., and Giacomini, K. M. (2001) *Mol Pharmacol* **59**, 339-348
24. Loewen, S. K., Ng, A. M., Mohabir, N. N., Baldwin, S. A., Cass, C. E., and Young, J. D. (2003) *Yeast* **20**, 661-675
25. Loewen, S. K., Yao, S. Y., Slugoski, M. D., Mohabir, N. N., Turner, R. J., Mackey, J. R., Weiner, J. H., Gallagher, M. P., Henderson, P. J., Baldwin, S. A., Cass, C. E., and Young, J. D. (2004) *Mol Membr Biol* **21**, 1-10
26. Yao, S. Y., Ng, A. M., Loewen, S. K., Cass, C. E., Baldwin, S. A., and Young, J. D. (2002) *Am J Physiol Cell Physiol* **283**, C155-168
27. Dresser, M. J., Gerstin, K. M., Gray, A. T., Loo, D. D., and Giacomini, K. M. (2000) *Drug Metab Dispos* **28**, 1135-1140
28. Smith, K. M., Ng, A. M., Yao, S. Y., Labedz, K. A., Knaus, E. E., Wiebe, L. I., Cass, C. E., Baldwin, S. A., Chen, X. Z., Karpinski, E., and Young, J. D. (2004) *J Physiol* **558**, 807-823

29. Larrayoz, I. M., Casado, F. J., Pastor-Anglada, M., and Lostao, M. P. (2004) *J Biol Chem* **279**, 8999-9007

30. Lostao, M. P., Mata, J. F., Larrayoz, I. M., Inzillo, S. M., Casado, F. J., and Pastor-Anglada, M. (2000) *FEBS Lett* **481**, 137-140

31. Duflot, S., Calvo, M., Casado, F. J., Enrich, C., and Pastor-Anglada, M. (2002) *Exp Cell Res* **281**, 77-85

32. Young, J. D., Cheeseman, C. I., Mackey, J. R., Cass, C. E., and Baldwin, S. A. (2001) *Current Topics in Membranes* **50**, 329-377

33. Wang, J., Su, S. F., Dresser, M. J., Schaner, M. E., Washington, C. B., and Giacomini, K. M. (1997) *Am J Physiol* **273**, F1058-1065

34. Lai, Y., Bakken, A. H., and Unadkat, J. D. (2002) *J Biol Chem* **277**, 37711-37717

35. Mangravite, L. M., Lipshutz, J. H., Mostov, K .E., Giacomini, K. M. (2001) *Am J Phisiol Renal Physiol* **280**, F879-885

36. Mangravite, L. M., Badagnani, I., and Giacomini, K. M. (2003) *Eur J Pharmacol* **479**, 269-281

37. Lu, H., Chen, C., and Klaassen, C. D. (2004) *Drug Metab Dispos*

38. Griffiths, M., Beaumont, N., Yao, S. Y., Sundaram, M., Boumah, C. E., Davies, A., Kwong, F. Y., Coe, I., Cass, C. E., Young, J. D., and Baldwin, S. A. (1997) *Nat Med* **3**, 89-93

39. Griffiths, M., Yao, S. Y., Abidi, F., Phillips, S. E., Cass, C. E., Young, J. D., and Baldwin, S. A. (1997) *Biochem J* **328**, 739-743

40. Crawford, C. R., Patel, D. H., Naeve, C., and Belt, J. A. (1998) *J Biol Chem* **273**, 5288-5293

41. Acimovic, Y., and Coe, I. R. (2002) *Mol Biol Evol* **19**, 2199-2210

42. Hyde, R. J., Cass, C. E., Young, J. D., Baldwin, S. A. (2001) *Mol Memb Biol* **18**, 53-63

43. Lieb, W. R., and Stein, W. D. (1972) *Biochim Biophys Acta* **265**, 187-207

44. Stein, A., Vaseduvan, G., Carter, N. S., Ullman, B., Landfear, S. M., and Kavanaugh, M. P. (2003) *J Biol Chem* **278**, 35127-35134

45. Osses, N., Pearson, J. D., Yudilevich, D. L., and Jarvis, S. M. (1996) *Biochem J* **317**, 843-848.

46. Yao, S. Y., Ng, A. M., Vickers, M. F., Sundaram, M., Cass, C. E., Baldwin, S. A., and Young, J. D. (2002) *J Biol Chem* **277**, 24938-24948

47. Baldwin, S. A., Beal, P. R., Yao, S. Y., King, A. E., Cass, C. E., and Young, J. D. (2004) *Pflugers Arch* **447**, 735-743

48. Sanchez, M. A., Tryon, R., Pierce, S., Vasudevan, G., and Landfear, S. M. (2004) *Mol Membr Biol* **21**, 11-18

49. Sundaram, M., Yao, S. Y., Ingram, J. C., Berry, Z. A., Abidi, F., Cass, C. E., Baldwin, S. A., and Young, J. D. (2001) *J Biol Chem* **2**, 2

50. Yao, S. M., Sundaram, M., Chomey, E. G., Cass, C. E., Baldwin, S. A., Young, J. D. (2001) *Biochem J* **353**, 387-393

51. SenGupta, D. J., and Unadkat, J. D. (2004) *Biochem Pharmacol* **67**, 453-458

52. Vasudevan, G., Ullman, B., and Landfear, S. M. (2001) *Proc Natl Acad Sci U S A* **98**, 6092-6097

53. Valdes, R., Vasudevan, G., Conklin, D., and Landfear, S. M. (2004) *Biochemistry* **43**, 6793-6802

54. Vasudevan, G., Carter, N. S., Drew, M. E., Beverley, S. M., Sanchez, M. A., Seyfang, A., Ullman, B., and Landfear, S. M. (1998) *Proc Natl Acad Sci U S A* **95**, 9873-9878

55. Arastu-Kapur, S., Ford, E., Ullman, B., and Carter, N. S. (2003) *J Biol Chem* **278**, 33327-33333

56. Vickers, M. F., Kumar, R., Visser, F., Zhang, J., Charania, J., Raborn, R. T., Baldwin, S. A., Young, J. D., and Cass, C. E. (2002) *Biochem Cell Biol* **80**, 639-644

57. Vickers, M. F., Zhang, J., Visser, F., Tackaberry, T., Robins, M. J., Nielsen, L. P., Nowak, I., Baldwin, S. A., Young, J. D., and Cass, C. E. (2004) *Nucleosides Nucleotides Nucleic Acids* **23**, 361-373

58. Yao, S. Y., Cass, C. E., and Young, J. D. (1996) *Mol Pharmacol* **50**, 388-393

59. Ward, J. L., Sherali, A., Mo, Z. P., and Tse, C. M. (2000) *J Biol Chem* **275**, 8375-8381

60. Mangravite, L. M., Xiao, G., and Giacomini, K. M. (2003) *Am J Physiol Renal Physiol* **284**, F902-910

61. Widdas, W. F. (1952) *J Physiol* **118**, 23-39
62. Locher, K. P., Bass, R. B., and Rees, D. C. (2003) *Science* **301**, 603-604
63. Agbanyo, F. R., Cass, C. E., and Paterson, A. R. (1988) *Mol Pharmacol* **33**, 332-337
64. Mackey, J. R., Baldwin, S. A., Young, J. D., and Cass, C. E. (1998) *Drug Resistance Updates* **1**, 310-324
65. Damaraju, V. L., Damaraju, S., Young, J. D., Baldwin, S. A., Mackey, J., Sawyer, M. B., and Cass, C. E. (2003) *Oncogene* **22**, 7524-7536
66. Cheson, B. D. (1997) in *Cancer: Principles and Practice of Oncology* (Devita, V. T., ed) Vol. 1, 5 Ed., pp. 490-498, Lippincott-Raven, Philadelphia
67. Gourdeau, H., Clarke, M. L., Ouellet, F., Mowles, D., Selner, M., Richard, A., Lee, N., Mackey, J. R., Young, J. D., Jolivet, J., Lafreniere, R. G., and Cass, C. E. (2001) *Cancer Res* **61**, 7217-7224.
68. Mackey, J. R., Mani, R. S., Selner, M., Mowles, D., Young, J. D., Belt, J. A., Crawford, C. R., and Cass, C. E. (1998) *Cancer Res* **58**, 4349-4357
69. Arner, E. S., and Eriksson, S. (1995) *Pharmacol Ther* **67**, 155-186
70. King, K. M., Damaraju, V. L., Vickers, M. F., Yao, S. Y., Lang, T., Tackaberry, T. E., Mowles, D. A., Ng, A. M., Young, J. D., and Cass, C. E. (2004) *Cancer Research* **Submitted**
71. Damaraju, V. L., Visser, F., Zhang, J., Mowles, D., Ng, A. M., Young, J. D., Hiremagalur, N., and Cass, C. E. (2004) *Mol Pharm* **Submitted**
72. Ritzel, M. W., Ng, A. M., Yao, S. Y., Graham, K., Loewen, S. K., Smith, K. M., Hyde, R. J., Karpinski, E., Cass, C. E., Baldwin, S. A., and Young, J. D. (2001) *Mol Membr Biol* **18**, 65-72.
73. Mackey, J. R., Yao, S. Y., Smith, K. M., Karpinski, E., Baldwin, S. A., Cass, C. E., and Young, J. D. (1999) *J Natl Cancer Inst* **91**, 1876-1881
74. Lang, T. T., Selner, M., Young, J. D., and Cass, C. E. (2001) *Mol Pharmacol* **60**, 1143-1152
75. Lang, T. T., Young, J. D., and Cass, C. E. (2004) *Mol Pharmacol* **65**, 925-933
76. Yao, S. Y., Ng, A. M., Sundaram, M., Cass, C. E., Baldwin, S. A., and Young, J. D. (2001) *Mol Membr Biol* **18**, 161-167.

77. Cohen, A., Ullman, B., and Martin, D. W., Jr. (1979) *J Biol Chem* **254**, 112-116

78. Cass, C. E., Kolassa, N., Uehara, Y., Dahlig-Harley, E., Harley, E. R., and Paterson, A. R. (1981) *Biochim Biophys Acta* **649**, 769-777

79. Reiman, T., Clarke, M. L., Dabbagh, L., Vsianska, M., Coupland, R. W., Belch, A. R., Baldwin, S. A., Young, J. D., Cass, C. E., and Mackey, J. R. (2002) *Leuk Lymphoma* **43**, 1435-1440

80. Mackey, J. R., Jennings, L. L., Clarke, M. L., Santos, C. L., Dabbagh, L., Vsianska, M., Koski, S. L., Coupland, R. W., Baldwin, S. A., Young, J. D., and Cass, C. E. (2002) *Clin Cancer Res* **8**, 110-116

81. Dabbagh, L., Coupland, R. W., Cass, C. E., and Mackey, J. R. (2003) *Clin Cancer Res* **9**, 3213-3214

82. Spratlin, J., Sangha, R., Glubrecht, D., Dabbagh, L., Young, J. D., Dumontet, C., Cass, C. E., Lai, R., and Mackey, J. R. (2004) *Clin Cancer Res* **In press**

83. Gray, J. H., Mangravite, L. M., Owen, R. P., Urban, T. J., Chan, W., Carlson, E. J., Huang, C. C., Kawamoto, M., Johns, S. J., Stryke, D., Ferrin, T. E., and Giacomini, K. M. (2004) *Mol Pharmacol* **65**, 512-519

84. Osato, D. H., Huang, C. C., Kawamoto, M., Johns, S. J., Stryke, D., Wang, J., Ferrin, T. E., Herskowitz, I., and Giacomini, K. M. (2003) *Pharmacogenetics* **13**, 297-301

85. Leabman, M. K., Huang, C. C., DeYoung, J., Carlson, E. J., Taylor, T. R., de la Cruz, M., Johns, S. J., Stryke, D., Kawamoto, M., Urban, T. J., Kroetz, D. L., Ferrin, T. E., Clark, A. G., Risch, N., Herskowitz, I., and Giacomini, K. M. (2003) *Proc Natl Acad Sci U S A* **100**, 5896-5901

86. Damaraju, S., Zhang, J., Visser, F., Tackaberry, T., Dufour, J., Baldwin, S. A., Young, J. D., and Cass, C. E. (2004) *Pharmacogenetics* **Submitted**

87. Van Belle, H. (1993) *Cardiovasc Res* **27**, 68-76

88. Headrick, J. P., Hack, B., and Ashton, K. J. (2003) *Am J Physiol Heart Circ Physiol* **285**, H1797-1818

89. Libert, F., Parmentier, M., Lefort, A., Dinsart, C., Van Sande, J., Maenhaut, C., Simons, M. J., Dumont, J. E., and Vassart, G. (1989) *Science* **244**, 569-572

90. Libert, F., Schiffmann, S. N., Lefort, A., Parmentier, M., Gerard, C., Dumont, J. E., Vanderhaeghen, J. J., and Vassart, G. (1991) *Embo J* **10**, 1677-1682

91. Maenhaut, C., Van Sande, J., Libert, F., Abramowicz, M., Parmentier, M., Vanderhaegen, J. J., Dumont, J. E., Vassart, G., and Schiffmann, S. (1990) *Biochem Biophys Res Commun* **173**, 1169-1178

92. Stehle, J. H., Rivkees, S. A., Lee, J. J., Weaver, D. R., Deeds, J. D., and Reppert, S. M. (1992) *Mol Endocrinol* **6**, 384-393

93. Meyerhof, W., Muller-Brechlin, R., and Richter, D. (1991) *FEBS Lett* **284**, 155-160

94. Zhou, Q. Y., Li, C., Olah, M. E., Johnson, R. A., Stiles, G. L., and Civelli, O. (1992) *Proc Natl Acad Sci U S A* **89**, 7432-7436

95. Lasley, R. D., and Mentzer, R. M., Jr. (1995) *Ann Thorac Surg* **60**, 843-846

96. Klinger, M., Freissmuth, M., and Nanoff, C. (2002) *Cell Signal* **14**, 99-108

97. Rudolphi, K. A., Schubert, P., Parkinson, F. E., and Fredholm, B. B. (1992) *Trends Pharmacol Sci* **13**, 439-445

98. Rudolphi, K. A., Schubert, P., Parkinson, F. E., and Fredholm, B. B. (1992) *Cerebrovasc Brain Metab Rev* **4**, 346-369

99. Chaudary, N., Shuralyova, I., Liron, T., Sweeney, G., and Coe, I. R. (2002) *Biochem Cell Biol* **80**, 655-665

100. Dhalla, A. K., Dodam, J. R., Jones, A. W., and Rubin, L. J. (2001) *J Mol Cell Cardiol* **33**, 1143-1152

101. Parkinson, F. E., and Clanachan, A. S. (1991) *Br J Pharmacol* **104**, 399-405

102. Jennings, L. L., Cass, C. E., Ritzel, M. W. L., Yao, S. Y. M., Young, J. D., Griffiths, M., Baldwin, S. A. (1998) *Drug Dev Res* **45**, 277-287

103. Anderson, C. M., Xiong, W., Geiger, J. D., Young, J. D., Cass, C. E., Baldwin, S. A., and Parkinson, F. E. (1999) *J Neurochem* **73**, 867-873

104. Anderson, C. M., Baldwin, S. A., Young, J. D., Cass, C. E., and Parkinson, F. E. (1999) *Brain Res Mol Brain Res* **70**, 293-297

105. Alanko, L., Stenberg, D., and Porkka-Heiskanen, T. (2003) *J Sleep Res* **12**, 299-304

106. Chaudary, N., Naydenova, Z., Shuralyova, I., and Coe, I. R. (2004) *Cardiovasc Res* **61**, 780-788

107. Jennings, L. L., Hao, C., Cabrita, M. A., Vickers, M. F., Baldwin, S. A., Young, J. D., and Cass, C. E. (2001) *Neuropharmacology* **40**, 722-731.

108. Chaudary, N., Naydenova, Z., Shuralyova, I., and Coe, I. R. (2004) *J Pharmacol Exp Ther* **310**, 1190-1198

109. Pickard, M. A., Brown, R. R., Paul, B., and Paterson, A. R. (1973) *Can J Biochem* **51**, 666-672

110. Paterson, A. R., Kolassa, N., and Cass, C. E. (1981) *Pharmacol Ther* **12**, 515-536

111. Young, J. D., and Jarvis, S. M. (1983) *Biosci Rep* **3**, 309-322

112. Plagemann, P. G. W., Wohlhueter, R. M., Woffendin, C. (1988) *Biochim Biophys Acta* **947**, 405-443

113. Jarvis, S. M., Hammond, J. R., Paterson, A. R., and Clanachan, A. S. (1982) *Biochem J* **208**, 83-88

114. Cass, C. E., Gaudette, L. A., and Paterson, A. R. (1974) *Biochim Biophys Acta* **345**, 1-10

115. Paul, B., Chen, M. F., and Paterson, A. R. (1975) *J Med Chem* **18**, 968-973

116. Cass, C. E., Dahlig, E., Lau, E. Y., Lynch, T. P., and Paterson, A. R. (1979) *Cancer Res* **39**, 1245-1252

117. Wiley, J. S., Brocklebank, A. M., Snook, M. B., Jamieson, G. P., Sawyer, W. H., Craik, J. D., Cass, C. E., Robins, M. J., McAdam, D. P., and Paterson, A. R. (1991) *Biochem J* **273**, 667-672

118. Li, N., Cook, L., Santos, C., Cass, C. E., Mackey, J. R., and Dovichi, N. J. (2002) *Anal Chem* **74**, 2573-2577

119. Gati, W. P., Paterson, A. R., Larratt, L. M., Turner, A. R., and Belch, A. R. (1997) *Blood* **90**, 346-353

120. Jarvis, S. M., McBride, D., and Young, J. D. (1982) *J Physiol (Lond)* **324**, 31-46

121. Cass, C. E., Gati, W. P., Odegard, R., and Paterson, A. R. (1985) *Mol Pharmacol* **27**, 662-665

122. Koren, R., Cass, C. E., and Paterson, A. R. (1983) *Biochem J* **216**, 299-308.

123. Jarvis, S. M., Janmohamed, S. N., and Young, J. D. (1983) *Biochem J* **216**, 661-667

124. Wohlhueter, R. M., Marz, R., and Plagemann, P. G. (1978) *J Membr Biol* **42**, 247-264

125. Hammond, J. R. (1991) *Mol Pharmacol* **39**, 771-779

126. Yao, S. Y., Ng, A. M., Muzyka, W. R., Griffiths, M., Cass, C. E., Baldwin, S. A., and Young, J. D. (1997) *J Biol Chem* **272**, 28423-28430

127. Kiss, A., Farah, K., Kim, J., Garriock, R. J., Drysdale, T. A., Hammond, J. R. (2000) *Biochem J* **352**, 363-372

128. Young, J. D., Jarvis, S. M., Robins, M. J., and Paterson, A. R. (1983) *J Biol Chem* **258**, 2202-2208

129. Fleming, S. A., Rawlins, D. B., and Robins, M. J. (1990) *Tetrahedron Lett* **31**, 4995-4998

130. Wu, J. S., Kwong, F. Y., Jarvis, S. M., and Young, J. D. (1983) *J Biol Chem* **258**, 13745-13751

131. Gati, W. P., Belt, J. A., Jakobs, E. S., Young, J. D., Jarvis, S. M., and Paterson, A. R. (1986) *Biochem J* **236**, 665-670

132. Almeida, A. F., Jarvis, S. M., Young, J. D., and Paterson, A. R. (1984) *FEBS Lett* **176**, 444-448

133. Young, J. D., Jarvis, S. M., Belt, J. A., Gati, W. P., and Paterson, A. R. (1984) *J Biol Chem* **259**, 8363-8365

134. Wu, J. S., and Young, J. D. (1984) *Biochem J* **220**, 499-506

135. Shi, M. M., Wu, J. S., Lee, C. M., and Young, J. D. (1984) *Biochem Biophys Res Commun* **118**, 594-600

136. Jarvis, S. M., and Young, J. D. (1987) *Pharmacol Ther* **32**, 339-359

137. Kwong, F. Y., Wu, J. S., Shi, M. M., Fincham, H. E., Davies, A., Henderson, P. J., Baldwin, S. A., and Young, J. D. (1993) *J Biol Chem* **268**, 22127-22134

138. Tse, C. M., Belt, J. A., Jarvis, S. M., Paterson, A. R., Wu, J. S., and Young, J. D. (1985) *J Biol Chem* **260**, 3506-3511

139. Crawford, C. R., Ng, C. Y., Ullman, B., and Belt, J. A. (1990) *Biochim Biophys Acta* **1024**, 289-297

140. Hammond, J. R. (1991) *Adv Exp Med Biol*, 423-426

141. Hammond, J. R., and Zarenda, M. (1996) *Arch Biochem Biophys* **332**, 313-322

142. Hammond, J. R. (1994) *J Pharmacol Exp Ther* **271**, 906-917

143. Hammond, J. R. (1997) *Biochem Pharmacol* **53**, 623-629.

144. Baldwin, S. A., Baldwin, J. M., and Lienhard, G. E. (1982) *Biochemistry* **21**, 3836-3842

145. Kwong, F. Y., Baldwin, S. A., Scudder, P. R., Jarvis, S. M., Choy, M. Y., and Young, J. D. (1986) *Biochem J* **240**, 349-356

146. Mueckler, M., Caruso, C., Baldwin, S. A., Panico, M., Blench, I., Morris, H. R., Allard, W. J., Lienhard, G. E., and Lodish, H. F. (1985) *Science* **229**, 941-945

147. Good, A. H., Craik, J. D., Jarvis, S. M., Kwong, F. Y., Young, J. D., Paterson, A. R., and Cass, C. E. (1987) *Biochem J* **244**, 749-755

148. Kwong, F. Y., Tse, C. M., Jarvis, S. M., Choy, M. Y., and Young, J. D. (1987) *Biochim Biophys Acta* **904**, 105-116

149. Kwong, F. Y., Davies, A., Tse, C. M., Young, J. D., Henderson, P. J., and Baldwin, S. A. (1988) *Biochem J* **255**, 243-249

150. Vickers, M. F., Mani, R. S., Sundaram, M., Hogue, D. L., Young, J. D., Baldwin, S. A., and Cass, C. E. (1999) *Biochem J* **339**, 21-32

151. Sundaram, M., Yao, S. Y. M., Ng, A. M. L., Cass, C. E., Baldwin, S. A., Young, J.D. (2001) *Biochemistry* **40**, 8146-8151

152. Endres, C. J., SenGupta, D. J., and Unadkat, J. D. (2004) *Biochem J* **Pt**

153. FitzGerald, G. A. (1987) *N Engl J Med* **316**, 1247-1257

154. Hammond, J. R. (1991) *J Pharmacol Exp Ther* **259**, 799-807.

155. Curtin, N. J., Bowman, K. J., Turner, R. N., Huang, B., Loughlin, P. J., Calvert, A. H., Golding, B. T., Griffin, R. J., and Newell, D. R. (1999) *Br J Cancer* **80**, 1738-1746

156. Smith, P. G., Thomas, H. D., Barlow, H. C., Griffin, R. J., Golding, B. T., Calvert, A. H., Newell, D. R., and Curtin, N. J. (2001) *Clin Cancer Res* **7**, 2105-2113

157. Paterson, A. R., Lau, E. Y., Dahlig, E., and Cass, C. E. (1980) *Mol Pharmacol* **18**, 40-44

158. Jarvis, S. M. (1986) *Mol Pharmacol* **30**, 659-665

159. Shi, M., Young, J. D. (1986) *Biochem J* **240**, 879-883

160. Deckert, J., Hennemann, A., Bereznai, B., Fritze, J., Vock, R., Marangos, P. J., and Riederer, P. (1994) *Life Sci* **55**, 1675-1682

161. Woffendin, C., and Plagemann, P. G. (1987) *J Membr Biol* **98**, 89-100

162. Jones, K. W., and Hammond, J. R. (1992) *J Neurochem* **59**, 1363-1371

163. Plagemann, P. G. W., Woffendin, C. (1988) *Biochim Biophys Acta* **969**, 1-8

164. Sundaram, M., Yao, S. Y. M., Ng, A. M. L., Griffiths, M., Cass, C. E., Baldwin, S. A., and Young, J. D. (1998) *J Biol Chem* **273**, 21519-21525

165. Visser, F., Vickers, M. F., Ng, A. M., Baldwin, S. A., Young, J. D., and Cass, C. E. (2002) *J Biol Chem* **277**, 395-401.

166. Appleford, P. J., Griffiths, M., Yao, S. Y., Ng, A. M., Chomey, E. G., Isaac, R. E., Coates, D., Hope, I. A., Cass, C. E., Young, J. D., and Baldwin, S. A. (2004) *Mol Membr Biol* **21**, 247-260

167. Li, G., Liu, K., Baldwin, S. A., and Wang, D. (2003) *J Biol Chem* **278**, 35732-35742

168. Chiang, C. W., Carter, N., Sullivan, W. J., Jr., Donald, R. G., Roos, D. S., Naguib, F. N., el Kouni, M. H., Ullman, B., and Wilson, C. M. (1999) *J Biol Chem* **274**, 35255-35261

169. Vickers, M. F., Yao, S. Y., Baldwin, S. A., Young, J. D., and Cass, C. E. (2000) *J Biol Chem* **275**, 25931-25938

170. Parker, M. D., Hyde, R. J., Yao, S. Y., McRobert, L., Cass, C. E., Young, J. D., McConkey, G. A., and Baldwin, S. A. (2000) *Biochem J* **349**, 67-75

171. Carter, N. S., Ben Mamoun, C., Liu, W., Silva, E. O., Landfear, S. M., Goldberg, D. E., and Ullman, B. (2000) *J Biol Chem* **275**, 10683-10691

172. Sano, N., Katsuki, S., and Kawada, M. (1972) *Arzneimittelforschung* **22**, 1655-1658

173. IJzerman, A. P., and Voorschuur, A. H. (1990) *Naunyn Schmiedebergs Arch Pharmacol* **342**, 336-341

174. Gati, W. P., Paterson, A. R. P. (1989) *Mol Pharm* **36**, 134-141

175. Pirovano, I. M., Van Belle, H., and Ijzerman, A. P. (1990) *Eur J Pharmacol* **189**, 419-422

176. Beukers, M. W., Kerkhof, C. J., AP, I. J., and Soudijn, W. (1994) *Eur J Pharmacol* **266**, 57-62

177. Ijzerman, A. P., Thedinga, K. H., Custers, A. F., Hoos, B., and Van Belle, H. (1989) *Eur J Pharmacol* **172**, 273-281

178. Hammond, J. R. (2000) *Nauyn Schmiedebergs Arch Pharmacol* **361**, 373-382

179. Griffith, D. A., Conant, A. R., and Jarvis, S. M. (1990) *Biochem Pharmacol* **40**, 2297-2303

180. Jones, K. W., and Hammond, J. R. (1993) *Eur J Pharmacol* **246**, 97-104

181. IJzerman, A. P., Kruidering, M., van Weert, A., van Belle, H., and Janssen, C. (1992) *Naunyn Schmiedebergs Arch Pharmacol* **345**, 558-563

182. Parkinson, F. E., Paterson, A. R., Young, J. D., and Cass, C. E. (1993) *Biochem Pharmacol* **46**, 891-896

183. Jarvis, S. M., and Ng, A. S. (1985) *J Neurochem* **44**, 183-188

184. Marangos, P. J., Patel, J., Clark-Rosenberg, R., and Martino, A. M. (1982) *J Neurochem* **39**, 184-191

185. Plagemann, P. G., and Wohlhueter, R. M. (1984) *Biochem Pharmacol* **33**, 1783-1788

186. Geiger, J. D., LaBella, F. S., and Nagy, J. I. (1985) *J Neurosci* **5**, 735-740

187. Kwan, K. F., and Jarvis, S. M. (1984) *Am J Physiol* **246**, H710-715

188. Parkinson, F. E., and Fredholm, B. B. (1991) *Eur J Pharmacol* **202**, 361-366

189. Balwierczak, J. L., Krulan, C. M., Wang, Z. C., Chen, J., and Jeng, A. Y. (1989) *J Pharmacol Exp Ther* **251**, 279-287

190. Plagemann, P. G., and Woffendin, C. (1987) *Biochim Biophys Acta* **928**, 243-250

191. Striessnig, J., Zernig, G., and Glossmann, H. (1985) *Eur J Biochem* **150**, 67-77

192. Deckert, J., Bereznai, B., Hennemann, A., Gsell, W., Gotz, M., Fritze, J., and Riederer, P. (1993) *Eur J Pharmacol* **238**, 131-133

193. Huang, M., Wang, Y., Collins, M., Gu, J. J., Mitchell, B. S., and Graves, L. M. (2002) *J Biol Chem* **277**, 28364-28367

194. Huang, M., Wang, Y., Cogut, S. B., Mitchell, B. S., and Graves, L. M. (2003) *J Pharmacol Exp Ther* **304**, 753-760

195. Baldwin, S. A., Mackey, J. R., Cass, C. E., and Young, J. D. (1999) *Mol Med Today* **5**, 216-224

Chapter 2: Experimental Procedures

Yeast culture

Strains and media (Chapters 3-6)

KY114 (MATα, gal, ura3-52, trp1, lys2, ade2, hisd2000) was the parental yeast strain used to generate KTK, which produces recombinant *Herpes simplex* thymidine kinase (1), and fui1::TRP1, which contains a disruption in the gene encoding the endogenous uridine permease (FUI1) (2). Other strains were generated by transformation of the yeast/*E. coli* shuttle vector pYPGE15 (3) into KTK and fui1::TRP1 using a standard lithium acetate method (4). cDNA inserts were under the transcriptional control of the constitutive PGK promoter. Yeast strains were maintained in complete minimal medium (CMM) containing 0.67% yeast nitrogen base (Difco, Detroit, MI), amino acids (as required to maintain auxotrophic selection) and 2% glucose (CMM/GLU). Agar plates contained CMM with various supplements and 2% agar (Difco, Detroit, MI).

Molecular biology

Plasmid construction (Chapters 3-6)

For *S. cerevisiae* expression, the complete hENT1, hENT2, CeENT1 and rENT1 open reading frames were amplified by polymerase chain reaction (PCR) methodology from a pBlue-script II KS contruct containing the cDNA clones of each transporter, (obtained from the laboratory of Dr. James Young) using the primers in Table 2-1 and inserted into pYPGE15 to generate pYPhENT1, pYPhENT2, pYPCeENT1 and pYPrENT1. Plasmids were propagated in *E. coli* strain TOP10F' (Invitrogen, Carlsbad, CA) and maintained in Luria broth with ampicillin (100 μg/ml) (Sigma, Mississauga, Ontario).

For *X. laevis* oocytes expression, the hENT1-M33I cDNA was cloned into pBlue-script II KS (+) (Stratagene) to generate pKS (+)-hENT1-M33I as previously described for the generation of pKS (+)-hENT1 (5,6).

Table 2-1. Nucleotide sequences of the primers used to amplify hENT1, hENT2, CeENT1 and rENT1.

Primer name	Location	Nucleotide sequence (restriction site underlined)
5'-XbaIes	5' end of hENT1 cDNA	5'-CCC TCT AGA ATG ACA ACC AGT CAC CAG CCT C-3'
3'-KpnIes	3' end of hENT1 cDNA	5'-CCC GGT ACC TCA CAC AAT TGC CCG GAA CAG G-3'
5'-XbaIei	5' end of hENT2 cDNA	5'-CCC TCT AGA ATG GCC CGA GGA GAC GCC-3'
3'-KpnIei	3' end of hENT2 cDNA	5'-CCC GGT ACC TCA GAG CAG CGC CTT GAA G-3'
5'-CeXbaI	5' end of CeENT1 cDNA	5'-CCC TCT AGA ATG TCG TCG GCA GTG GAG-3'
3'-CeXbaI	3' end of CeENT1 cDNA	5'-CCC GGT ACC TTA GGC CGT GAC GAC CAT C-3'
XbaIrENT1	5' end of rENT1 cDNA	5'-CCC TCT AGA ATG ACA ACC AGT CAC CAG-3'
KpnIrENT1	3' end of rENT1 cDNA	5'-CCC GGT ACC TCA CAC AAG TGC CCT TAA-3'

Site-directed mutagenesis (Chapters 3-6)

All point mutations were generated using either megaprimer PCR methodology (Chapters 3, 4) (7) with Pwo polymerase (Roche, Laval, Quebec, Canada) or the QuikChange XL site-directed mutagenesis kit (Stratagene, La Jolla, CA) (Chapters 5, 6). All plasmid constructs were verified by DNA sequencing using an ABI PRISM 310 sequence detection system (Applied Biosystems, Foster City, CA).

Random mutagenesis and screening

Hydroxylamine random mutagenesis of pYPhENT1 (Chapter 3)

Double stranded plasmid DNA (10 μg) was precipitated with ethanol/sodium acetate and resuspended in 500 μl of freshly prepared hydroxylamine (Sigma, Mississauga, Ontario, Canada) solution (90 mg NaOH, 350 mg hydroxylamine-HCl, pH~6.5 in 5 ml H_2O). The DNA was incubated for 16 h at 37°C and the reactions were terminated by the addition of 15 μl 4 M NaCl, 50 μl of 1 mg/ml BSA followed by precipitation of the DNA with 1 ml 95% ethanol. The DNA was resuspended in 100 μl TE (10 mM Tris, 1 mM EDTA pH 8.0) and precipitated again with 15 μl 4.0 M NaCl/250 μl 95% ethanol. The DNA resuspension-precipitation procedure was repeated 3 times in total with a final resuspension in 20 μl TE.

XL-1 RED E. coli-mediated random mutagenesis of pYPhENT1 and pYPCeENT1 (Chapters 5 and 6)

Random mutagenesis of pYPCeENT1 and pYPhENT1 was performed by propagating the plasmid in the XL-1 RED mutator strain of *E. coli* (Stratagene) for 45 generations to obtain 1 mutation per cDNA, according to the procedure of Greener *et al.* (8).

Phenotypic complementation and screening of mutants (Chapters 3, 5 and 6)

The complementation assay was based on the ability of recombinant hENT1 produced in yeast to salvage exogenously supplied thymidine under conditions of dTMP

starvation (9). In brief, KTK cells transformed with pYPhENT1 or pYPCeENT1 using a lithium acetate procedure (4) were plated directly onto CMM/GLU plates containing methotrexate (MTX) at 50 μg/ml and sulfanilamide (SAA) at 6 mg/ml (CMM/GLU/MTX/SAA). Colonies formed with an efficiency of ~10^5 transformants/μg DNA after incubation at 30°C for 3.5 days in the presence of 10 μM thymidine, and complementation was prevented when 10 μM dilazep, 100 μM dipyridamole, 1 μM draflazine or 10 μM soluflazine was also present. Draflazine and soluflazine were kind gifts from Janssen Pharamceuticals (Beers, Belgium), there were insufficient quantities of soluflazine for screening. Randomly mutated pYPhENT1 or pYPCeENT1 (20 μg) was transformed into KTK cells, which were then plated onto CMM/GLU/MTX/SAA with 10 μM thymidine and 10 μM dilazep, 100 μM dipyridamole or 1 μM draflazine and incubated at 30°C for 3.5 days. Colonies with apparent resistance to inhibitors were isolated, grown in 5 ml liquid CMM/GLU for 2 days, and restreaked onto CMM/GLU/MTX/SAA plates with 10 μM thymidine and 10 μM dilazep, 100 μM dipyridamole or 1 μM draflazine. The mutant hENT1 or CeENT1 cDNAs were amplified from the yeast colonies by PCR, subcloned back into nonmutated pYPGE15 and subjected to DNA sequencing.

Nucleoside transport assays

Oil-stop uridine transport assays in S. cerevisiae (Chapter 3)

The plasmids pYPhENT1, pYPhENT1-M33I, pYPhENT2 and pYPhENT2-I33M were transformed into fui1::TRP1 yeast, a strain that lacks the endogenous uridine permease FUI1 (2). The transport of ^{3}H-uridine (Moravek Biochemicals, Brea, CA) by logarithmically proliferating yeast was measured as described previously using the "oil stop" method (10,11) with the following modifications. Yeast were grown in CMM/GLU to an A_{600} of 0.7-1.5, washed once with fresh medium and resuspended to an A_{600} of 2.0 in fresh medium. All transport assays were performed at room temperature and pH 7.0. One-ml portions of yeast culture were distributed into 15 ml plastic centrifuge tubes to which 5 to 10-µl portions of stock dilazep, dipyridamole, or NBMPR (Sigma, Mississauga, Ontario) solution or solvent alone (H_2O, ethanol or dimethyl sulfoxide) were added to achieve the desired final concentration. To allow for steady-state equilibration, the yeast were incubated in the presence of inhibitor for 30 min before addition of [^{3}H]-uridine (12-15). Transport reactions were initiated by the rapid addition of a small volume of ^{3}H-uridine to a final concentration of 2 µM. Transport reactions were terminated at graded time intervals by pipetting triplicate 200-µl portions of yeast suspension into 1.5-ml microcentrifuge tubes containing 200-µl transport oil; the tubes were immediately centrifuged at 12000x*g* for 2 min. The supernatants were removed by aspiration, the resulting pellets were solubilized with 5% Triton X-100 for 24 h, and the radioactive content was determined by liquid scintillation counting.

The protein content of yeast suspensions used in transport assays was determined with the Bio-Rad protein assay reagent (Bio-Rad, Hercules, CA) using bovine serum albumin solutions ranging from 0 to 10 µg/ml to generate a standard curve.

Cell harvester nucleoside transport assays in S. cerevisiae (Chapters 4, 5 and 6)

Yeast cells containing pYPhENT1, pYPhENT2 or plasmid with one of the constructs encoding the various mutant transporters were grown in CMM/GLU media to A_{600} = 0.5-1.0, washed twice in CMM/GLU and resuspended to A_{600} = 4.0. All transport assays were performed at room temperature and pH 7.4 in CMM/GLU. All unlabeled

nucleosides and nucleoside analogs, dilazep, dipyridamole and NBMPR were obtained from Sigma, St. Louis, MO. The radiolabeled compounds [5,6-^{3}H]-uridine, [5-^{3}H(N)]-cytidine, [methyl-^{3}H]-thymidine, [2,8-^{3}H]-adenosine, [2,8-^{3}H]-inosine, [8-^{3}H]-guanosine, [6-^{3}H]-5-fluorouridine, [5-^{3}H]-2',2'-difluoro-2'-deoxycytidine (gemcitabine), [5-^{3}H]-cytosine-β-D-arabinofuranoside (cytarabine), [8-^{3}H]-2-chloro-2'-deoxyadenosine (cladribine) and [8-^{3}H]-2-fluoro-2'-deoxyadenosine (fludarabine) were purchased from Moravek Biochemicals, Brea, CA. A final specific activity of 0.5 μCi/μl was used in all transport reactions. A high-throughput method developed by Zhang et. al. (16) was used as follows. Fifty-μl portions of yeast suspensions in CMM/GLU were added to 50-μl portions of CMM/GLU that contained 2X concentrated [^{3}H]-nucleoside in 96-well microtiter plates. At a given time point, the yeast cells were collected on filtermats using a Micro96 Cell Harvester (Skatron Instruments, Norway) that were rapidly washed with deionized water. The individual filter circles corresponding to individual wells of microtiter plates were removed from the filtermats using forceps and transferred to vials for liquid scintillation counting.

For determination of nucleoside concentration-effect relationships, unlabeled nucleosides and [^{3}H]-adenosine were added simultaneously to yeast suspensions. For inhibitor concentration-effect relationships, the yeast suspensions were first incubated for 15-30 min with inhibitor to allow equilibration of inhibitors their binding sites before the addition of [^{3}H]-uridine or [^{3}H]-adenosine as previously described (12-15,17). Trace uridine transport activity in fui1::TRP1 yeast due to the presence of the endogenous uracil/uridine permease, FUR4, was subtracted by determining background uptake in the presence of 10 mM thymidine, which does not interact with endogenous yeast transporters (18).

The protein content of yeast suspensions used in transport assays was determined with the Bio-Rad protein assay reagent (Bio-Rad, Hercules, CA) using bovine serum albumin solutions ranging from 0 to 10 μg/ml to generate a standard curve.

pCMBS experiments (Chapter 4)

Yeast containing pYPhENT2 or one of the various mutant plasmids were grown in CMM/GLU medium to A_{600} of 0.5-1.0, washed twice in ice-cold fresh CMM/GLU medium (pH 7.4) and resuspended to an A_{600} of 2.0. All reactions were performed on ice (19-21). The yeast cell suspensions were distributed into microcentrifuge tubes into which pCMBS (Toronto Research Chemicals, Toronto, ON) was added alone or together with either uridine, adenosine, dilazep, dipyridamole or NBMPR. Following 30-min incubation periods, the cells were centrifuged and washed 3X with ice-cold CMM/GLU to remove unreacted pCMBS, nucleosides and inhibitors. The cells were resuspended to an A_{600} of 4.0 and distributed in 96-well microtiter plates for nucleoside transport assays, which were conducted as described above.

Functional expression of hENT1 and hENT1-M33I in X. laevis oocytes (Chapter 3)

In vitro synthesized transcripts were prepared from pKS(+)-hENT1 and pKS(+)-hENT1-M33I (SP6 MEGAscript Kit Ambion, Austin, TX) in water and injected into isolated mature stage VI oocytes from *X. laevis* as described previously (22). Mock-injected oocytes were injected with water alone. Transport assays were performed as described previously (5,6) on groups of 10 oocytes at 20°C using ^{14}C-uridine (Amersham Pharmacia Biotech) (1 μCi/ml) in 200 μl of transport buffer containing 100 mM NaCl, 2 mM KCl, 1 mM $CaCl_2$, 1 mM $MgCl_2$, and 10 mM HEPES, pH 7.5. Initial rates of uridine uptake (10 μM) were determined using incubation periods of 5 min. These experiments were conducted by Ms. Amy Ng of Dr. Young's research group.

Data analysis

All the data resulting from transport experiments were analyzed using GraphPad Prism version 3.0 or 4.0 software. For time courses, rates were determined by linear regression analysis. For concentration-effect relationships, the IC_{50} values were determined by nonlinear regression analysis. In experiments where the data were normalized, the uptake observed in the absence of inhibitory test compound was set to 100 % whereas uptake observed in the presence of 10 mM thymidine was set to 0 %. For

concentration dependence of nucleoside transport experiments, the K_m and V_{max} values were determined by nonlinear regression analysis.

Immunofluorescence

Immunostaining (Chapter 6)

Monoclonal antibodies specific for hENT1 were previously produced by immunization of mice with a synthetic peptide corresponding to residues 254-271 in the large cytoplasmic loop of hENT1 (23), were used to identify hENT1 by immunostaining. The generation and characterization of the anti-hENT1 IgG monoclonal antibodies, which have high specificity and avidity for the hENT1, is described in detail elsewhere (23). The antibodies used in studies described in this thesis were produced by Ms. Milada Selner and Ms. Pat Carpenter.

Yeast cells producing hENT1 or one of the hENT1 mutants were subjected to immunostaining procedures according to previously established methods (24). Briefly, yeast cultures (10 ml) at A_{600}=0.7-1.5 were fixed with 37 % formaldehyde, washed in 4 ml of solution B (100 mM potassium phosphate, pH 7.5, 1.2 M sorbitol), resuspended in 2 ml of solution B containing 0.5 mg/ml zymolyase 100T (MP Biomedicals, Irvine, CA) and incubated at 30°C. Cell wall digestion was monitored for 20 to 60 min using a light microscope to achieve a high proportion of spheroblasts. Fifty-µl portions of cell suspensions were spotted onto poly L-lysine coated coverslips and fixed using cold 1:1 methanol/acetone. The coverslips were then dried and immersed in 200 µl blocking solution (2% goat serum in PBS) for 1 hr in a dark humid box to minimize evaporation. The cells were then incubated with primary antibodies for 1 h, washed 3X with 2-3 ml of PBST (phosphate-buffered saline, pH 7.2, 1 % Triton X-100) and 1X with 2-3 ml of PBS. The secondary antibodies, Alexa Fluor 488 goat-anti mouse IgG (H+L) (Molecular Probes, Burlington, Ontario, Canada), were then applied for 1 h, after which the cells were washed with PBST and PBS as described above. The coverslips were then mounted on slides using a permanent mounting media (9.4 % (w/v) mowiol 4-88, 23 % (w/v)

glycerol, 0.1 M phosphate buffer pH 7.4 and 0.1 % n-propylgallate as antifade) and dried overnight in a dark cupboard.

Microscopy and image collection (Chapter 6)

Images were recorded on a Zeiss LSM510 Confocal Laser Scanning Microscope, which was mounted on a Zeiss Axiovert 100M Microscope (Carl Zeiss Canada, Toronto, Ontario). All images were collected with a 40X objective (NA 1.3, F-Fluar) with a frame size of 1024X1024 pixels, a pixel resolution of 0.11 μm and a pixel depth of 12 bits. The fluorescent probes were excited with a 488-nm laser line and the emission signal was collected using a long-pass filter of 505 nm. For all images, the gain and offset values were held constant so that no pixels in the images were at saturation or at zero level.

Image analysis (Chapter 6)

The images were analyzed using Metamorph version 6.1 software (Univeral Imaging Corp, Downingtown, PA). Briefly, background values (average intensities of non-stained areas) were subtracted from the image values. The integrated intensities per cell were obtained by drawing circles over cells of interest. At least 50 to 100 cells were measured and the results were exported to GraphPad Prism version 4.0 software for further analysis.

Molecular modeling

Helical wheel diagrams of TMs 1,2, 8 and 11 (Chapter 6)

The residues implicated as being part of TMs 1, 2, 8 or 11 were generated using the helix wheel program on the EXPASY molecular biology server and transposed onto a high-resolution template to depict a view from the extracellular side of the membrane. An asymmetric distribution of polar and non-polar side chains was considered as characteristic of an amphipathic helix. Aromatic and aliphatic side chains were predicted to be more likely to face the hydrophobic membrane bilayer environment whereas residues with polar side chains such as Asn, Gln, Asp, Glu, Ser, Thr, Arg and Lys were predicted to be more likely to face away from the lipid bilayer and towards the permeant

translocation channel where they could participate in hydrogen bond interactions with permeants/inhibitors or other transmembrane helices. However, Ser and Thr could also form intrahelical hydrogen bonds and face the lipid bilayer. Secondly, highly conserved residues were also predicted to line the permeant translocation channel.

References

1. Hogue, D. L., Ellison, M. J., Young, J. D., and Cass, C. E. (1996) *J Biol Chem* **271**, 9801-9808
2. Vickers, M. F., Yao, S. Y., Baldwin, S. A., Young, J. D., and Cass, C. E. (2000) *J Biol Chem* **275**, 25931-25938
3. Brunelli, J. P., Pall, M.L. (1993) *Yeast* **9**, 1309-1318
4. Gietz, D., St. Jean, A., Woods, R. A., Schiestl, R. H. (1992) *Nucleic Acids Res* **20**, 1425
5. Griffiths, M., Beaumont, N., Yao, S. Y., Sundaram, M., Boumah, C. E., Davies, A., Kwong, F. Y., Coe, I., Cass, C. E., Young, J. D., and Baldwin, S. A. (1997) *Nat Med* **3**, 89-93
6. Sundaram, M., Yao, S. Y. M., Ng, A. M. L., Griffiths, M., Cass, C. E., Baldwin, S. A., and Young, J. D. (1998) *J Biol Chem* **273**, 21519-21525
7. Sarkar, G., Sommer, S. S. (1990) *Biotechniques* **8**, 404-407
8. Greener, A., Callahan, M., and Jerpseth, B. (1996) *Methods Mol Biol* **57**, 375-385
9. Vickers, M. F., Mani, R. S., Sundaram, M., Hogue, D. L., Young, J. D., Baldwin, S. A., and Cass, C. E. (1999) *Biochem J* **339**, 21-32
10. Harley, E. R., Paterson, A. R., and Cass, C. E. (1982) *Cancer Res* **42**, 1289-1295
11. Hogue, D. L., Hodgson, K. C., and Cass, C. E. (1990) *Biochem Cell Biol* **68**, 199-209
12. Morrison, J. F., and Walsh, C. T. (1988) *Adv Enzymol Relat Areas Mol Biol* **61**, 201-301
13. Gati, W. P., Paterson, A. R. P. (1989) *Mol Pharm* **36**, 134-141
14. Shi, M., Young, J. D. (1986) *Biochem J* **240**, 879-883
15. Jarvis, S. M., Janmohamed, S. N., and Young, J. D. (1983) *Biochem J* **216**, 661-667
16. Zhang, J., Visser, F., Vickers, M. F., Lang, T., Robins, M. J., Nielsen, L. P. C., Nowak, I., Baldwin, S. A., Young, J. D., and Cass, C. E. (2003) *Mol Pharm* **64**, 1512-1520

17. Visser, F., Vickers, M. F., Ng, A. M., Baldwin, S. A., Young, J. D., and Cass, C. E. (2002) *J Biol Chem* **277**, 395-401.
18. Grenson, M. (1969) *Eur J Biochem* **11**, 249-260
19. Jarvis, S. M., and Young, J. D. (1982) *J Physiol* **324**, 47-66
20. Jarvis, S. M., and Young, J. D. (1986) *J Membr Biol* **93**, 1-10
21. Tse, C. M., Wu, J. S., and Young, J. D. (1985) *Biochim Biophys Acta* **818**, 316-324
22. Huang, Q. Q., Harvey, C. M., Paterson, A. R., Cass, C. E., and Young, J. D. (1993) *J Biol Chem* **268**, 20613-20619
23. Jennings, L. L., Hao, C., Cabrita, M. A., Vickers, M. F., Baldwin, S. A., Young, J. D., and Cass, C. E. (2001) *Neuropharmacology* **40**, 722-731.
24. Pringle, J. R., Adams, A. E., Drubin, D. G., and Haarer, B. K. (1991) *Methods Enzymol* **194**, 565-602

Chapter 3: Mutation of Residue 33 of Human Equilibrative Nucleoside Transporters 1 and 2 (hENT1 and hENT2) Alters Sensitivity to Inhibition of Transport by Dilazep and Dipyridamole[1]

[1]*A version of this chapter has been published:*

F. Visser, M. F. Vickers, A. M. L. Ng, S. A. Baldwin, J. D. Young and C. E. Cass (2002) J. Biol. Chem. 277(1): 395-401

Acknowledgements

Dr. Mark Vickers contributed to this project by developing the nucleoside transport assay methodology and generating the fui1::TRP1 yeast strain. Ms. Amy Ng conducted the *X. laevis* nucleoside transport experiments displayed in Fig. 3-5. Dr. Stephen Baldwin and Dr. James Young are collaborative principle investigators who helped obtained research funding for this project and aided in manuscript preparation.

Introduction

Cellular uptake and release of nucleosides and nucleoside analog drugs is mediated by integral membrane nucleoside transporter proteins (1-4). These proteins are involved in salvage of extracellular nucleosides for nucleotide biosynthesis in mammalian cells, especially those that lack *de novo* synthesis pathways such as enterocytes and haemopoietic cells. They are critical for the cellular uptake of cytotoxic nucleoside analogs used in the treatment of human hematologic malignancies, solid tumors, and viral diseases (5,6). Nucleoside transporters also affect the cell surface concentration of adenosine, which is a signaling molecule that binds to G-protein coupled cell-surface adenosine receptors, affecting physiological processes such as coronary vasodilation, renal vasoconstriction, neuromodulation, platelet aggregation, and lipolysis (7,8).

Mammalian nucleoside transporters are classified into two structurally and functionally distinct families, the concentrative nucleoside transporters (CNTs) and the equilibrative nucleoside transporters (ENTs). CNTs mediate Na^+-dependent transport against nucleoside concentration gradients and are found primarily in specialized cells such as intestinal and renal epithelia. Three CNT isoforms, a pyrimidine-nucleoside preferring (CNT1), a purine-nucleoside and uridine preferring (CNT2) and a broadly selective (CNT3) protein, have been identified by molecular cloning from mammalian tissues (9-14). Mammalian ENTs are responsible for facilitated diffusion of nucleosides across cell membranes and have a broad tissue distribution. Two ENT isoforms have been identified by molecular cloning and functional expression from mammalian tissues and mediate nucleoside transport processes that are functionally distinguished by their differential sensitivity to inhibition by NBMPR (1-4). NBMPR-sensitive nucleoside transport processes that bind NBMPR with high affinity (K_d, 0.1-1 nM) have been assigned the functional designation *e*quilibrative *s*ensitive (*es*) and are mediated by ENT1 proteins. NBMPR-insensitive nucleoside transport processes are resistant to inhibition by micromolar concentrations of NBMPR, are functionally designated as *e*quilibrative *i*nsensitive (*ei*) and are mediated by ENT2 proteins. ENTs are pharmacological targets for the coronary vasodilators dilazep, dipyridamole and draflazine, which have been

shown to inhibit transport and NBMPR binding (3,15-17). Adenosine interacts with G-protein coupled cell-surface receptors of endothelial and smooth muscle cells to induce vasodilation. Transporter-mediated adenosine uptake is the major means by which this interaction is terminated, a mechanism that is blocked by coronary vasodilator binding to the human ENT isoforms hENT1 and hENT2 (7).

hENT2 shares 50% amino acid identity with hENT1 and is two and three orders of magnitude less sensitive, respectively, to inhibition by dipyridamole and dilazep than hENT1 whereas both rat isoforms (rENT1 and rENT2) are completely insensitive to these inhibitors (18,19). Human and rat ENT1 and ENT2 proteins share a common membrane architecture, recently confirmed by hydropathy analysis and glycosylation-scanning mutagenesis (20), with 11 transmembrane segments (TMs), a large glycosylated loop between TMs 1 and 2 and a large intracellular loop between TMs 6 and 7. In previous work, chimeric recombinant proteins were created between hENT1 and rENT1 to identify the structural regions of hENT1 that are responsible for interaction with dilazep and dipyridamole (21). The inhibitor sensitivities of the chimeras suggested that TMs 3-6 contain the major site(s) of interaction with secondary contributions from TMs 1-2, providing the first insight into regions of hENT1 that are important for interaction with dilazep and dipyridamole. The individual amino acid residues responsible for interaction with dilazep and dipyridamole have not yet been identified.

The goal of the study described in this chapter was to identify amino acid residues involved in dilazep and dipyridamole interaction by using a phenotypic complementation assay to screen a library of randomly mutated yeast expression plasmids containing the hENT1 cDNA (pYPhENT1) for functional thymidine-transport competent mutants with reduced sensitivity to dilazep. The complementation assay is based on the ability of recombinant hENT1 produced in *S. cerevisiae* to import thymidine under conditions of dTMP starvation, thereby allowing growth, that can be inhibited by the addition of dilazep to the assay medium (22-24). hENT1 cDNAs were isolated from the resulting mutant clones and sequenced, revealing a mutation in codon 33 that converted Met 33 to Ile (M33I). When mutant and "wildtype" recombinant hENT1 were produced in *S. cerevisiae* and *X. laevis* oocytes to quantitate dilazep and dipyridamole sensitivities, a significant decrease in sensitivity was observed for the mutated protein. The

corresponding residue in hENT2 (Ile 33) was, therefore, converted to a Met by site-directed mutagenesis and the sensitivity of the resulting mutant to dilazep and dipyridamole was assessed. The results suggested that residue 33 in the first TM (Met versus Ile) contributes importantly to the ability of dilazep and dipyridamole to interact with hENT1 and hENT2.

Results

Uridine transport by recombinant hENT1 and hENT2 in yeast

Time courses for influx of [^{3}H]-uridine were measured into fui1::TRP1, a uridine transport-defective strain of yeast (25), that contained pYPhENT1 or pYPhENT2 to determine incubation times that provided significant signal-to-noise ratios while also maintaining initial rates of uptake (Fig. 3-1). The time course for endogenous uridine influx was obtained by assessing uridine uptake into pYPGE15-containing yeast and yielded a rate of 0.11 ± 0.01 pmol/mg protein/s. Time courses for uridine uptake into pYPhENT1- and pYPhENT2-containing yeast for the first 10 s (see inset) gave rates of 1.03 ± 0.40 and 1.63 ± 0.45 pmol/mg protein/s, respectively. Uptake was linear over 40 min were linear for both pYPhENT1- and pYPhENT2-containing yeast and yielded rates, respectively, of 0.93 ± 0.02 and 1.4 ± 0.02 pmol/mg protein/s. Uptake rates over the first 10 s were not different from the rates calculated from 40 min time courses, indicating that initial rates representing uridine transport were maintained over long periods of time. The extended linear time courses were likely due to efficient substrate "trapping" by conversion of uridine to UMP by uridine kinase, thereby minimizing back-flow of [^{3}H]-uridine from the small intracellular compartment to the much larger extracellular volume. Uridine transport rates were determined for all subsequent experiments using incubation times of 10 or 20 min.

Random mutagenesis and screening

Methotrexate (MTX) and sulfanilamide (SAA) prevent the conversion of dUMP to dTMP by yeast thymidylate synthase and thus cause depletion of intracellular dTMP pools and inhibition of growth (22). KTK yeast producing recombinant hENT1 and *Herpes simplex* thymidine kinase can salvage thymidine via transporter-mediated uptake when low concentrations (e.g., 10 μM) are present in the growth medium, thereby allowing yeast to circumvent MTX/SAA-imposed growth arrest. Since thymidine salvage can be blocked by the inclusion of 10 μM dilazep in the complementation growth medium (23), this inhibition of thymidine rescue was used to screen a hENT1 random mutant library for functional proteins with reduced affinity for dilazep. pYPhENT1 was

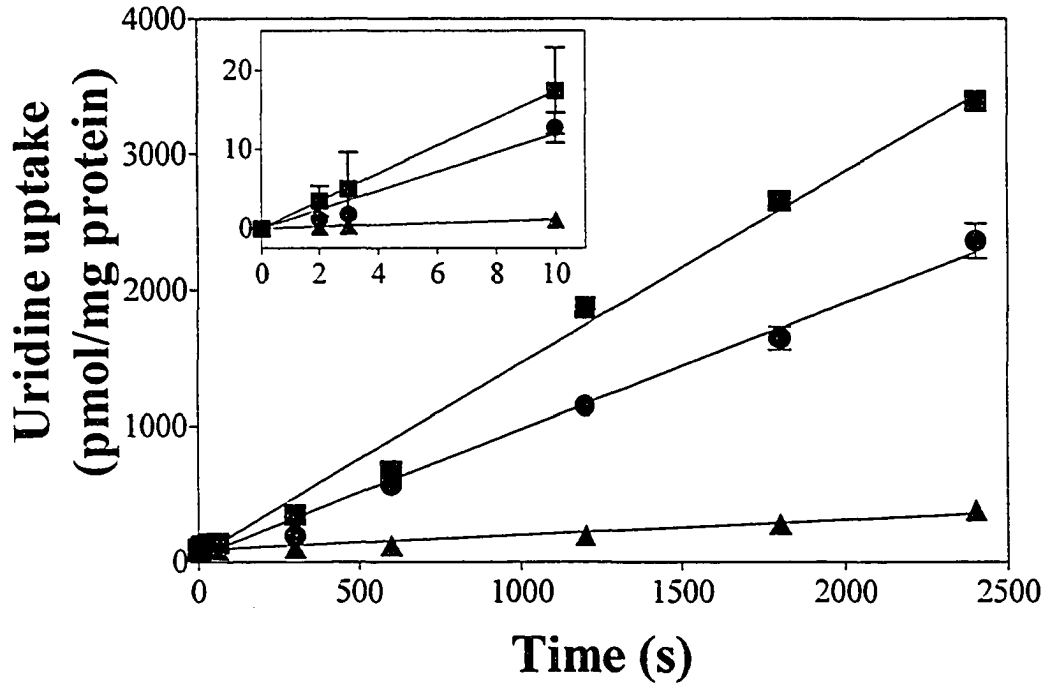

Figure 3-1. Time courses of [^{3}H]-uridine uptake for recombinant hENT1 and hENT2 produced in S. cerevisiae.

Yeast cells containing pYPhENT1 (●), pYPhENT2 (■), or pYPGE15 (▲) were incubated with 2 μM [^{3}H]-uridine for the indicated time periods. The *inset* shows time courses for the first 10 s of [^{3}H]-uridine influx. Each point represents mean uridine uptake (± S.E. n=3); S.E. values are not presented where the size of the point is larger than the S.E..

treated *in vitro* with the mutagen hydroxylamine, transformed into KTK yeast and screened for dilazep resistance. Dilazep-resistant yeast colonies were isolated and the hENT1 cDNA was amplified and subcloned into non-mutated pYPGE15. Twenty-one resistant mutant cDNA clones were sequenced and shown to be identical, with a point mutation in codon 33 that converted Met to Ile.

A comparison of sequences of inhibitor-sensitive and insensitive mammalian ENTs

Recombinant human and mouse ENT1 proteins are highly sensitive to transport inhibition by dipyridamole whereas recombinant human and mouse ENT2 proteins are much less sensitive (18,26). For example, the reported IC_{50} values for mENT1 and mENT2 produced in *X. laevis* oocytes were 75 and 2204 nM, respectively, which corresponds to a 29.4-fold difference (26). A transport-deficient cultured cell line stably transfected with recombinant hENT1 or hENT2 exhibited a 70-fold difference between the two proteins in sensitivity to dipyridamole with IC_{50} values of 5 and 356 nM, respectively (19). The rat ENT isoforms (rENT1 and rENT2) are completely insensitive to dipyridamole and dilazep transport inhibition when produced in *X. laevis* oocytes (18).

Multiple sequence alignment of the predicted amino acid sequences for the human, mouse and rat ENT1 and ENT2 proteins revealed that the identity of the amino acid at residue 33 was consistent with the dilazep and dipyridamole-sensitivity of the recombinant transporters (Fig. 3-2). Residue 33 is a Met in human and mouse ENT1, the most inhibitor-sensitive transporters, whereas it is an Ile in rat ENT1 and human, mouse and rat ENT2 proteins, all of which exhibit transport activity that is insensitive to inhibition by dilazep and dipyridamole (18,26-28). The predicted topology model for hENT1 suggests that position 33 is the last residue in the first TM and may therefore be solvent accessible and/or in the plane of the extracellular bilayer/solvent interface (Fig. 6-1) (20,27).

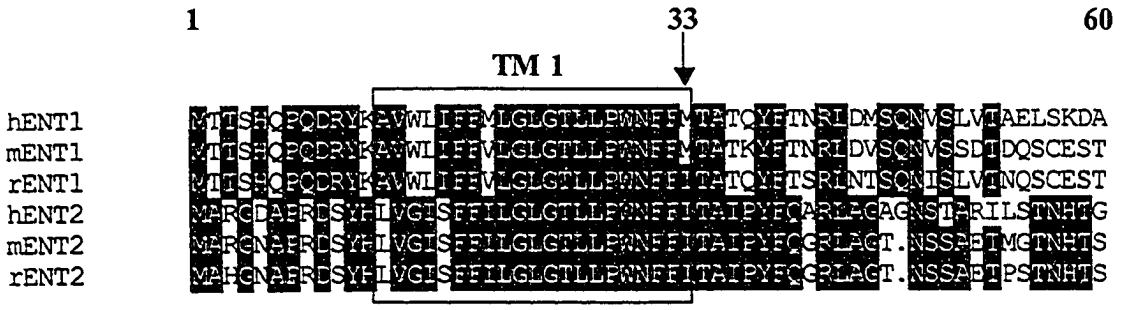

Figure 3-2. Multiple sequence alignment of the amino acid sequences of the ENT1 and ENT2 proteins in transmembrane segment 1 (TM 1) of humans (h), mice (m) and rats (r).

The position of the M33I mutation is indicated by the arrow. Genbank accession numbers are AAC51103 (hENT1) (27), AAF78452 (mENT1) (26), AAB88049 (rENT1) (18), AAC39526 (hENT2) (28), AAF78477 (mENT2) (26) and AAB88050 (rENT2) (18). Multiple sequence alignment was performed with DNAMAN version 4.03 software using the BLOSUM 62 substitution matrix.

Effect of Met-Ile interconversion at residue 33 of hENT1 and hENT2 on uridine transport inhibition by dilazep, dipyridamole and NBMPR

Uridine transport was measured in fui1::TRP1 yeast containing pYPhENT1 or pYPhENT1-M33I in the presence or absence of a single high concentration of dilazep, dipyridamole or NBMPR (Fig. 3-3A). hENT1-mediated uridine transport was inhibited ≥80% by 0.1 μM dilazep and 0.3 μM dipyridamole whereas hENT1-M33I was capable of transport at 60% of the maximal rate in the presence of both inhibitors. These results suggested that hENT1-M33I was substantially less sensitive to dilazep and dipyridamole than wildtype hENT1. In contrast, uridine transport was completely inhibited by 0.1 μM NBMPR in yeast with either recombinant protein, suggesting that residue 33 was not involved in binding of NBMPR.

Although hENT2 can be inhibited by high concentrations of dilazep and dipyridamole, it is two and three orders of magnitude less sensitive, respectively, to these compounds than hENT1 (19). To investigate the role of residue 33 in inhibitor sensitivity of hENT2, Ile 33 was converted to Met using site-directed mutagenesis and the effects of dilazep, dipyridamole and NBMPR on uridine transport were determined in fui1::TRP1 yeast containing either pYPhENT2 or pYhENT2-I33M (Fig. 3-3B). Dilazep (10 μM) and dipyridamole (1 μM) had no effect on hENT2-mediated uridine transport whereas both strongly inhibited hENT2-I33M-mediated transport. In contrast, uridine transport in yeast with either mutant or wildtype hENT2 remained insensitive to NBMPR, a result that was consistent with the lack of an effect of the opposite conversion on NBMPR sensitivity of hENT1. These data, together with those from Fig. 3-3A, indicated that residue 33 plays a key role in dilazep and dipyridamole inhibition of transport of both hENT1 and hENT2 and is not involved in NBMPR inhibition of transport.

Kinetic properties of uridine transport for hENT1, hENT1-M33I, hENT2 and hENT2-I33M

The effects of mutating residue 33 (Met vs Ile) of hENT1 and hENT2 on the kinetics of uridine transport were assessed by determining the concentration dependence of initial rates of uridine uptake (Table 3-1). hENT1 and hENT1-M33I showed similar kinetic parameters for uridine transport with K_m values of 110 ± 12 and 110 ± 28 μM,

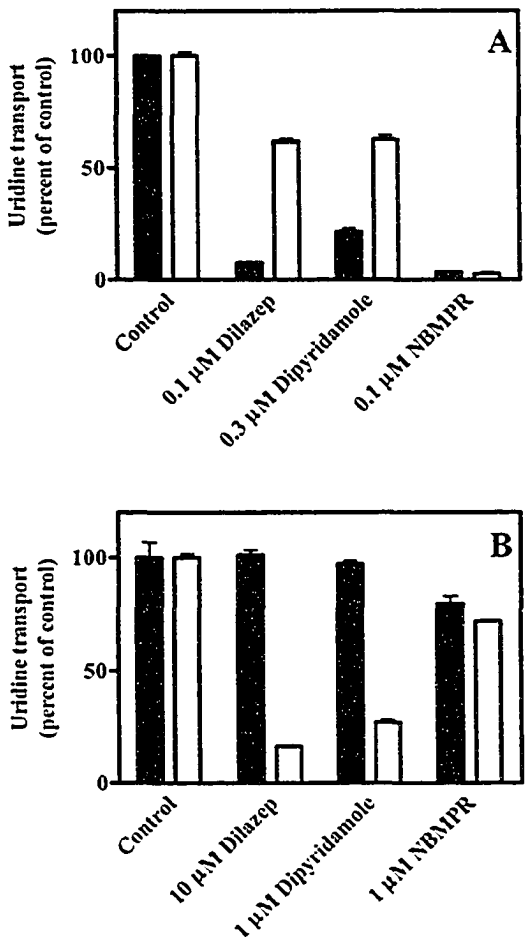

Figure 3-3. Inhibition of uridine transport mediated by recombinant hENT1, hENT1-M33I, hENT2 and hENT2-I33M by dilazep, dipyridamole and NBMPR.

Yeast cells containing pYPhENT1 (A, *solid bars*), pYPhENT1-M33I (A, *open bars*), pYPhENT2 (B, *solid bars*) or pYPhENT2-I33M (B, *open bars*) were incubated for 20 min in the presence of 2 μM [^{3}H]-uridine with or without the indicated concentration of inhibitor. Uridine transport rates (mean ± S. E., n=3) in the presence of inhibitor are represented as a percentage of the rates observed in the absence of inhibitor (*contr* which were 48.1 ± 4.7, 40.6 ± 1.5, 27.4 ± 0.2 and 100.2 ± 0.7 pmol/mg protein/min, respectively, for hENT1, hENT1-M33I, hENT2 and hENT2-I33M. Three separate experiments gave qualitatively similar results.

Table 3-1: Kinetic properties of uridine transport for hENT1, hENT1-M33I, hENT2 and hENT2-I33M

Uridine transport was assessed in yeast cells containing pYPhENT1, pYPhENT1-M33I, pYPhENT2 or pYPhENT2-I33M that were incubated in the presence of graded concentrations of [^{3}H]-uridine (1-3000 μM) for 10 min. Average K_m and V_{max} values (± S. E.) from three experiments were determined using GraphPad Prism version 3.0 software by nonlinear regression analysis.

Protein	Apparent K_m	Apparent V_{max}	V_{max}:K_m
	μM	*pmol/mg/min*	*pmol/mg/min/μM*
hENT1	110 ± 12	5893 ± 1399	53
hENT1-M33I	110 ± 28	5215 ± 562	47
hENT2	729 ± 53	8370 ± 1091	12
hENT2-I33M	87.2 ± 13.8	6555 ± 1616	75

respectively, and V_{max} values of 5893 ± 1399 and 5215 ± 562 pmol/mg protein/min, respectively, suggesting that uridine interaction with hENT1 was unaffected by the mutation. In contrast, K_m values were 729 ± 53 and 87.2 ± 13.8 μM, respectively, for hENT2 and hENT2-I33M, indicating an 8.4-fold increase in the apparent affinity for uridine. V_{max} values of 8370 ± 1091 and 6555 ± 1616 were obtained, respectively, for wildtype and mutant hENT2. The V_{max} values for the mutant and wildtype hENT1 and hENT2 proteins were not significantly different ($p > 0.05$) based on an unpaired two-tailed t-test, suggesting that expression of the recombinant proteins in yeast was not affected by mutation of residue 33. A method for determining recombinant hENT1 protein abundance was developed in Chapter 6 (Fig. 6-4). The V_{max}:K_m ratios for mutant and wildtype hENT1 were similar (47 and 53 pmol/mg protein/min/μM respectively), whereas the ratios for mutant hENT2 were much larger than those for wildtype hENT2 (75 and 12 pmol/mg protein/min/μM, respectively).

Concentration-effect relationships for dilazep, dipyridamole, and NBMPR

The relative changes in inhibitor sensitivities of mutant and wildtype hENT1 and hENT2 were determined by assessing the concentration dependence of uridine transport inhibition for the recombinant proteins produced in fui1::TRP1 yeast. The yeast were incubated with graded concentrations of inhibitors and then assayed for [^{3}H]-uridine transport (Fig. 3-4). The Hill coefficients determined from these relationships were not significantly different from unity based on a t-test against the theoretical value of 1.00 resulting in $p > 0.05$, which was consistent with (i) the presence of a single class of binding sites, and (ii) the findings of previous studies (21,23).

The IC_{50} values obtained from the data of Fig. 3-4 and the kinetic constants of Table 3-1 were used to compute apparent K_i values, assuming that dilazep, dipyridamole and NBMPR inhibit uridine transport in a reversible and strictly competitive manner at the concentration equal to the IC_{50} value (Table 3-2) (17,29-32). The transport of uridine by wildtype hENT1 was potently inhibited by dilazep (K_i, 18.7 ± 2.0 nM) whereas hENT1-M33I-mediated transport was an order of magnitude less sensitive to dilazep inhibition (K_i, 195 ± 51 nM). In contrast, hENT2-I33M was 45-fold more sensitive to

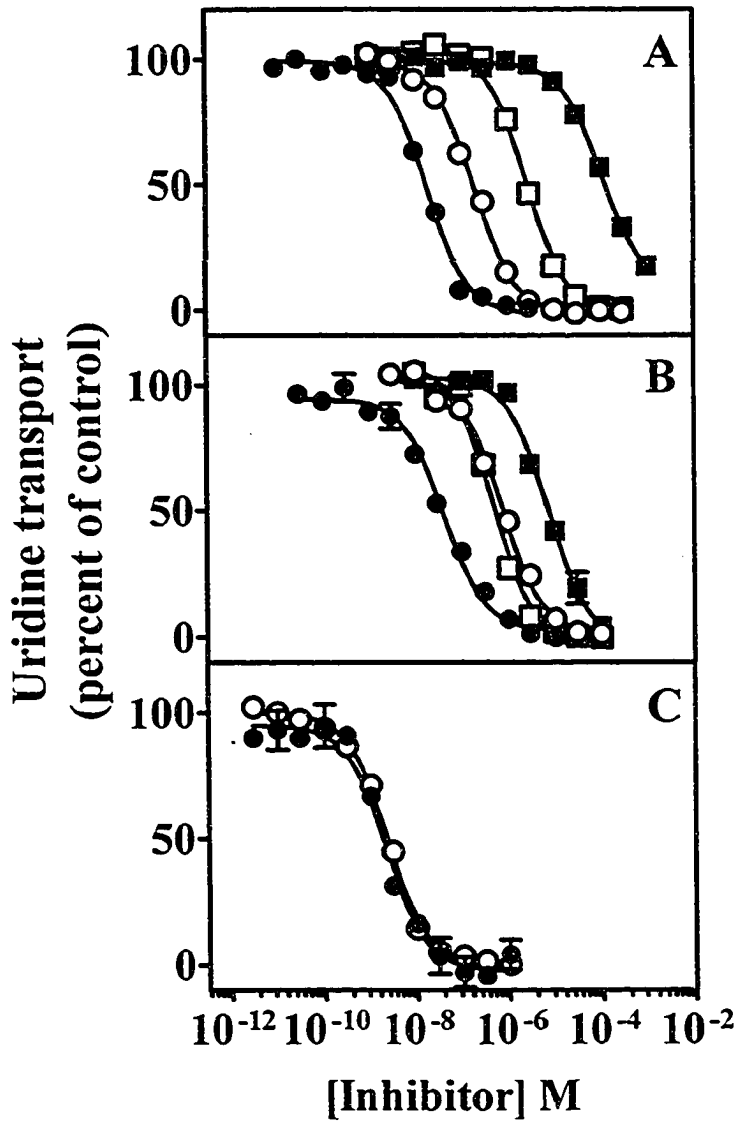

Figure 3-4. The concentration dependence of transport inhibition of recombinant hENT1, hENT1-M33I, hENT2 and hENT2-I33M by dilazep, dipyridamole and NBMPR.

Yeast cells containing pYPhENT1 (*closed circles*), pYPhENT1-M33I (*open circles*), pYPhENT2 (*closed squares*) or pYPhENT2-I33M (*open squares*) were incubated for 20 min in the presence of 2 μM [^{3}H]-uridine with or without graded concentrations of dilazep (A), dipyridamole (B) or NBMPR (C). Uridine transport rates (mean ± S. E., n=3) in the presence of inhibitor are represented as a percentage of the rates observed in

the absence of inhibitor (*control*), and S. E. values are not presented where the size of the point is larger than the S. E.. Mean values (± S. E.) for control uridine transport rates were 78.4 ± 5.5, 70.1 ± 2.6, 31.8 ± 0.7 and 143.6 ± 2.2 pmol/mg protein/min for hENT1, hENT1-M33I, hENT2 and hENT2-I33M, respectively. Three separate experiments gave similar results. IC_{50} values and Hill coefficients were determined using GraphPad Prism version 3.0 software by nonlinear regression analysis. The K_i values given in Table 3-2 were calculated using the equation of Cheng and Prusoff (29) with the experimentally determined IC_{50} values for each inhibitor and the uridine K_m values for each recombinant protein (Table 3-1).

TABLE 3-2: K_i values for dilazep, dipyridamole and NBMPR inhibition of uridine transport for hENT1, hENT1-M33I, hENT2 and hENT2-I33M

Average IC_{50} values from three experiments were (i) determined using GraphPad Prism version 3.0 software by nonlinear regression analysis of the curves presented in Fig. 3-4 and (ii) used to calculate K_i values using the equation of Cheng and Prusoff (46) with the experimentally determined K_m values shown in Table I. The P-values were determined using an unpaired two-tailed t-test of the K_i values presented.

Inhibitor	Inhibition of hENT1/hENT1-M33I (K_i, nM)			
	hENT1	hENT1-M33I	Ratio[α]	P-value
Dilazep	18.7 ± 2.0	195 ± 51	10.4	0.026
Dipyridamole	47.9 ± 8.9	528 ± 165	11.0	0.044
NBMPR	5.83 ± 1.08	3.34 ± 0.97	0.57	0.16
	Inhibition of hENT2/hENT2-I33M (K_i, nM)			
	hENT2	hENT2-I33M	Ratio[β]	P-value
Dilazep	134000 ± 40000	2910 ± 790	46.0	0.031
Dipyridamole	6230 ± 900	461 ± 74	13.5	0.0031
NBMPR	ND[γ]	ND[γ]	ND[γ]	ND[γ]

[α]Ratio= K_i(hENT1-M33I)/ K_i(hENT1)
[β] Ratio= K_i(hENT2)/ K_i (hENT2-I33M)
[γ] ND, not determined

dilazep inhibition than wildtype hENT2 with K_i values of 2.91 ± 0.79 and 134 ± 40 μM, respectively. Thus, the mutations at residue 33 decreased the differences in dilazep sensitivity between hENT1 and hENT2. The mutant proteins displayed a 15-fold difference (hENT1-M33I > hENT2-I33M) whereas the wildtype proteins displayed a 7000-fold difference (hENT1 > hENT2) in sensitivity to inhibition by dilazep.

For both hENT1 and hENT2, the relative differences between the mutant and wildtype proteins in dipyridamole sensitivity were similar to those observed for dilazep (Table 3-2). K_i values of 47.9 ± 8.9 and 528 ± 165 nM were obtained for dipyridamole inhibition of transport for wildtype and mutant hENT1, respectively, translating into an 11-fold decrease in sensitivity. The dipyridamole sensitivities of hENT2 (K_i, 6230 ± 900 nM) and hENT2-I33M (K_i, 461 ± 74 nM) differed by 13.5-fold. Wildtype hENT1 was 128-fold more sensitive to dipyridamole than hENT2, which is consistent with the results of previous studies (19), whereas mutant hENT1 and hENT2 displayed approximately equal sensitivities to dipyridamole.

The results of Fig. 3-3 had suggested that wildtype and mutant hENT1 were highly sensitive to NBMPR since complete inhibition of transport was observed for both at 0.1 μM. In the experiments of Table 3-2, K_i values of 5.83 ± 1.08 and 3.34 ± 0.97 nM were obtained for hENT1 and hENT1-M33I, respectively, demonstrating that both were potently inhibited by NBMPR, with no statistically significant difference in K_i values. The NBMPR sensitivities of hENT2 and hENT2-I33M were not determined because the experiments of Fig. 3-3B had established that neither protein was inhibited by NBMPR.

In a previous study (21), recombinant chimeric proteins (i) were constructed by region substitutions between hENT1, which is sensitive to inhibition by dilazep and dipyridamole, and its rat isoform, rENT1, which is insensitive to both compounds, and (ii) functionally characterized in *Xenopus laevis* oocytes. The results suggested that TMs 1-6 of hENT1 are required for interaction with dilazep and dipyridamole, with TMs 3-6 being the major site of interaction and TMs 1-2 making a secondary contribution. Since residue 33 is predicted to be the last residue in TM 1, recombinant hENT1-M33I was produced in *Xenopus laevis* oocytes (Fig. 3-5) to assess the functional characteristics of the mutated protein in the same recombinant expression system as the chimera study. When oocytes producing mutant and wildtype hENT1 were assayed for uridine uptake in

the presence of graded concentrations of dipyridamole, IC_{50} values were 3640 ± 1410 and 300 ± 79 nM, respectively, corresponding to a 12.1-fold lower sensitivity for the mutant protein. This relative decrease in sensitivity was similar to that observed when the recombinant proteins were produced in yeast.

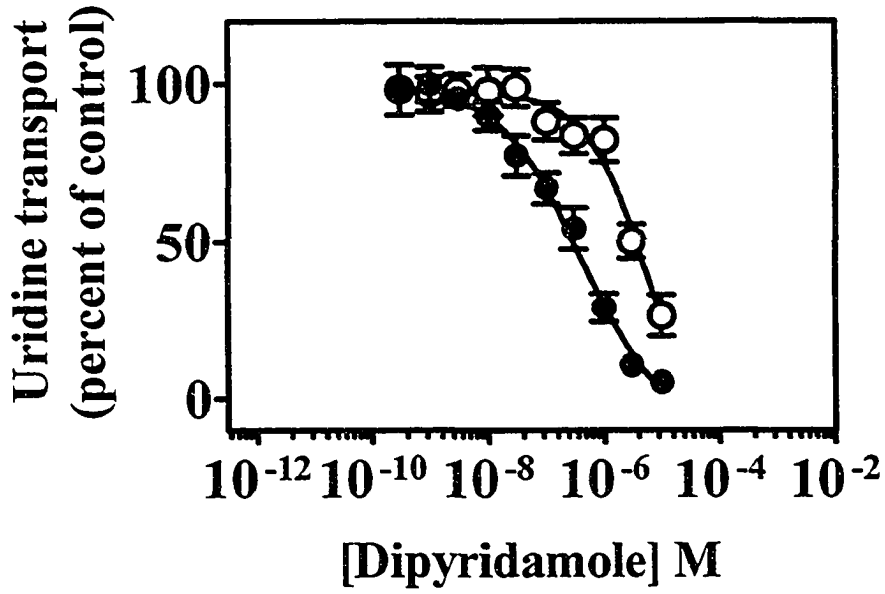

Figure 3-5. The concentration dependence of inhibition of recombinant hENT1 and hENT1-M33I by dipyridamole in Xenopus laevis oocytes.

Initial rates of ^{14}C-uridine uptake were determined in the presence of graded concentrations of dipyridamole and were corrected for endogenous uridine transport activity by subtracting uptake values obtained in water-injected oocytes. Oocytes were pretreated with dipyridamole for 1 h to allow for complete binding site equilibration. Uridine transport rates (mean ± S. E., n=10-12) in the presence of inhibitor are represented as a percentage of the rates observed in the absence of inhibitor (*control*), and S. E. values are not presented where the size of the point is larger than the S. E.. Mean values (± S. E.) for control uridine transport rates were 2.13 ± 0.10 and 2.15 ± 0.11 pmol/oocyte/5 min, respectively, for hENT1 and hENT1-M33I. IC_{50} values were determined using GraphPad Prism version 3.0 software by nonlinear regression analysis amd were 300 ± 79 and 3640 ± 1400, respectively, for hENT1 and hENT1-M33I.

Discussion

The results of molecular cloning and functional expression studies on recombinant ENTs are consistent with the findings of studies on *es* and *ei*-type transport processes in cultured cell lines and erythrocytes. The human and mouse *es*-type transporters, which correspond, respectively, to the hENT1 and mENT1 proteins, are highly sensitive to dilazep and dipyridamole (3,16,33,34). In contrast, rat *es* and human, mouse and rat *ei* transporters are relatively insensitive to transport inhibition by dilazep and dipyridamole and these observed effects have been correlated with the transport-inhibition phenotypes of recombinant rENT1, hENT2, mENT2 and rENT2 (3,33,34). This study provided evidence that mutation of residue 33 of the hENT1 and hENT2 proteins affects their interactions with dilazep and dipyridamole significantly. The amino acid residue at this position (Met vs Ile) corresponds with the relative dilazep and dipyridamole sensitivities of the known mammalian ENTs, being a Met in human and mouse ENT1 and an Ile in rat ENT1 and human, mouse and rat ENT2 proteins (Fig. 3-2) (18,19,21,26-28).

Mutation of Met 33 to Ile in hENT1 decreased the sensitivity of uridine transport to inhibition by dilazep and dipyridamole (as seen by the >10-fold increase in K_i values) but did not alter the affinity for uridine (similar K_m values) or the sensitivity to inhibition of uridine transport by NBMPR (similar K_i values). In contrast, when Ile was converted to Met, the sensitivities of hENT2 to dilazep and dipyridamole were increased >10 fold, the affinity for uridine increased 8.4-fold and NBMPR sensitivity was not affected. These results, which implicated residue 33 in uridine interaction with hENT2, but not hENT1, suggested a difference in the permeant-binding pockets of the two proteins. hENT1 and hENT2 are known to have different permeant-binding properties since hENT2 is capable of transporting nucleobases and antiviral dideoxynucleoside analogs, whereas hENT1 is not (35,36).

The apparent K_m value for uridine transport obtained for recombinant hENT1 in yeast (Table 3-1) was 110 ± 12 μM whereas values of 200-260 μM have been obtained for recombinant hENT1 in other expression systems (cultured cells, *X. laevis* oocytes)

and for the native protein in human erythrocytes (19,27,37). The basis for this discrepancy is uncertain but may have been due to the human protein being inserted into the yeast plasma membrane environment and/or an altered state of glycosylation, resulting is subtle changes in the conformation of the uridine-binding pocket.

Previous work in which chimeric recombinant proteins were created by substituting regions between inhibitor-sensitive hENT1 and inhibitor-insensitive rENT1 suggested that the region including residues 100-231 (which includes TMs 3-6) is the major site of interaction with dilazep and dipyridamole and that residues 1-99 (TMs 1-2) play a secondary role (21). TMs 3-6 were also implicated in the interaction of rENT1 with NBMPR (20). The chimera studies demonstrated that the N-terminal half of hENT1 is critical for interaction with the inhibitors. When recombinant hENT1-M33I was characterized in the same expression system (*Xenopus laevis* oocytes) as was utilized in the chimera study, the relative effect of the mutation on dipyridamole sensitivity was comparable to that observed in yeast. These oocyte results confirmed participation of Met 33, which is predicted to be the last residue in TM 1, in binding of dilazep and dipyridamole. That the M33I mutation reduced, but did not abolish, inhibitor sensitivity in hENT1 (compared to rENT1 and rENT2, which are totally resistant to inhibition), suggests that binding of dipyridamole and dilazep is likely to be complex, involving contributions from several amino acid residues from different regions of hENT1.

Results of equilibrium binding studies in cells with the *es* transport process, for which ENT1 proteins are believed to be responsible, have led to the conclusion that dilazep and dipyridamole are competitive inhibitors for a single, or an overlapping, exofacial NBMPR and permeant binding site (17,30,31,38,39). However, results from other studies have suggested that dilazep and dipyridamole display characteristics of allosteric ligands when present at high concentrations (30,32,40,41). A unifying model that has been suggested for permeant and inhibitor binding to hENT1 describes two binding sites in which permeants, NBMPR and other inhibitors (e.g., dilazep and dipyridamole) compete for a single "high-affinity" site, which is subject to allosteric modulation by a distinct broad-specificity "low-affinity" site that binds nucleosides, nucleobases and inhibitors when present at very high concentrations (3). The contribution of the potential allosteric binding site of hENT1 was likely to be negligible

in the experiments presented here, since the Hill coefficients indicated the presence of a single class of binding sites. These results suggested that mutation of residue 33 affected dilazep and dipyridamole binding to the competitive binding site.

The current study established that residue 33 of hENT1 and hENT2 is important for dilazep and dipyridamole interaction. It is not clear whether residue 33 of hENT1 and hENT2 is directly involved in permeant or inhibitor binding or if the effects observed when it was mutated were due to changes in the tertiary structure of these proteins. The alternatives are difficult to resolve in the absence of detailed structural data. Future studies include using different random mutagenesis and screening approaches to identify other residues that may be important for interaction with nucleoside transport inhibitors.

References

1. Vickers, M. F., Young, J. D., Baldwin, S. A., and Cass, C. E. (2000) *Emerging Therapeutic Targets* **4**, 515-539
2. Cass, C. E., Young, J. D., Baldwin, S. A., Cabrita, M. A., Graham, K. A., Griffiths, M., Jennings, L. L., Mackey, J. R., Ng, A. M. L., Ritzel, M. W. L., Vickers, M. F., and Yao, S. Y. M. (1999) in *Membrane Transporters as Drug Targets* (Amidon, G. L., and Sadee, W., eds) Vol. 12, 1 Ed., 12 vols., Kluwer Academic/Plenum Publishers
3. Griffith, D. A., and Jarvis, S. M. (1996) *Biochim Biophys Acta* **1286**, 153-181
4. Baldwin, S. A., Mackey, J. R., Cass, C. E., and Young, J. D. (1999) *Mol Med Today* **5**, 216-224
5. Cass, C. E. (1995) in *Drug Transport in Antimicrobial and Anticancer Chemotherapy* (Georgopapadakou, N. H., ed), pp. 403-451, Marcel Deker, New York, NY
6. Mackey, J. R., Baldwin, S. A., Young, J. D., and Cass, C. E. (1998) *Drug Resistance Updates* **1**, 310-324
7. Jennings, L. L., Cass, C. E., Ritzel, M. W. L., Yao, S. Y. M., Young, J. D., Griffiths, M., Baldwin, S. A. (1998) *Drug Dev Res* **45**, 277-287
8. Belardinelli, L., Linden, J., Berne, R. M. (1989) *Prog Cardiovasc Dis* **32**, 73-97
9. Ritzel, M. W., Yao, S. Y., Huang, M. Y., Elliott, J. F., Cass, C. E., and Young, J. D. (1997) *Am J Physiol* **272**, C707-714
10. Ritzel, M. W., Yao, S. Y., Ng, A. M., Mackey, J. R., Cass, C. E., and Young, J. D. (1998) *Mol Membr Biol* **15**, 203-211
11. Ritzel, M. W. L., Ng, A. M., Yao, S. Y. M., Graham, K., Loewen, S. K., Smith, K. M., Ritzel, R. G., Mowles, D. A., Carpenter, P., Chen, X., Karpinski, E., Hyde, R. J., Baldwin, S. A., Cass, C. E., and Young, J. D. (2001) *J Biol Chem* **276**, 2914-2927
12. Yao, S. Y., Ng, A. M., Ritzel, M. W., Gati, W. P., Cass, C. E., and Young, J. D. (1996) *Mol Pharmacol* **50**, 1529-1535
13. Che, M., Ortiz, D. F., and Arias, I. M. (1995) *J Biol Chem* **270**, 13596-13599

14. Huang, Q. Q., Harvey, C. M., Paterson, A. R., Cass, C. E., and Young, J. D. (1993) *J Biol Chem* **268**, 20613-20619
15. Van Belle, H. (1993) *Cardiovasc Res* **27**, 68-76
16. Hammond, J. R. (2000) *Nauyn Schmiedebergs Arch Pharmacol* **361**, 373-382
17. Jarvis, S. M. (1986) *Mol Pharmacol* **30**, 659-665
18. Yao, S. Y., Ng, A. M., Muzyka, W. R., Griffiths, M., Cass, C. E., Baldwin, S. A., and Young, J. D. (1997) *J Biol Chem* **272**, 28423-28430
19. Ward, J. L., Sherali, A., Mo, Z. P., and Tse, C. M. (2000) *J Biol Chem* **275**, 8375-8381
20. Sundaram, M., Yao, S. Y., Ingram, J. C., Berry, Z. A., Abidi, F., Cass, C. E., Baldwin, S. A., and Young, J. D. (2001) *J Biol Chem* **2**, 2
21. Sundaram, M., Yao, S. Y. M., Ng, A. M. L., Griffiths, M., Cass, C. E., Baldwin, S. A., and Young, J. D. (1998) *J Biol Chem* **273**, 21519-21525
22. Hogue, D. L., Ellison, M. J., Young, J. D., and Cass, C. E. (1996) *J Biol Chem* **271**, 9801-9808
23. Vickers, M. F., Mani, R. S., Sundaram, M., Hogue, D. L., Young, J. D., Baldwin, S. A., and Cass, C. E. (1999) *Biochem J* **339**, 21-32
24. Hogue, D. L., Ellison, M. J., Vickers, M., and Cass, C. E. (1997) *Biochem Biophys Res Commun* **238**, 811-816
25. Vickers, M. F., Yao, S. Y., Baldwin, S. A., Young, J. D., and Cass, C. E. (2000) *J Biol Chem* **275**, 25931-25938
26. Kiss, A., Farah, K., Kim, J., Garriock, R. J., Drysdale, T. A., Hammond, J. R. (2000) *Biochem J* **352**, 363-372
27. Griffiths, M., Beaumont, N., Yao, S. Y., Sundaram, M., Boumah, C. E., Davies, A., Kwong, F. Y., Coe, I., Cass, C. E., Young, J. D., and Baldwin, S. A. (1997) *Nat Med* **3**, 89-93
28. Griffiths, M., Yao, S. Y., Abidi, F., Phillips, S. E., Cass, C. E., Young, J. D., and Baldwin, S. A. (1997) *Biochem J* **328**, 739-743
29. Cheng, Y., and Prusoff, W. H. (1973) *Biochem Pharmacol* **22**, 3099-3108
30. Koren, R., Cass, C. E., and Paterson, A. R. (1983) *Biochem J* **216**, 299-308.
31. Jarvis, S. M., McBride, D., and Young, J. D. (1982) *J Physiol (Lond)* **324**, 31-46

32. Gati, W. P., Paterson, A. R. P. (1989) *Mol Pharm* **36**, 134-141

33. Plagemann, P. G. W., Wohlhueter, R. M., Woffendin, C. (1988) *Biochim Biophys Acta* **947**, 405-443

34. Plagemann, P. G. W., Woffendin, C. (1988) *Biochim Biophys Acta* **969**, 1-8

35. Osses, N., Pearson, J. D., Yudilevich, D. L., and Jarvis, S. M. (1996) *Biochem J* **317**, 843-848.

36. Hamilton, S. R., Yao, S. Y., Ingram, J. C., Hadden, D. A., Ritzel, M. W., Gallagher, M. P., Henderson, P. J., Cass, C. E., Young, J. D., and Baldwin, S. A. (2001) *J Biol Chem* **276**, 27981-27988.

37. Jarvis, S. M., Hammond, J. R., Paterson, A. R., Clanachan, A. S. (1982) *Biochem J* **208**, 83-88

38. Paterson, A. R., Lau, E. Y., Dahlig, E., and Cass, C. E. (1980) *Mol Pharmacol* **18**, 40-44

39. Shi, M., Young, J. D. (1986) *Biochem J* **240**, 879-883

40. Hammond, J. R. (1991) *Mol Pharmacol* **39**, 771-779

41. Jarvis, S. M., Janmohamed, S. N., and Young, J. D. (1983) *Biochem J* **216**, 661-667

Chapter 4: Residue 33 of Human Equilibrative Nucleoside Transporter 2 is a Functionally Important Component of Both the Dipyridamole and Nucleoside Binding Sites[2]

[2] *A version of this chapter has been submitted for publication:*
F. Visser, J. Zhang, R. T. Raborn, S. A. Baldwin, J. D. Young and C. E. Cass (2004) Mol. Pharmacol.

Acknowledgements

Ms. Jing Zhang contributed to this project by developing the high-throughput nucleoside transport assay methodology and providing intellectual guidance. Mr. R. Taylor Raborn conducted some preliminary concentration-dependence of nucleoside transport experiments for this project. Dr. Stephen Baldwin and Dr. James Young are collaborative principle investigators who helped obtained research funding for this project and aided in manuscript preparation.

Introduction

Integral membrane proteins mediate the transport of hydrophilic nucleosides and anticancer or antiviral nucleoside analogs across biological membranes (1). Equilibrative nucleoside transporters (ENTs) in mammalian cells mediate facilitated diffusion of nucleosides down their concentration gradients. Four ENT family members have been identified by molecular cloning: hENT1, hENT2, hENT3 and hENT4. hENT1 and hENT2 display equilibrative sensitive (*es*) and equilibrative insensitive (*ei*) transport activities, respectively, based on their differential sensitivities to the inhibitor nitrobenzylmercaptopurine ribonucleoside (NBMPR) (2-4). Neither hENT3 or hENT4 have been functionally characterized, but hENT3 is believed to be a transporter located in intracellular membranes (5,6). Although hENT1 and hENT2 mediate the transport of a broad variety of nucleoside permeants, kinetic analyses have revealed that hENT2 generally displays lower affinities (higher K_m values) for its permeants and, unlike hENT1, can also transport nucleobases (7,8). The amino acid residues responsible for these functional differences have not been identified.

ENT proteins control extracellular concentrations of adenosine, a ligand for cell-surface adenosine receptors that facilitate a variety of physiological responses, such as coronary vasodilation, renal vasoconstriction, platelet aggregation, and neuromodulation (9). hENT1 and hENT2 are the pharmacological targets of the coronary vasodilators dilazep and dipyridamole and differ in their sensitivities to these inhibitors by two to three orders of magnitude with hENT1 being more sensitive (10).

Despite limited sequence identities, all members of the ENT family share a common topology model consisting of 11 transmembrane segments (TMs), a large extracellular loop between TMs 1 and 2 and a large cytoplasmic loop between TMs 6 and 7 (11). The current level of knowledge of the structure and function of these transporter proteins is limited. A number of studies on chimeric constructs involving region swaps between different members of the ENT family have implicated TMs 3 – 6 as a region involved in permeant and inhibitor binding (7,12-14). In addition, Cys 140 in TM 4 of rat ENT2 has been demonstrated by sulfhydryl modification experiments to form part of the permeant translocation pore, and the corresponding residue of hENT1, Gly 154, is

critical for NBMPR sensitivity (15-17). Other mutagenesis studies have identified Gly 179 in TM 4 and Leu 92 in TM 2 of hENT1 as residues that, when mutated, impair inhibitor binding and transporter function (18,19). Single residues in TMs 5, 7 and 8 of the LdNT transporters, which are ENT family members from the parasitic protozoan *Leishmania donovani*, were demonstrated to play important roles in transporter function (20,21). Furthermore, by use of the substituted cysteine accessibility method, TM 5 of LdNT1.1 was shown to line the permeant translocation pathway (22).

In Chapter 3, mutation of Met 33 of hENT1 to Ile, the corresponding residue in hENT2, resulted in ~10-fold reduced affinities for dilazep and dipyridamole, whereas the reciprocal mutation of Ile 33 of hENT2 to Met resulted in ~10-fold increased sensitivities to these inhibitors (10). hENT1-M33I displayed similar kinetic parameters for uridine transport to wildtype hENT1, whereas hENT2-I33M displayed kinetic parameters that were more similar to hENT1 than to hENT2. In this chapter, an improved method for functional characterization of recombinant hENT1 and hENT2 in yeast (10,23,24) was utilized to determine the kinetic properties of hENT1-M33I, hENT2-I33M and a series of hENT2 mutants at residue 33 for a variety of different nucleoside permeants. These experiments revealed that hENT2-I33M had higher transport activities than wildtype hENT2 for all the permeants tested whereas hENT1-M33I was functionally similar to wildtype hENT1. The residue 33 hENT2 mutants were also tested for their sensitivities to dipyridamole and the membrane impermeant sulfhydryl-reactive reagent p-chloromercuribenzyl sulphonate (pCMBS). The results indicated that residue 33 is accessible from the extracellular side of the membrane and suggested that it is a common functional determinant of the nucleoside and dipyridamole binding sites.

Results

Initial rates of nucleoside transport by recombinant hENT1 and hENT2 produced in yeast.

Fui1::TRP1 yeast cells containing either pYPhENT1, pYPhENT2 or pYPGE15 (vector without insert) were incubated in the presence of 1 μM [^{3}H]-labeled uridine, cytidine, thymidine, adenosine, inosine or guanosine for various intervals within 0 to 60 s and 0 to 60 min (Fig. 4-1). For yeast with recombinant hENT1, the rates of uptake of 1 μM uridine, cytidine, adenosine, inosine and guanosine from 0 to 30 s were linear and not significantly different from the rates observed from 0 to 10 min, and for uridine and adenosine from 0 to 60 min. For yeast producing hENT2, rates of uptake of 1 μM uridine, adenosine and inosine were linear from 0 to 60 s and not significantly different from the rates observed at time points up to 10 min. Uptake of [^{3}H]-cytidine and [^{3}H]-guanosine by yeast producing hENT2 was significant but with poor signal-to-noise ratios, and subsequent kinetic experiments did not yield reproducible data. Uptake of [^{3}H]-thymidine by yeast producing either hENT1 or hENT2 was very poor even though thymidine is a known permeant of both transporters (2,3) and unlabeled thymidine was a potent inhibitor of nucleoside transport in yeast with either transporter (Fig. 4-1). The low uptake of thymidine was likely because fui1::TRP1 yeast do not possess thymidine kinase and thus cannot metabolically "trap" thymidine once inside the cell. However, metabolism did not appear to be rate-limiting for uptake of the other nucleoside permeants since functional differences were observed between hENT1, hENT2 and mutants thereof, indicating that the transported permeants were rapidly trapped and the intracellular concentrations of free nucleosides were, therefore, negligible. For yeast containing pYPGE15, the rates of uptake for all [^{3}H]-labeled nucleosides were low and similar to those of yeast producing recombinant hENT1 or hENT2 in the presence of 10 mM unlabeled thymidine or uridine. For all subsequent experiments initial rates of nucleoside transport were estimated from values of total uptake at 10 min minus values observed in the presence of 10 mM unlabeled thymidine.

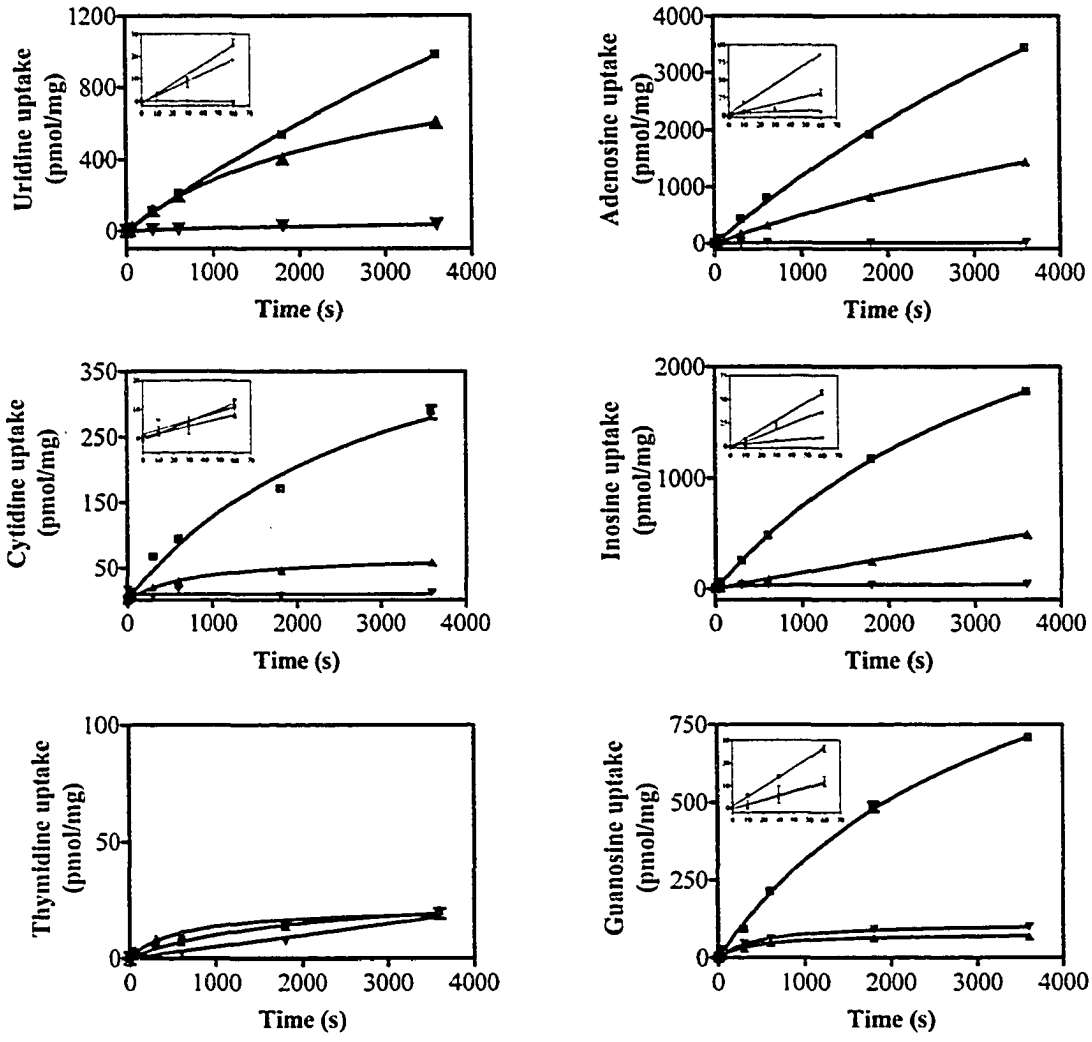

Figure 4-1. Time courses for the uptake of [^{3}H]-uridine, cytidine, thymidine, adenosine, inosine and guanosine into yeast containing pYPhENT1, pYPhENT2 or pYPGE15.

Yeast cells containing pYPhENT1 (■), pYPhENT2 (▲) or pYPGE15 (▼) were incubated with 1 μM [^{3}H]-uridine, cytidine, thymidine, adenosine, inosine or guanosine for various timepoints up to 3600 s (60 min). Time points from 0 – 60 s are presented in the *insets*. Each point represents the mean ± S.E. of three separate determinations and where the point is larger than the S.E., it is not shown. The graphs were generated using GraphPad Prism version 4.0 software.

Nucleoside transport by hENT1, hENT1-M33I, hENT2 and hENT2-I33M.

Yeast cells containing either pYPhENT1, pYPhENT1-M33I, pYPhENT2, pYPhENT2-I33M or pYPGE15 were incubated in the presence of 10 μM [^{3}H]-labeled uridine, cytidine, adenosine, inosine or guanosine for 10 min (Fig. 4-2A). hENT1 and hENT1-M33I displayed similar rates of uptake for all of the nucleosides whereas hENT2-I33M displayed rates of uptake that were higher than those of wildtype hENT2 and similar to those of hENT1. This experiment demonstrated total uptake observed at a 10-min timepoint and did not distinguish between mediated and non-mediated uptake.

Uptake of the [^{3}H]-labeled nucleoside analog drugs (5-fluorouridine, gemcitabine, cytarabine, cladribine and fludarabine) into yeast cells containing pYPhENT1, pYPhENT2, pYPhENT2-I33M or pYPGE15 was also determined (Fig. 4-2B). Consistent with what was observed for the naturally occurring nucleosides, hENT2-I33M displayed rates of uptake that were higher than those of hENT2 and similar to those of hENT1 with the exception of the cytidine analogs gemcitabine and cytarabine, for which hENT2-I33M-mediated uptake was higher than that of either wildtype protein.

Inhibition of adenosine transport mediated by recombinant hENT1 and hENT2 by physiological permeants.

Concentration-effect relationships for inhibition of 1 μM [^{3}H]-adenosine transport by recombinant hENT1 and hENT2 in yeast by graded concentrations of either uridine, cytidine, thymidine, adenosine, inosine or guanosine were determined. The resulting IC_{50} values were used to calculate K_i values using the equation of Cheng and Prusoff: $K_i = IC_{50}/(1 + [S]/K_m)$ where [S] is the permeant concentration (25). The results are given in Tables 4-1 (hENT1 series) and 4-2 (hENT2 series). The K_i values obtained for inhibition of adenosine transport were similar to the observed K_m values for transport of the same permeant, indicating that a common transporter (hENT1 or hENT2) was responsible for uptake of the permeants tested. Furthermore, the K_i values served as surrogate measures of the affinities of the transporters for their permeants, which enabled assessment of hENT2 interactions with cytidine and guanosine (Table 4-2).

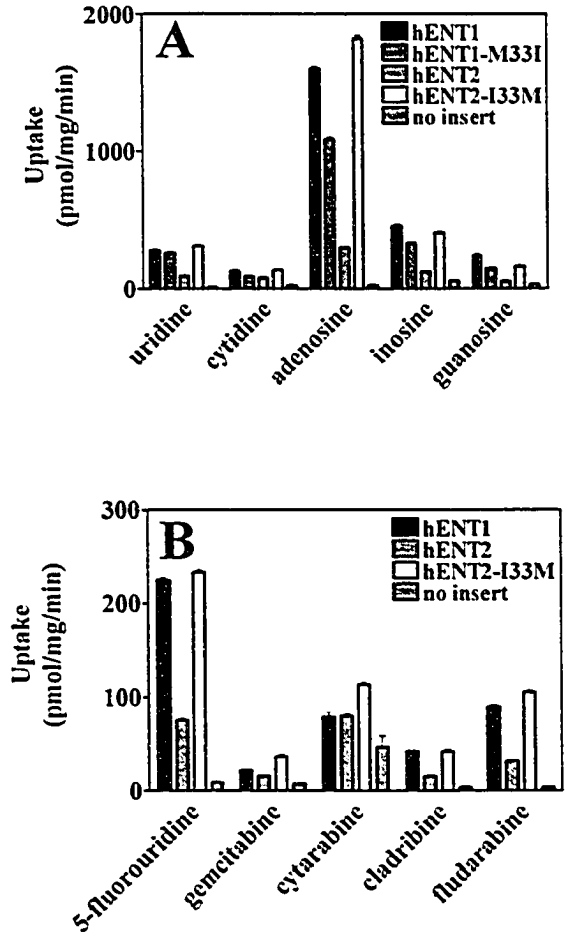

Figure 4-2. Nucleoside and nucleoside analog uptake rates by hENT1, hENT1-M33I, hENT2 and hENT2-I33M.

Yeast cells containing pYPhENT1, pYPhENT1-M33I, pYPhENT2, pYPhENT2-I33M or pYPGE15 (no insert) were incubated for 10 min with the following [^{3}H]-labeled nucleosides or nucleoside analogs: (A) uridine, cytidine, adenosine, inosine, guanosine, and (B) 5-fluorouridine, gemcitabine, cytarabine, cladribine or fludarabine at a concentration of 10 μM. The representative uptake values are presented as the means ± S.E. of triplicate determinations. Three separate experiments gave similar results. For each single experiment, all five yeast strains were assayed simultaneously for all the permeants indicated so that direct uptake rate comparisons could be made.

Kinetic parameters of hENT1 and hENT1-M33I.

The concentration dependence of [^{3}H]-labeled uridine, cytidine, adenosine, inosine and guanosine transport was determined for yeast cells containing either pYPhENT1 or pYPhENT1-M33I (Table 4-1). Both wildtype and mutant hENT1 conformed to simple Michaelis-Menten kinetics for all nucleosides tested. Recombinant hENT1-M33I displayed apparent K_m values that were similar to those of hENT1 whereas the mutant consistently displayed lower V_{max} values than hENT1, which likely reflected a lower abundance of the mutant protein in the plasma membrane. The V_{max}:K_m ratios, which reflect transporter efficiencies for the various nucleoside permeants, for hENT1-M33I were similar to those of hENT1. These results suggested that there were no apparent functional differences between mutant and wildtype hENT1.

Kinetic parameters of hENT2 and various residue 33 mutants.

The concentration dependence of [^{3}H]-labeled uridine, cytidine, adenosine, inosine and guanosine transport was determined for yeast cells containing pYPhENT2 or pYPhENT2-I33M (Table 4-2). As was observed for hENT1, both wildtype hENT2 and hENT2-I33M conformed to simple Michaelis-Menten kinetics for all the nucleoside permeants tested. Recombinant hENT2-I33M displayed K_m values for the pyrimidine nucleosides uridine and cytidine that were similar to those of hENT1 and ~25 % of those of wildtype hENT2. Although the K_m values of hENT2-I33M for adenosine, inosine and guanosine were lower than those of wildtype hENT2, they were higher than those of hENT1. The V_{max} values of hENT2-I33M for the purine nucleosides, particularly adenosine, were significantly higher than those of either hENT1 or hENT2. The V_{max}:K_m ratios of hENT2-I33M for all the nucleoside permeants tested were higher than those of hENT2 and similar to those of hENT1, providing an explanation for the differences in nucleoside uptake results observed in Fig. 4-2A.

To test the effects of substituting different amino acid side chains at residue 33 of hENT2, additional mutations were generated (hENT2-I33A, I33C and I33S) and the kinetic parameters of uridine and adenosine transport were determined (Table 4-2). Representative rate vs concentration plots and Eadie Hofstee plots for adenosine transport

Table 4-1. Kinetic properties of hENT1 and hENT1-M33I

The K_m, V_{max} and K_i values shown are the means ± S.E. of 3-5 separate experiments. Representative curves for uridine are presented in Fig. 3-2A.

Protein	Permeant	Apparent K_m	Apparent V_{max}	V_{max}:K_m	K_i
		μM	*pmol/mg/min*	*pmol/mg/min/μM*	*μM*
hENT1					
	uridine	44.1 ± 2.6	1060 ± 20	24.0	51.9 ± 2.8
	cytidine	234 ± 47	1280 ± 70	5.4	346 ± 49
	thymidine	ND	ND	ND	81.6 ± 3.1
	adenosine	17.8 ± 0.8	1330 ± 20	74.7	10.3 ± 0.4
	inosine	28.5 ± 2.6	1300 ± 30	45.6	34.6 ± 1.9
	guanosine	47.5 ± 4.8	1080 ± 30	22.7	48.6 ± 3.6
hENT1-M33I					
	uridine	30.0 ± 1.4	707 ± 10	23.6	
	cytidine	150 ± 38	814 ± 68	5.4	
	adenosine	12.2 ± 0.5	1010 ± 10	82.8	
	inosine	24.0 ± 4.0	804 ± 36	33.5	
	guanosine	49.8 ± 4.7	784 ± 36	15.7	

ND = not determined

Table 4-2. Kinetic properties of hENT2, hENT2-I33M, hENT2-I33A, hENT2-I33C and hENT2-I33S

The K_m, V_{max} and K_i values shown are the means ± S.E. of 3-5 separate experiments. Representative curves for uridine and adenosine are presented in Fig. 3-2B and 3-3, respectively.

Protein	Permeant	Apparent K_m	Apparent V_{max}	V_{max}:K_m	K_i
		μM	*pmol/mg/min*	*pmol/mg/min/μM*	*μM*
hENT2					
	uridine	195 ± 14	1940 ± 60	9.9	216 ± 17
	cytidine	ND	ND	ND	1380 ± 170
	thymidine	ND	ND	ND	129 ± 9
	adenosine	106 ± 6	3420 ± 60	32.2	93.7 ± 8.1
	inosine	180 ± 37	2020 ± 150	11.2	192 ± 29
	guanosine	ND	ND	ND	394 ± 70
hENT2-I33M					
	uridine	49.0 ± 2.3	1110 ± 20	22.6	
	cytidine	393 ± 77	1700 ± 70	4.3	
	adenosine	52.0 ± 2.0	10000 ± 110	231	
	inosine	95.6 ± 6.5	3420 ± 70	35.8	
	guanosine	81.2 ± 15.6	2300 ± 110	28.3	
hENT2-I33A					
	uridine	213 ± 28	1410 ± 70	6.6	
	adenosine	104 ± 11	2010 ± 50	19.3	
hENT2-I33C					
	uridine	39.1 ± 5.0	1640 ± 40	41.9	
	adenosine	43.6 ± 2.2	6830 ± 80	157	
hENT2-I33S					
	uridine	67.1 ± 5.7	2080 ± 40	31.0	
	adenosine	98.5 ± 4.4	10200 ± 130	104	

ND = not determined

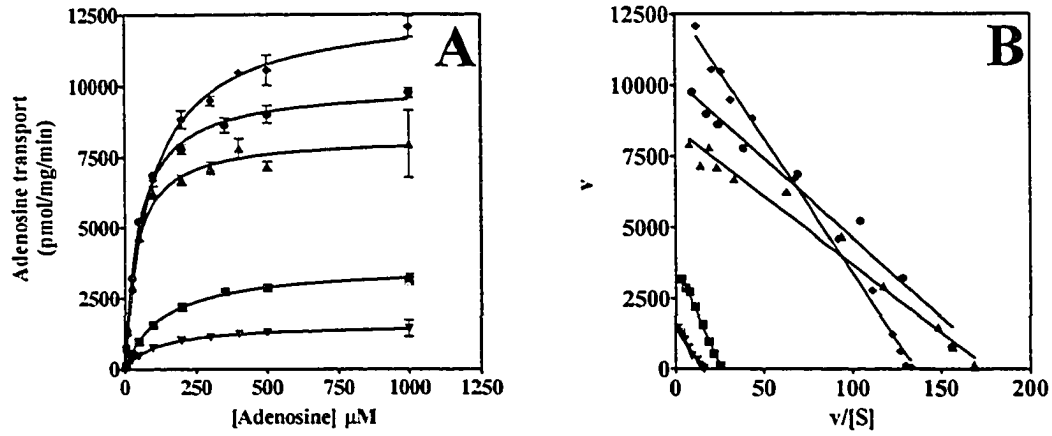

Figure 4-3. Concentration-dependence of adenosine transport by hENT2 and various residue 33 mutants.

(A) Yeast cells containing pYPhENT2 (■), pYPhENT2-I33M (●), pYPhENT2-I33C (▲), pYPhENT2-I33A (▼) or pYPhENT2-I33S (◆) were incubated for 10 min with increasing concentrations of [^{3}H]-adenosine. The transport rates presented were derived from the difference between the uptake observed in the absence and presence of 10 mM unlabeled thymidine at each uridine concentration. K_m and V_{max} values were obtained by nonlinear regression analysis using GraphPad Prism version 4.0 software, and the average values from 3 - 5 separate experiments are presented in Table 4-2. (B) Eadie-Hofstee plot of the data presented in panel A. Each point is presented as the mean ± S.E. (n=4-9), and where the size of the point is larger than the S.E., it is not shown.

by hENT2 and all the residue 33 mutants are presented in Fig. 4-3. hENT2-I33A displayed K_m and V_{max} values that were similar to those of hENT2, whereas the values for hENT2-I33C and I33S were similar to those of hENT2-I33M in that the K_m values for uridine were 20 to 30 % of wildtype and the V_{max} values for adenosine were 2 to 3 - fold higher. hENT2-I33M and hENT2-I33C displayed modestly lower K_m values for adenosine compared to hENT2 whereas hENT2-I33S only displayed an increased V_{max} with no change in K_m. These results suggested that the presence of either Met, Cys or Ser side chains at residue 33 of hENT2 resulted in transporters with similar functional properties with respect to either uridine or adenosine.

Concentration-effect relationships for dipyridamole inhibition of hENT2 and various residue 33 mutants.

hENT2-I33M was previously shown to be more sensitive to dipyridamole then wildtype hENT2 (10). Yeast cells producing either hENT2 or one of the residue 33 mutants were incubated in the presence of 1 μM [^{3}H]-uridine in the absence (control) or presence of graded concentrations of dipyridamole (Fig. 4-4, Table 4-3). hENT2 and hENT2-I33A displayed similar IC_{50} values whereas hENT2-I33M and I33C were 14 and 18 - fold more sensitive, respectively, and hENT2-I33S was only 1/5 as sensitive to dipyridamole inhibition as wildtype.

Sulfhydryl modification of hENT2 and various residue 33 mutants.

Yeast cells producing hENT2, hENT2-I33M, hENT2-I33C, hENT2-I33A or hENT2-I33S were incubated with graded concentrations of pCMBS, a membrane-impermeant sulfhydryl-reactive reagent, followed by measurement of 1 μM [^{3}H]-uridine uptake (Fig. 4-5). hENT2, hENT2-I33A, hENT2-I33S and hENT2-I33M-mediated uridine uptake was highly resistant to concentrations of pCMBS up to 3 mM, whereas hENT2-I33C-mediated uridine uptake was inhibited in a dose-dependent manner to a maximum inhibition of 64% and an average IC_{50} value of 8.8 ± 1.0 μM (n=3). The average Hill slope of hENT2-I33C inhibition by pCMBS was 1.08 ± 0.14, suggesting that modification of a single Cys residue was responsible for the observed effect. The observation that hENT2-I33A and I33S were insensitive to inhibition by pCMBS

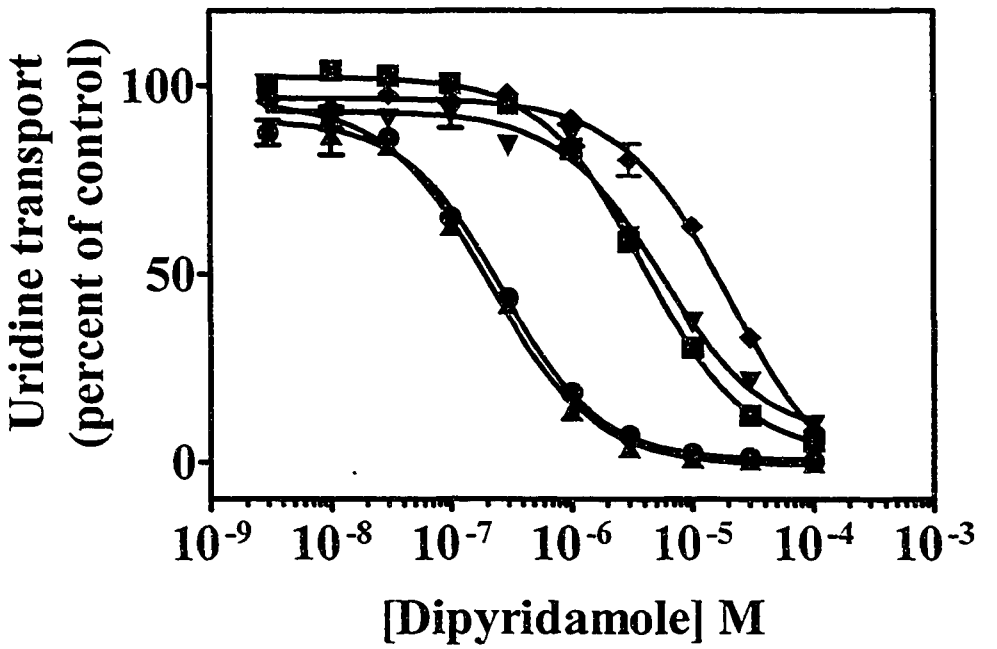

Figure 4-4. Concentration dependence of dipyridamole inhibition of hENT2, hENT2-I33M, hENT2-I33C, hENT2-I33A and hENT2-I33S.

Yeast cells containing pYPhENT2 (■), pYPhENT2-I33M (●), pYPhENT2-I33C (▲), pYPhENT2-I33A (▼) or pYPhENT2-I33S (◆) were incubated with 1 μM [^{3}H]-uridine for 10 min in the absence (control) or presence of graded concentrations of dipyridamole. IC_{50} values were determined by nonlinear regression analysis using GraphPad Prism version 4.0 software, and the average values from 3 separate experiments are presented in Table 4-3. Each point is presented as the mean ± S.E. (n=4), and where the size of the point is larger than the S.E., it is not shown.

Table 4-3. Inhibition of hENT2, hENT2-I33M and hENT2-I33C-mediated [^{3}H]-uridine transport by dipyridamole

Ki values are the mean ± S.E. calculated using the equation of Cheng and Prusoff (Cheng and Prusoff, 1973) with the IC_{50} values obtained by nonlinear regression analysis of the curves presented in Fig. 5 using GraphPad Prism version 4.0 software.

Protein	K_i	Ratio[α]	ΔG°
	uM		*kcal/mol*
hENT2	3.77 ± 0.25	1.00	7.4
hENT2-I33M	0.263 ± 0.011	14.3	9.0
hENT2-I33A	4.95 ± 0.55	0.76	7.2
hENT2-I33C	0.206 ± 0.018	18.3	9.1
hENT2-I33S	18.6 ± 4.7	0.20	6.4

[α]Ratio=K_i hENT2/K_i mutant

suggested that the substitution of an amino acid residue with a small side chain did not induce a conformational change leading to the exposure of an endogenous pCMBS-reactive Cys residue. Furthermore, the observation that wildtype hENT2 was insensitive to inhibition by pCMBS was consistent with previously published work (17). The current topology model of hENT2 places residue 33 as the last position on the extracellular end of TM 1 (3,11,17) and the observation that residue 33 was accessible to pCMBS supported this model (Fig. 6-1).

Permeant and inhibitor protection of hENT2-I33C from pCMBS modification.

Yeast cells producing hENT2-I33C were incubated in the presence or absence of 0.1 mM pCMBS either alone or together with (i) 1 mM adenosine or uridine, (ii) 10 μM dilazep or dipyridamole, or (iv) 1 μM NBMPR and then assayed for [^{3}H]-uridine uptake (Fig. 4-6A). The presence of either adenosine, uridine or dipyridamole protected hENT2-I33C from pCMBS inhibition whereas dilazep and NBMPR had no effect on pCMBS-dependent inhibition. That NBMPR did not protect hENT2-I33C from pCMBS was consistent with its inability to bind with high affinity to hENT2. Yeast cells producing hENT2-I33C that had been incubated with 0.1 mM pCMBS and subsequently incubated with 1 mM dithiothreitol exhibited full recovery of uridine uptake activity, demonstrating involvement of a sulfhydryl group in the pCMBS-dependent inhibition.

To determine the extent to which either adenosine, uridine, dipyridamole or dilazep protected yeast cells producing hENT2-I33C from pCMBS inhibition, graded concentrations of compound were tested in the experiments of Fig. 4-6B. Uridine (EC_{50}, 320 ± 50 μM, n=3), adenosine (EC_{50}, 67.1 ± 8.9 μM, n=3) and dipyridamole (EC_{50}, ≥ 10 μM, n=3) protected hENT2-I33C from pCMBS inhibition in a dose-dependent manner whereas dilazep had no protective effects at concentrations up to 1 mM. The highest dipyridamole concentration used for protection from pCMBS modification was 10 μM because this was the solubility limit on ice, the temperature at which the reactions were performed. The data suggested that binding of adenosine, uridine or dipyridamole prevented pCMBS from inhibiting hENT2-I33C and implied that residue 33 formed a common component of the binding site for these compounds.

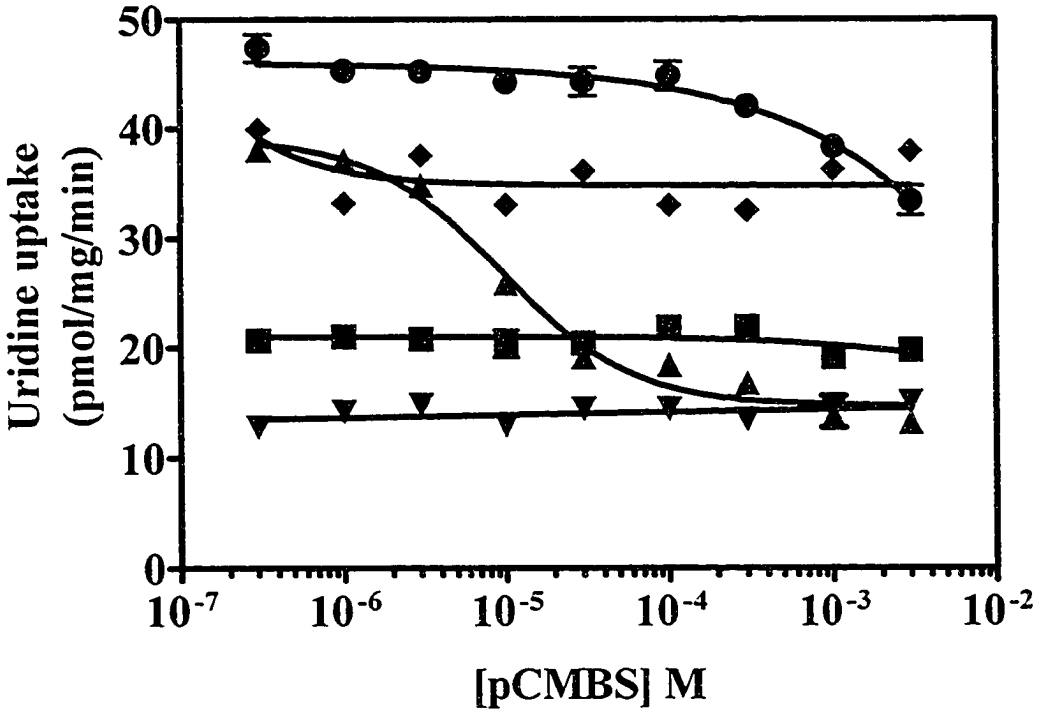

Figure 4-5. Concentration-dependence of pCMBS inhibition of hENT2 and various residue 33 mutants.

Yeast cells containing pYPhENT2 (■), pYPhENT2-I33M (●), pYPhENT2-I33C (▲), pYPhENT2-I33A (▼) or pYPhENT2-I33S (◆) were incubated in the absence or presence of graded concentrations of pCMBS followed by incubation with 1 μM [^{3}H]-uridine for 10 min. Each point represents the mean ± S.E. (n=4), and where the size of the point is larger than the S.E., it is not shown. IC_{50} values were determined by nonlinear regression using GraphPad Prism version 4.0 software, and average values are presented in the text. Three separate experiments gave similar results.

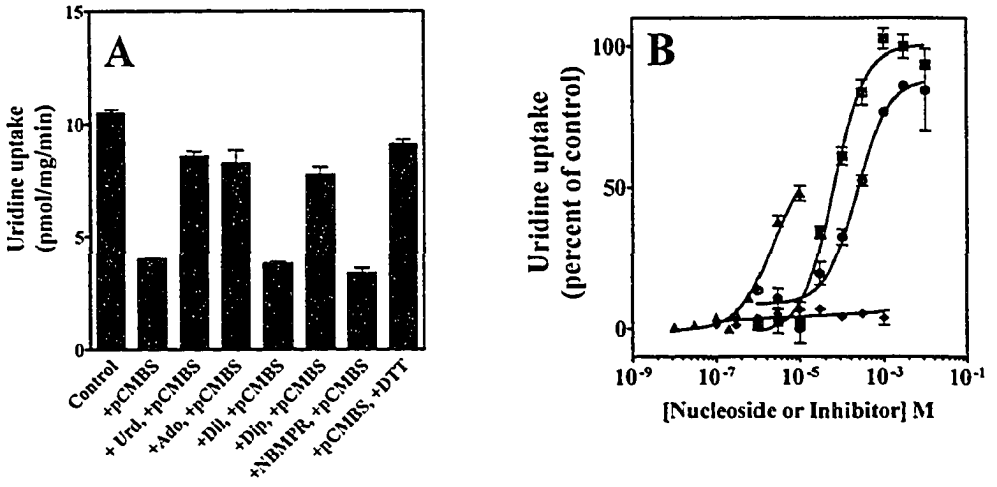

Figure 4-6. Protection of hENT2-I33C from pCMBS modification by various permeants and inhibitors.

(A) Yeast cells producing hENT2-I33C were incubated in the absence (control) or presence of 0.1 mM pCMBS with or without 1 mM uridine (Urd), 1 mM adenosine (Ado), 10 μM dilazep (Dil), 10 μM dipyridamole (Dip) or 1 μM NBMPR. Some of the yeast cells incubated with 0.1 mM pCMBS alone were subsequently incubated with 1 mM DTT. The yeast cells were then incubated for 10 min with 1 μM [^{3}H]-uridine in the absence of the test protecting agents. Uridine uptake is presented as the mean ± S.E., n=4 and was analyzed using GraphPad Prism version 4.0 software. Three separate experiments gave similar results. (B) Yeast cells producing hENT2-I33C were incubated in the absence or presence of 0.1 mM pCMBS with or without graded concentrations of uridine (●), adenosine (■), dilazep (◆) or dipyridamole (▲) followed by incubation for 10 min with 1 μM [^{3}H]-uridine in the absence of the test protecting agents. Uridine transport rates in the absence of 0.1 mM pCMBS were set as 100 % of control whereas rates in the presence of 0.1 mM pCMBS were set as 0 % of control. EC_{50} values were determined by nonlinear regression using GraphPad Prism version 3.0 software, and average values are presented in the text. Each point represents the mean ± S.E. (n=4), and where the size of the point is larger than the S.E., it is not shown. Three separate experiments gave similar results.

Discussion

In this study, fui1::TRP1 yeast cells displayed little or no endogenous transport activity for uridine, cytidine, thymidine, adenosine, inosine and guanosine and are therefore a powerful heterologous expression system for the comprehensive functional analysis of recombinant hENT1 and hENT2. The observed affinity parameters, K_i or K_m, were similar to those reported in other studies for recombinant hENT1 and hENT2 produced in yeast (15,19,24,26). However, these parameters differed from those obtained in other recombinant expression systems such as *Xenopus laevis* oocytes and transfected mammalian cells (2,3,8,27). These discrepancies were likely due to differences in post-translational processing of the transporter protein and in the lipid composition of plasma membranes. Nonetheless, the relative affinities of hENT1 and hENT2 for their permeants were consistent with those reported in transfected cells with the exception of inosine and thymidine for hENT2 (8). Recombinant hENT1 and hENT2 were previously reported to have similar apparent affinities for uridine (2,3,8) although earlier studies of endogenous *es* and *ei* transport systems in cultured cells and rat erythrocytes had demonstrated lower affinities of the *ei* transporter (i.e., ENT2) for uridine (28,29).

hENT2-I33M, I33C and I33S all displayed increased affinities for uridine (Table 4-2), suggesting that residue 33 is an important functional determinant for the binding of uridine and other pyrimidine nucleosides. Furthermore, the observation that hENT2-I33M displayed increased apparent V_{max} values for all purine nucleoside permeants and that hENT2-I33M, I33C and I33S all displayed notably increased apparent V_{max} values for adenosine suggested that residue 33 was also an important functional determinant for the purine nucleoside transport activity of hENT2. That increased V_{max} values were observed with adenosine and not with uridine suggested that the observed effects were not due to an increase in the plasma membrane abundance of the protein but rather to an increase in catalytic activity brought about by increases in the rate of conformational turnover and/or increases in protein flexibility. A method to determine the protein abundance of ENTs in yeast was developed in Chapter 6 (Fig. 6-5). However, hENT2-I33S did not display a reduced K_m value for adenosine (Table 4-2), as was observed for

hENT2-I33M and I33C, suggesting that it contributed to permeant recognition and transport via a unique mechanism. The Met and Cys side chains contain highly polarizable sulphur atoms that likely interacted with hydrophobic moieties on the base portions of uridine and adenosine (30), whereas the Ser side chain contributed hydrogren bond interactions to uridine binding. Furthermore, Met was favored over Ile in this regard due to its relatively high degree of conformational flexibility. The apparent ability of this residue to interact with different parts of the permeant molecule likely stems from the conformational flexibility in TM 1 brought about by the highly conserved glycine residues G22 and G24 (5).

The observation that hENT1 and hENT1-M33I did not display functional differences suggested that this residue 33 did not contribute to permeant interactions in hENT1 (Table 4-1). This was likely due to minor structural differences between hENT1 and hENT2. In particular, the large extracellular loop that extends from TM 1 is considerably more hydrophobic in hENT1 than hENT2 and may affect the conformation and solvent accessibility of residue 33. Because TM 1 is likely alpha-helical, as would be predicted from the crystal structures of other major facilitator superfamily proteins such as lac permease (31), W29 is predicted to be in close proximity to residue 33, suggesting that this region of hENT1 is involved in permeant recognition and transport.

Cys and Met at residue 33 increased sensitivity to dipyridamole by 18 and 14-fold, respectively, whereas Ile (wildtype), Ala and Ser were less favourable for dipyridamole inhibition (Fig. 4-4, Table 4-3). That hENT2-I33S exhibited increased transport activity but decreased dipyridamole sensitivity strongly suggested that this residue could not engage in hydrogen bond interactions with the more hydrophobic dipyridamole molecule. Met or Cys at residue 33 likely participated in interactions with the pi electron cloud of the aromatic moieties on the dipyridamole structure, which was supported by the fact that the strength of the interaction (1.6 to 1.7 kcal/mol) is consistent with the strength of similar interactions observed in alpha-helices (0.7 to 2 kcal/mol) and is based on the high degree of polarizability of the sulphur atom (32,33).

hENT2-I33C was the only hENT2 mutant that displayed a dose-dependent sensitivity to the membrane-impermeant sulfhydryl reactive reagent pCMBS (Fig. 4-5). These results independently confirmed the location of residue 33 on the putative topology

model of hENT2, which placed it as the last residue on the extracellular end of TM 1 (11). hENT2-I33C was protected from pCMBS modification by uridine, adenosine and dipyridamole (Fig. 4-6). These results suggested that the binding of permeants or dipyridamole prevented pCMBS from reacting either by directly blocking access to residue 33 or by altering accessibility to residue 33 by a long-range conformational effect on the tertiary structure of hENT2. Given the functional significance of residue 33, the results of these experiments suggested a direct interaction between residue 33 and either nucleoside permeants or dipyridamole. Earlier studies had provided contradictory evidence for both competitive and allosteric binding of dipyridamole to hENT1 (34). However, the current results suggested that dipyridamole competes with permeants for binding to the outward-facing conformation of mammalian ENTs, supporting the conclusion that dipyridamole and nucleoside permeant bind to the same or an overlapping site (35-37). That Met was favoured at residue 33 for permeant and inhibitor binding is consistent with the ability of ENTs to bind a large variety of chemically unrelated permeants and inhibitors. Met residues of the signal-recognition particle 45 (SRP45) and calmodulin have been implicated as critical for recognition of a wide variety of unrelated protein targets (30).

Dilazep was unable to protect against pCMBS inhibition of hENT2-I33C even though this mutant transporter was inhibited by dilazep with an average IC_{50} value of 18.7 ± 1.2 μM (Fig. 4-7). Dilazep and dipyridamole are believed to bind to the same or overlapping sites of hENT1, which was supported by the results of Chapter 3, in which residue 33 mutations similarly affected the potency of these two inhibitors (10,12,38). The results of the current study suggested that dilazep may bind adjacent to residue 33 in a manner that does not occlude this residue.

In conclusion, this in-depth study of the impact of mutations of residue 33 in hENT2 in the yeast expression system has yielded novel information about the role of this residue in permeant and inhibitor interactions with hENT2 and hENT1. The earlier conclusions were confirmed (Chapter 3), that residue 33 is a determinant of the overall functional differences between hENT1 and hENT2. This chapter demonstrated that residue 33 is extracellular, thereby validating the predicted topology model for hENT2, and indicated that nucleosides and dipyridamole interact directly with residue 33. These

results established residue 33 as a common exofacial component of the binding sites for nucleosides and inhibitors, providing molecular evidence that dipyridamole competes with nucleosides for binding to hENT2. Although these conclusions are consistent with the data presented in this study, a crystal structure of the transporter would be necessary to further address the role of residue 33 in permeant and inhibitor interactions with hENT2.

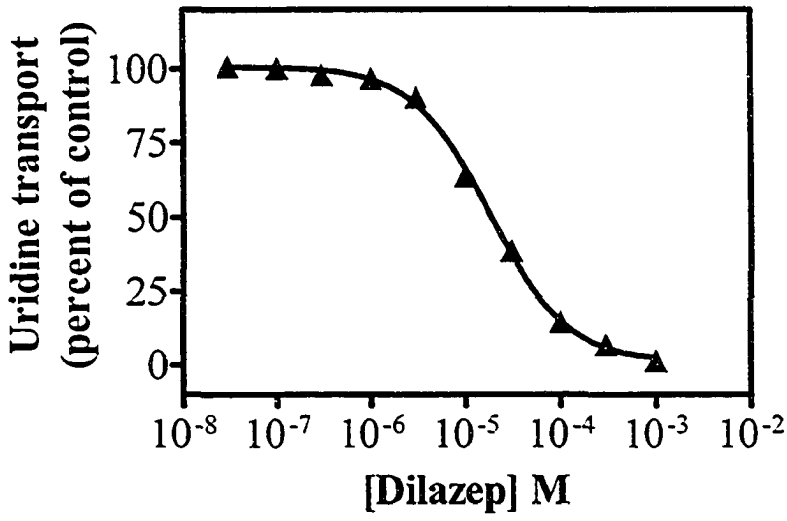

Figure 4-7. Concentration dependence of dilazep inhibition of hENT2-I33C.

Yeast cells producing recombinant hENT2-I33C were incubated in the presence of 1 μM [^{3}H]-uridine for 10 min in the absence (control) or presence of graded concentrations of dilazep. Each point represents the mean ± S. E. of four separate determinations, and where the point is larger than the S.E., it is not shown. The data were analyzed by nonlinear regression using GraphPad Prism version 4.0 software. The average IC_{50} value from three separate experiments are presented in the text.

References

1. Cass, C. E., Young, J. D., Baldwin, S. A., Cabrita, M. A., Graham, K. A., Griffiths, M., Jennings, L. L., Mackey, J. R., Ng, A. M. L., Ritzel, M. W. L., Vickers, M. F., and Yao, S. Y. M. (1999) in *Membrane Transporters as Drug Targets* (Amidon, G. L., and Sadee, W., eds) Vol. 12, 1 Ed., 12 vols., Kluwer Academic/Plenum Publishers
2. Griffiths, M., Beaumont, N., Yao, S. Y., Sundaram, M., Boumah, C. E., Davies, A., Kwong, F. Y., Coe, I., Cass, C. E., Young, J. D., and Baldwin, S. A. (1997) *Nat Med* **3**, 89-93
3. Griffiths, M., Yao, S. Y., Abidi, F., Phillips, S. E., Cass, C. E., Young, J. D., and Baldwin, S. A. (1997) *Biochem J* **328**, 739-743
4. Crawford, C. R., Patel, D. H., Naeve, C., and Belt, J. A. (1998) *J Biol Chem* **273**, 5288-5293
5. Hyde, R. J., Cass, C. E., Young, J. D., Baldwin, S. A. (2001) *Mol Memb Biol* **18**, 53-63
6. Acimovic, Y., and Coe, I. R. (2002) *Mol Biol Evol* **19**, 2199-2210
7. Yao, S. Y., Ng, A. M., Vickers, M. F., Sundaram, M., Cass, C. E., Baldwin, S. A., and Young, J. D. (2002) *J Biol Chem* **277**, 24938-24948
8. Ward, J. L., Sherali, A., Mo, Z. P., and Tse, C. M. (2000) *J Biol Chem* **275**, 8375-8381
9. Van Belle, H. (1993) *Cardiovasc Res* **27**, 68-76
10. Visser, F., Vickers, M. F., Ng, A. M., Baldwin, S. A., Young, J. D., and Cass, C. E. (2002) *J Biol Chem* **277**, 395-401.
11. Sundaram, M., Yao, S. Y., Ingram, J. C., Berry, Z. A., Abidi, F., Cass, C. E., Baldwin, S. A., and Young, J. D. (2001) *J Biol Chem* **2**, 2
12. Sundaram, M., Yao, S. Y. M., Ng, A. M. L., Griffiths, M., Cass, C. E., Baldwin, S. A., and Young, J. D. (1998) *J Biol Chem* **273**, 21519-21525
13. Sundaram, M., Yao, S. Y. M., Ng, A. M. L., Cass, C. E., Baldwin, S. A., Young, J.D. (2001) *Biochemistry* **40**, 8146-8151

14. Yao, S. Y., Ng, A. M., Sundaram, M., Cass, C. E., Baldwin, S. A., and Young, J. D. (2001) *Mol Membr Biol* **18**, 161-167.
15. SenGupta, D. J., and Unadkat, J. D. (2004) *Biochem Pharmacol* **67**, 453-458
16. Hyde, R. J., Abidi, F., Griffiths, M., Yao, S. Y. M., Sundaram, M., Phillips, S. E. V., Cass, C. E., Young, J. D. (2000) *Drug Dev Res* **50**, 38
17. Yao, S. M., Sundaram, M., Chomey, E. G., Cass, C. E., Baldwin, S. A., Young, J. D. (2001) *Biochem J* **353**, 387-393
18. SenGupta, D. J., Lum, P. Y., Lai, Y., Shubochkina, E., Bakken, A. H., Schneider, G., and Unadkat, J. D. (2002) *Biochemistry* **41**, 1512-1519
19. Endres, C. J., SenGupta, D. J., and Unadkat, J. D. (2004) *Biochem J* **Pt**
20. Arastu-Kapur, S., Ford, E., Ullman, B., and Carter, N. S. (2003) *J Biol Chem* **278**, 33327-33333
21. Vasudevan, G., Ullman, B., and Landfear, S. M. (2001) *Proc Natl Acad Sci U S A* **98**, 6092-6097
22. Valdes, R., Vasudevan, G., Conklin, D., and Landfear, S. M. (2004) *Biochemistry* **43**, 6793-6802
23. Zhang, J., Visser, F., Vickers, M. F., Lang, T., Robins, M. J., Nielsen, L. P. C., Nowak, I., Baldwin, S. A., Young, J. D., and Cass, C. E. (2003) *Mol Pharm* **64**, 1512-1520
24. Vickers, M. F., Zhang, J., Visser, F., Tackaberry, T., Robins, M. J., Nielsen, L. P., Nowak, I., Baldwin, S. A., Young, J. D., and Cass, C. E. (2004) *Nucleosides Nucleotides Nucleic Acids* **23**, 361-373
25. Cheng, Y., and Prusoff, W. H. (1973) *Biochem Pharmacol* **22**, 3099-3108
26. Osato, D. H., Huang, C. C., Kawamoto, M., Johns, S. J., Stryke, D., Wang, J., Ferrin, T. E., Herskowitz, I., and Giacomini, K. M. (2003) *Pharmacogenetics* **13**, 297-301
27. Yao, S. Y., Ng, A. M., Muzyka, W. R., Griffiths, M., Cass, C. E., Baldwin, S. A., and Young, J. D. (1997) *J Biol Chem* **272**, 28423-28430
28. Boleti, H., Coe, I. R., Baldwin, S. A., Young, J. D., and Cass, C. E. (1997) *Neuropharmacology* **36**, 1167-1179
29. Jarvis, S. M., and Young, J. D. (1986) *J Membr Biol* **93**, 1-10

30. Gellman, S. H. (1991) *Biochemistry* **30**, 6633-6636

31. Abramson, J., Smirnova, I., Kasho, V., Verner, G., Kaback, H. R., and Iwata, S. (2003) *Science* **301**, 610-615

32. Viguera, A. R., and Serrano, L. (1995) *Biochemistry* **34**, 8771-8779

33. Pal, D., and Chakrabarti, P. (2001) *J Biomol Struct Dyn* **19**, 115-128

34. Griffith, D. A., and Jarvis, S. M. (1996) *Biochim Biophys Acta* **1286**, 153-181

35. Jarvis, S. M., Janmohamed, S. N., and Young, J. D. (1983) *Biochem J* **216**, 661-667

36. Jarvis, S. M. (1986) *Mol Pharmacol* **30**, 659-665

37. Paterson, A. R., Lau, E. Y., Dahlig, E., and Cass, C. E. (1980) *Mol Pharmacol* **18**, 40-44

38. Koren, R., Cass, C. E., and Paterson, A. R. (1983) *Biochem J* **216**, 299-308.

Chapter 5: Identification and Mutational Analysis of Amino Acid Residues Involved in Dipyridamole Interactions with Human and *Caenorhabditis elegans* Equilibrative Nucleoside Transporters[3]

[3] *A version of this chapter has been submitted for publication:*

F. Visser, S. A. Baldwin, R. E. Isaac, J. D. Young, C. E. Cass (2004) J. Biol. Chem.

Acknowledgements

Dr. Stephen Baldwin, Dr. R. Elwyn Isaac and Dr. James Young are collaborative principle investigators who helped obtained research funding for this project and aided in manuscript preparation.

Introduction

Nucleosides are hydrophilic molecules that require the presence of integral membrane transporter proteins to move across biological membranes (1-3). Nucleoside transporters are also responsible for cellular uptake of many nucleoside analogs used in the treatment of solid tumors, hematologic malignancies and viral diseases (4,5). Extracellular concentrations of adenosine, a signalling molecule that binds to G-protein coupled cell-surface receptors, are regulated by nucleoside transporters (6).

Members of the equilibrative nucleoside/nucleobase transporter (ENT) family have been identified in many eukaryotes and most mediate facilitated diffusion of nucleosides although some members are proton-coupled (7). All ENT family transporters appear to share a common membrane architecture with 11 transmembrane segments (TMs)[1] and a large cytoplasmic loop between TMs 6 and 7, and in many cases they possess a large glycosylated loop between TMs 1 and 2 (8).

Four ENT family members have been identified by molecular cloning from human tissues. The inhibitor nitrobenzylmercaptopurine ribonucleoside (NBMPR) functionally distinguishes human ENT1 (hENT1), which mediates equilibrative sensitive (*es*) transport activity, from hENT2, which mediates equilibrative insensitive (*ei*) transport activity (9-11). Moreover, hENT1 is two to three orders of magnitude more sensitive to inhibition by coronary vasodilator drugs such as dilazep and dipyridamole than hENT2 (12). No functional characteristics have been published for hENT3 or hENT4 (7,13,14).

Five ENT family members have been identified by sequence homology in the genomic database for *Caenorhabditis elegans* (15). *C. elegans* ENT1 and 2 (CeENT1 and 2) share 94% amino acid sequence identity and have been functionally characterized and determined to be sensitive to inhibition by the coronary vasodilator dipyridamole but insensitive to NBMPR and dilazep (15).

Several studies have addressed the mechanism of dipyridamole binding, which appears to compete with permeants and NBMPR for binding to the extracellular outward-facing conformation of mammalian *es* transporters at nanomolar concentrations, although

allosteric properties have been observed at micromolar concentrations (16-19). The mechanism of dipyridamole inhibition of CeENT1 has not been reported.

Knowledge of the amino acid residues involved in dipyridamole interactions with ENTs is extremely limited. In Chapter 3, a library of hENT1 mutants was screened for clones with reduced sensitivity to dilazep, resulting in the identification of residues 33 of hENT1 and hENT2 as important determinants of dilazep and dipyridamole interactions (12). The work described in this chapter used a similar approach to identify amino acid residues of hENT1 and CeENT1 involved in dipyridamole interactions. Dipyridamole was shown to be a competitive inhibitor of both uridine and adenosine influx mediated by recombinant hENT1 and CeENT1 produced in the yeast *Saccharomyces cerevisiae*, a result that supports a common structural model for dipyridamole binding by the two proteins. hENT1 and CeENT1 were then subjected to random mutagenesis and screened for dipyridamole-resistant clones by phenotypic complementation in *S. cerevisiae*. The hENT1 clones contained mutations in Met 33 in TM 1 whereas the CeENT1 clones contained mutations in Ile 429 in TM 11. Several different mutations of the corresponding residues of both proteins were generated and tested for dipyridamole sensitivity and uridine transport characteristics. The mutations that yielded the highest dipyridamole sensitivity for both proteins (Met in TM 1, Ile in TM11) were introduced into hENT2 to assess the involvement of these residues in dipyridamole interactions with this other important ENT family member. The hENT1 and CeENT1 mutants were also assessed for their ability to transport uridine. The combined results of the studies reported here indicated that the TM 1 and 11 residues were important for dipyridamole interactions and uridine transport by hENT1 and CeENT1.

Results

Dixon plot analysis of dipyridamole inhibition of hENT1 and CeENT1

To determine whether dipyridamole inhibited hENT1 and CeENT1 by a common mechanism, yeast cells producing recombinant hENT1 or CeENT1 were incubated with 10, 25 or 100 μM [^{3}H]-adenosine in the absence or presence of increasing concentrations of dipyridamole. Dixon plot analysis (32) of these data suggested that dipyridamole was a competitive inhibitor of adenosine transport for both proteins, with K_i values of 30.2 ± 1.4 and 395 ± 16 nM, respectively, for hENT1 and CeENT1 (Fig. 5-1A, B).

In a similar experiment, yeast cells producing recombinant hENT1 or CeENT1 were incubated with 50, 150 or 500 μM [^{3}H]-uridine in the absence or presence of increasing concentrations of dipyridamole. Dixon plot analysis of the resulting data suggested that dipyridamole was also a competitive inhibitor of uridine transport for both hENT1 and CeENT1 with K_i values of 40.2 ± 4.0 and 307 ± 41 nM, respectively (Fig. 5-1C, D) (32).

Random mutagenesis and screening of CeENT1

Growth of yeast cells in the presence of methotrexate and sulfanilamide results in depletion of TTP pools and growth arrest (33). Yeast lack endogenous plasma membrane transport systems for thymidine (34) but heterologous production of hENT1 results in transport of extracellular thymidine, which is subsequently metabolized to TMP by recombinant *Herpes simplex* thymidine kinase in KTK cells, thereby providing a functional complementation assay that bypasses the methotrexate/sulfanilamide-induced growth arrest (20,26,35). The yeast expression plasmids, pYPCeENT1 and pYPhENT1, were randomly mutated by propagation in the XL-1 RED mutator strain of *E. coli* (Stratagene, La Jolla, CA) and screened by complementation in KTK yeast cells for functional mutants with reduced sensitivity to dipyridamole. Screening of a hENT1 cDNA mutant library for dipyridamole resistance resulted in the isolation of >20 clones, all of which contained mutations in codon 33, which corresponds to Met 33, a residue previously identified in screens of a hydroxylamine-mutated hENT1 library for resistance to dilazep, a structurally unrelated inhibitor of hENT1 and hENT2 (12). Four separate

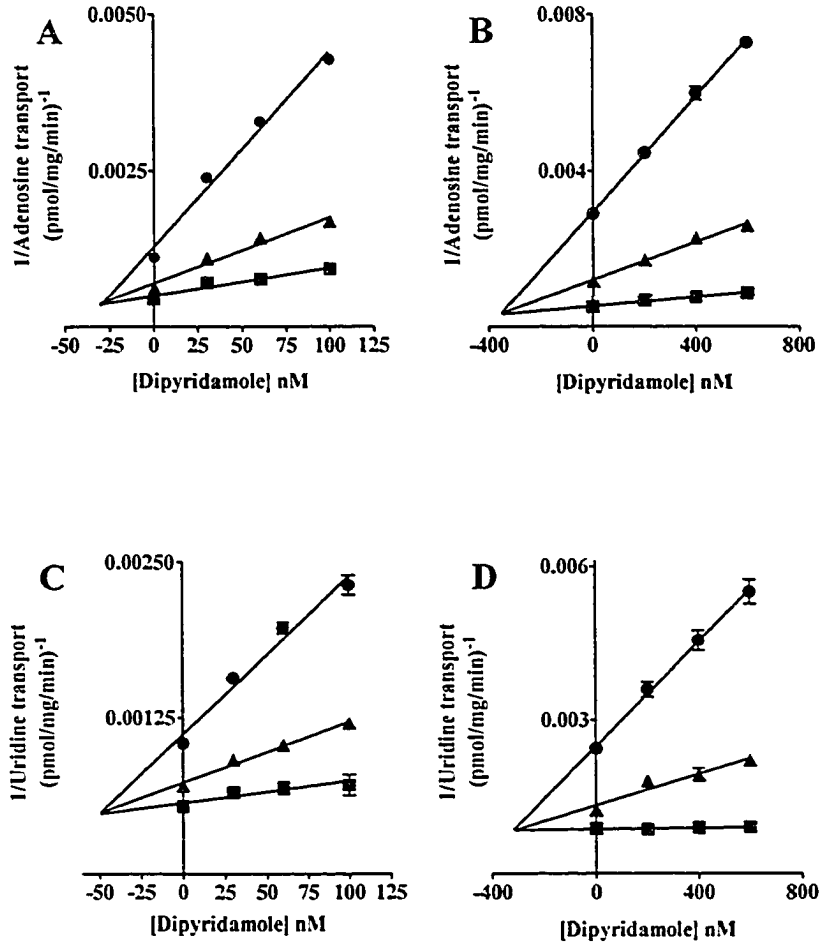

Figure 5-1. Dixon plot analysis of dipyridamole inhibition of hENT1 and CeENT1-mediated uridine and adenosine transport.

Yeast cells producing recombinant hENT1 or CeENT1 were incubated in the presence of 10 (●), 25 (▲) or 100 μM (■) [^{3}H]-adenosine (A, hENT1; B, CeENT1) or 50 (●), 150 (▲) or 500 μM (■) [^{3}H]-uridine (C, hENT1; D, CeENT1) for 10 min in the absence or presence of increasing concentrations of dipyridamole. Each point represents the mean ± S. E. of five determinations and where the point is larger than the S. E., it is not shown. The data were analyzed by linear regression using GraphPad Prism version 4.0 software. the slope and *y*-intercept of which were used to calculate the K_i values as the average *x*-value of the point of intersection for all the lines on the graph. The average K_i values from three separate experiments are presented in the text.

screens of the CeENT1 libraries resulted in the isolation of five clones, four of which did not contain mutations in the CeENT1 cDNA, and one of which contained a mutation in codon 429, resulting in the conversion of Ile 429 in TM 11 to Thr.

Multiple sequence alignments of the TM 1 regions of human, rat and *C. elegans* ENT1 and ENT2 revealed that a methionine is present at residue 33 in dipyridamole-sensitive hENT1 whereas an Ile is present in the insensitive transporters rENT1, rENT2 and hENT2 (Fig. 5-2). The corresponding residue in CeENT1 and CeENT2 (i.e., Ile 49) was the same as in the dipyridamole-insensitive mammalian transporters.

Multiple sequence alignments of the TM 11 regions of the human, rat and *C. elegans* ENT1 and ENT2 proteins revealed that the four mammalian transporters contained a Leu whereas both CeENT1 and CeENT2 contained an Ile at the corresponding positions (i.e., positions 442 in hENT1 and 429 in CeENT1). Thus, this residue could not be responsible for the observed differences in dipyridamole sensitivity of the transporters. Furthermore, these sequence alignments suggested that the determinants of high sensitivity to dipyridamole were complex, involving the contributions of several residues on different parts of the protein.

Concentration-effect relationships for dipyridamole inhibition of hENT1, CeENT1 and various mutants

To determine the effects of mutations at the identified amino acid residues of hENT1 (Met 33 and Leu 442) and CeENT1 (Ile 49 and Ile 429), site-directed mutagenesis was undertaken to generate additional mutants at these positions in addition to those identified by random mutagenesis and screening. Several of the resulting mutants exhibited functional activity: hENT1-M33I, M33A, L442T, L442I and CeENT1-I49M, I49A, I429L and I429T. Two mutants, hENT1-M33T and L442A, did not display any measurable transport activity.

To determine dipyridamole sensitivities, yeast cells producing CeENT1, hENT1 or one of the various mutants were incubated in the absence (control) or presence of increasing concentrations of dipyridamole (Table 5-1, Fig. 5-3). The hENT1-M33I and hENT1-M33A mutants, respectively, displayed significantly higher ($p < 0.05$) IC_{50} values (either 27-fold higher than that of hENT1 or totally insensitive), whereas CeENT1,

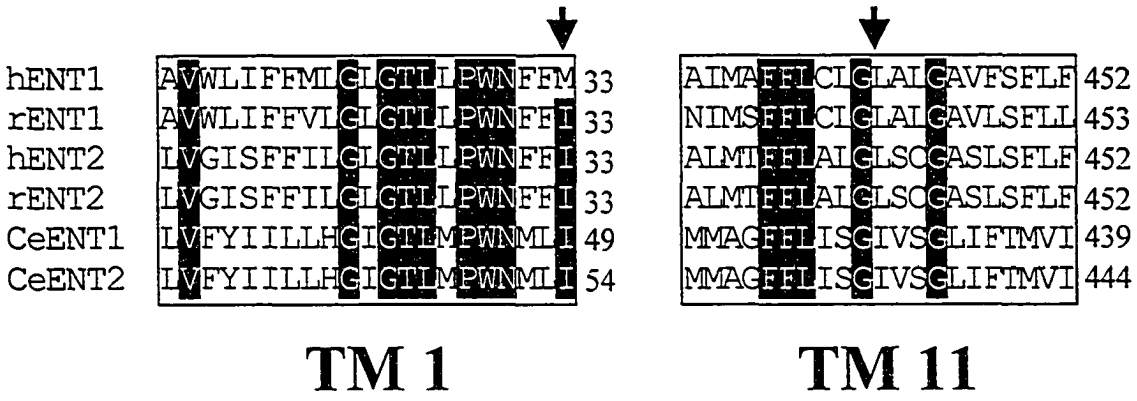

Figure 5-2. Multiple sequence alignment of the TM 1 and TM 11 segments of the human, rat and C. elegans ENT1 and 2 proteins.

The positions of the TM 1 (Met 33 in hENT1 and Ile 49 in CeENT1) and TM 11 (Leu 442 in hENT1 and Ile 429 in CeENT1) residues analyzed in this study are indicated by arrows. Genbank accession numbers are AAC51103 (hENT1), AAB88049 (rENT1), AAC39526 (hENT2), AAB88050 (rENT2), AAM46663 (CeENT1) and CAB01882 (CeENT2). Residues are shaded if they are homologous in $\geq$ 75% of the sequences. Multiple sequence alignment was performed using DNAMAN version 4.03 using the BLOSUM 62 substitution matrix.

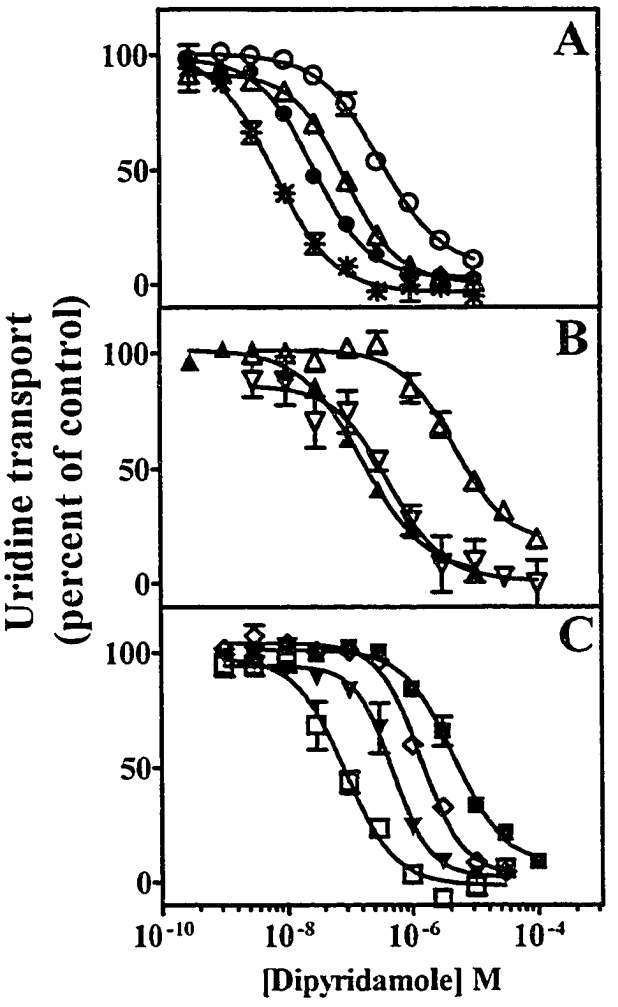

Figure 5-3. Concentration-effect relationships for dipyridamole inhibition of uridine transport by hENT1, CeENT1, hENT2 and various mutants.

Yeast cells producing recombinant hENT1 (A, ●), hENT1-M33I (A, O), hENT1-L442I (A, ✳), hENT1-M33I/L442I (A, △), CeENT1 (B, ▲), CeENT1-I429T (B, △), CeENT1-I49M/I429T (B, ▽), hENT2 (C, ■), hENT2-I33M (C, ▼), hENT2-L442I (C, ◇) and hENT2-I33M/L443I (C, □) were incubated with 1 μM [^{3}H]-uridine for 10 min in the absence (control) or presence of graded concentrations of dipyridamole. Each point is presented as the mean ± S. E. (n = 4) and where the points are larger than the S. E., it is not shown. Average IC_{50} values from three separate experiments were determined by nonlinear regression using GraphPad Prism version 4.0 software and are presented in Table 5-1.

Table 5-1. IC_{50} values for dipyridamole inhibition of the hENT1, rENT1, CeENT1 or hENT2 TM1 and 11 mutants

Average IC_{50} values (± S.E.) from three separate experiments were determined using GraphPad Prism version 4.0 software by nonlinear regression analysis. Some representative curves are presented in Fig. 5-3.

Protein	TM	IC_{50}	Ratio[α]	*p* value
		nM		
hENT1		29.7 ± 2.0	1.0	1.0[β]
M33I	1	811 ± 139	27	0.0049[β]
M33A	1	>30,000	>>>	ND
L442T	11	22.4 ± 1.9	0.75	0.057[β]
L442I	11	10.1 ± 1.4	0.34	0.0013[β]
M33I/L442I	1/11	103 ± 6	3.5	0.0070[γ]
M33A/L442I	1/11	597 ± 71	20	ND
CeENT1		181 ± 11	1.00	1.0000[δ]
I49M	1	152 ± 11	0.84	0.14[δ]
I49A	1	135 ± 15	0.75	0.069[δ]
I429L	11	733 ± 114	4.05	0.0085[δ]
I429T	11	3560 ± 620	20	0.0055[δ]
I49M/I429L	1/11	173 ± 19	0.96	0.0084[ε]
I49M/I429T	1/11	766 ± 261	4.2	0.014[φ]
rENT1		10500± 2300	1.0	1.0000
hENT2		4440 ± 510	1.0	1.0000[π]
I33M	1	484 ± 49	0.11	0.0015[π]
L442I	11	1500 ± 137	0.34	0.0051[π]
I33M/L442I	1/11	87.5 ± 21.3	0.02	0.0010[π]

[α]Ratio= Mutant IC50/Wildtype IC50.
[β]tested against hENT1
[γ]tested against hENT1-M33I
[δ]tested against CeENT1
[ε]tested against CeENT1-I429L
[φ]tested against CeENT1-I429T
[π]tested against hENT2
ND, not determined

CeENT1-I49M and I49A displayed similar IC_{50} values ($p > 0.05$). CeENT1-I429L and I429T displayed IC_{50} values that were 4.1 and 20-fold higher ($p < 0.05$), respectively, than those of CeENT1, whereas the values of hENT1-L442T and L442I were, respectively, similar to and 34 % ($p < 0.05$) of the hENT1 value. These results showed that only TM 11 mutations affected the dipyridamole sensitivity of CeENT1 whereas both TM 1 and 11 mutations affected the dipyridamole sensitivity of hENT1.

rENT1, the rat isoform of hENT1, is relatively insensitive to dipyridamole (36). The multiple sequence alignments of Fig. 5-2 demonstrated that rENT1 contains an Ile at the TM 1 position and a Leu at the TM 11 position. The concentration-effect relationship for dipyridamole inhibition of rENT1 was determined, revealing an IC_{50} value of 10500 ± 2300 nM, which was 58 and 350-fold higher than the values for CeENT1 and hENT1, respectively (Table 5-1). Although it was much less sensitive than hENT1 and CeENT1, rENT1 was capable of interacting with dipyridamole. That both hENT1 and rENT1 contain a Leu residue at the TM 11 position suggested that this residue contributed to dipyridamole binding by both transporters rather than being responsible for their differences in sensitivity.

For both hENT1 and CeENT1, a Met at the TM 1 position and an Ile at the TM 11 position were consistent with high sensitivities to dipyridamole. This was further investigated by combining the CeENT1 TM 11 mutants with reduced sensitivities, I429L and I429T, with the TM 1 mutant with high sensitivity, I49M. The concentration-effect relationships for dipyridamole inhibition of uridine transport by CeENT1-I49M/I429L and I49M/I429T were determined (Table 5-1). CeENT1-I49M/I429T displayed an IC_{50} value that was 22 % of that of CeENT1-I429T ($p < 0.05$) and 4.2-fold higher than that of CeENT1 (Fig. 5-3B). CeENT1-I49M/I429L displayed an IC_{50} value that was 24 % of that of CeENT1-I429L ($p < 0.05$) and similar to that of CeENT1. This partial and complete restoration, respectively, of sensitivity to dipyridamole in the two residue 429 mutants, brought about by the presence of a Met residue at position 49, suggested the involvement of a functional interaction between TM 1 and TM 11 in binding of dipyridamole by CeENT1.

To complement these observations on CeENT1, the hENT1 TM 1 mutants, which were less sensitive to dipyridamole than wildtype hENT1, were combined with the L442I

mutation. The concentration-effect relationships for dipyridamole inhibition of uridine transport by hENT1-M33I/L442I and M33A/L442I were then determined (Table 5-1). hENT1-M33I/L442I displayed an IC_{50} value that was 13 % of that of hENT1-M33I ($p < 0.05$) and 3.5-fold higher than that of hENT1 (Fig. 5-3A). hENT1-M33A/L442I displayed an IC_{50} value that was much lower than that of the highly insensitive hENT1-M33A and 20-fold higher than that of hENT1. The observation that the introduction of the L442I mutation to hENT1, hENT1-M33I and M33A decreased their IC_{50} values for dipyridamole inhibition implies a functional interaction between TM 1 and TM 11 in dipyridamole binding by hENT1, similar to the interaction hypothesized above for CeENT1. Thus, the mutational analyses of dipyridamole sensitivity in ENT family members from divergent sources suggested that both the TM 1 and 11 positions contributed to dipyridamole sensitivities.

Concentration-effect relationships for dipyridamole inhibition of hENT2 and various mutants

To determine if the TM 1 and 11 positions also contributed to the relative insensitivity of hENT2 to dipyridamole, site-directed mutagenesis was employed to generate hENT2-I33M, L442I and I33M/L442I. The concentration-effect relationships for dipyridamole inhibition of uridine transport by hENT2, or the various hENT2 mutants, were then determined (Table 5-1, Fig. 5-3C). hENT2-I33M and L442I displayed IC_{50} values that were 11 % and 34 %, respectively, of that of hENT2 ($p < 0.05$). The double mutant, I33M/L442I, displayed an IC_{50} value that was 2 % of that of hENT2 ($p < 0.05$). The additive effect of these mutations suggested that both the TM 1 and 11 positions contributed to the weakness of dipyridamole interaction with hENT2.

Kinetic parameters of uridine transport for hENT1, CeENT1 and various mutants

To assess the effects of mutations at either the TM 1 or 11 positions on permeant transport characteristics, the apparent K_m and V_{max} values of uridine transport by yeast cells producing hENT1, CeENT1 or one of the mutants were determined by assaying transport rates at increasing concentrations of [^{3}H]-uridine (Table 5-2, Fig. 5-4). Recombinant hENT1- and CeENT1-mediated uridine transport conformed to simple

Michaelis-Menten kinetics and displayed apparent K_m values of 36.4 ± 6.0 and 100 ± 13 μM, respectively, and apparent V_{max} values of 537 ± 18 and 955 ± 35 pmol/mg/min, respectively (Fig. 5-4). That CeENT1 displayed a lower apparent affinity for uridine than hENT1 was consistent with the results generated by production of these proteins in *Xenopus laevis* oocytes (37).

Although there were no differences between the kinetic values obtained for hENT1 and hENT1-M33I, hENT1-M33A displayed a modestly increased K_m value and a reduced V_{max} value. CeENT1-I49M displayed a reduced K_m value whereas CeENT1-I49A displayed a modestly increased K_m value and a modestly reduced V_{max} value. These data suggested that the presence of an Ala residue at the TM 1 position resulted in reduced apparent affinities and transport capacities of both hENT1 and CeENT1.

Like the mutations in TM 1, conservative substitutions of the hydrophobic Leu and Ile residues at the TM 11 positions in hENT1 and CeENT1, respectively, had only minor effects on transport activity. hENT1-L442I displayed a modestly higher K_m value than hENT1, while CeENT1-I429L displayed similar kinetic properties to CeENT1 (Table 5-2). In contrast, the less conservative substitution of these residues by Thr markedly reduced the apparent affinities of the transporters for uridine: hENT1-L442T displayed a K_m value that was 10-fold higher than that of hENT1 (Fig. 5-4A, Table 5-2), and CeENT1-I429T displayed a K_m value that was 3.4-fold higher than that of CeENT1 (Fig. 5-4B, Table 5-2).

The kinetic properties of the TM 1 / TM 11 double mutants of hENT1 and CeENT1 were roughly consistent with those of the corresponding single mutants. Thus, while the K_m values for M33I and L442I were, respectively, smaller and larger than that of wildtype hENT1, the K_m value of the double mutant hENT1-M33I/L442I was similar to the wildtype value. hENT1-M33A/L442I exhibited a modestly raised K_m, similar to the K_m values of either single mutation alone. Likewise, CeENT1-I49M/I429L displayed similar kinetic parameters to those of the wildtype protein. In contrast, the double mutant CeENT1-I49M/I429T, which contained the less conservative Thr substitution at the TM 11 position, displayed a K_m value that was not only 9.6-fold higher than that of the wildtype protein but 2.8-fold higher than that of the corresponding single mutant (i.e.,

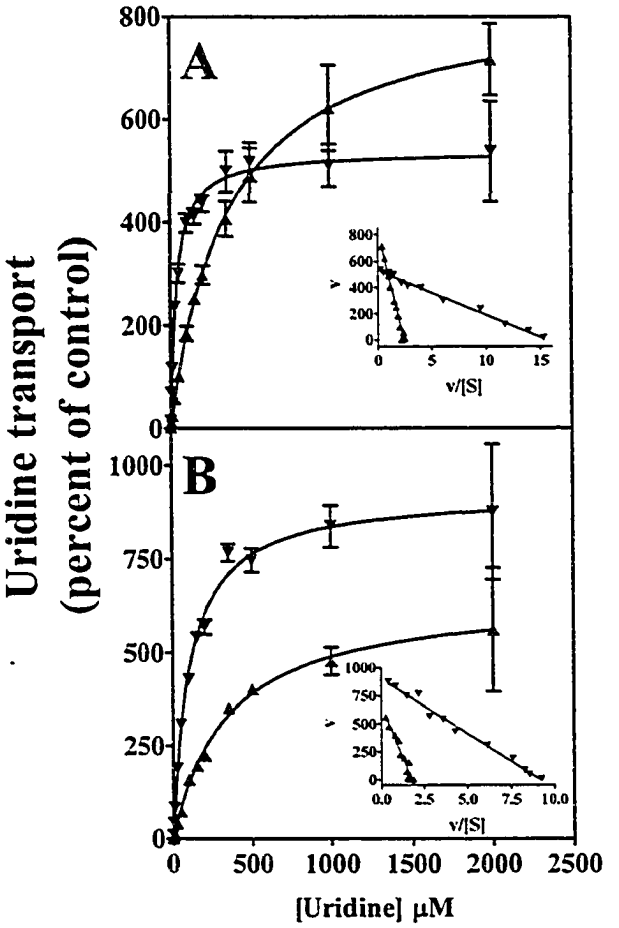

Figure 5-4. Concentration-dependence of uridine transport by hENT1, hENT1-L442T, CeENT1 and CeENT1-I429T.

Yeast cells containing pYPhENT1 (A, ▼), pYPhENT1-L442T (A, ▲), pYPCeENT1 (B, ▼) or pYCeENT1-L429T (B, ▲) were incubated for 20 min with increasing concentrations of [^{3}H]-uridine. The Eadie-Hofstee plots are presented in the *insets*. The transport rates presented were derived from the difference between uptake observed in the absence and presence of 10 mM unlabeled thymidine at each uridine concentration. K_m and V_{max} values were obtained by nonlinear regression analysis using GraphPad Prism version 4.0 software and are presented in Table 5-2. Each point is presented as the mean ± S.E. (n=4), and where the size of the point is larger than the S.E., it is not shown.

Table 5-2. Kinetic properties of uridine transport for hENT1, CeENT1 and their respective TM 1 and TM 11 mutants

K_m and V_{max} values were determined using GraphPad Prism version 4.0 software, by nonlinear regression analysis. Representative plots for hENT1, hENT2-L442T, CeENT1 and CeENT1-I429T are presented in Fig. 5-4. The V_{max} values and V_{max}:K_m ratios are expressed in units of pmol/mg total protein/min.

Protein	Apparent K_m	Apparent V_{max}	V_{max}:K_m
	μM	*pmol/mg/min*	*pmol/mg/min/μM*
hENT1	36.4 ± 6.0	537 ± 18	14.8
M33I	30.2 ± 3.1	411 ± 8.7	13.6
M33A	57.5 ± 10.8	263 ± 13	4.6
L442I	66.0 ± 6.1	715 ± 17	10.8
L442T	364 ± 46	847 ± 46	2.3
M33I/L442I	27.8 ± 4.8	658 ± 23	23.7
M33A/L442I	63.7 ± 9.9	424 ± 17	6.7
CeENT1	100 ± 13	955 ± 35	9.6
I49M	63.5 ± 12.7	978 ± 48	15.4
I49A	156 ± 12.9	809 ± 21	5.2
I429L	86.2 ± 8.3	925 ± 24	10.7
I429T	338 ± 48	655 ± 48	1.9
I49M/I429L	135 ± 24	892 ± 50	6.6
I49M/I429T	958 ± 144	1680 ± 130	1.8

CeENT1-I429T). Taken together, these results indicated that a Thr at the TM 11 position compromised the uridine transport functions of both hENT1 and CeENT1.

Discussion

In the study described in this chapter, dipyridamole was shown to be a potent competitive inhibitor of uridine and adenosine transport for both recombinant hENT1 and CeENT1 (Fig. 5-1). Therefore, despite limited amino acid sequence identity (26%), both hENT1 and CeENT1 were able bind dipyridamole with high affinities and in competitive manner with respect to the physiological permeants uridine and adenosine. This common mechanism of inhibition suggested that the residues involved in dipyridamole binding by recombinant hENT1 and CeENT1 may be conserved and was consistent with previous studies, which suggested that the dipyridamole binding site overlaps with the exofacial permeant binding site of ENT transporters (16,18,38).

Random mutagenesis and screening for dipyridamole resistance by functional complementation in yeast resulted in identification of Ile 429 in TM 11 of CeENT1 and Met 33 in TM 1 of hENT1 as key residues. Multiple sequence alignments of highly dipyridamole-sensitive transporters (hENT1, CeENT1 and CeENT2) versus much less dipyridamole-sensitive transporters (rENT1, rENT2 and hENT2) revealed that these positions were always occupied by residues with large hydrophobic side chains, namely either Met or Ile in TM 1, and either Leu or Ile in TM 11 (Fig. 5-2). Interestingly, while a Met at position 33 of mammalian transporters is associated with high dipyridamole sensitivity (12), CeENT1 and CeENT2 contain an Ile at the corresponding position. Conversely, while all the mammalian transporters contain a Leu at the TM 11 position, regardless of their dipyridamole sensitivity, the corresponding residue in CeENT1 and CeENT2 is Ile. The multiple sequence alignments therefore suggested that binding of dipyridamole is complex, involving contributions from several residues on different parts of the proteins. The presence of a common, complex dipyridamole binding site in multiple members of the ENT family is supported by the demonstration here, that not only hENT1 and CeENT1, but also hENT2 and rENT1, exhibited dipyridamole sensitivity, albeit to very different extents. The observed differences were consistent with the findings of previous studies (9,10,36,37,39,40).

The results of the mutagenesis and dipyridamole concentration-effect relationship studies (Table 5-1, Fig. 5-3) suggested that both the TM 1 and 11 residues contributed to dipyridamole binding by hENT1, CeENT1 and hENT2. The fact that similar single mutations of either hENT1 or CeENT1 had opposite effects on dipyridamole sensitivity warrants explanation (Table 5-1). It is possible that the TM 1 residue of hENT1 plays the same role in dipyridamole binding as the TM 11 residue of CeENT1. In hENT1, the TM 11 residue only contributes to dipyridamole interactions when mutated to Ile and/or when the TM 1 residue is first mutated. Similarly, the TM 1 residue of CeENT1 is not involved in dipyridamole binding unless the TM 11 residue is first mutated. That the TM 1 and 11 residues are able to compensate for each other with respect to dipyridamole binding in hENT1 and CeENT1 suggests that mutation of one residue affects the conformation of the other. The structure of dipyridamole has a two-fold symmetry (Fig. 1-4), suggesting that similar interactions are possible at identical moieties on opposite ends of the molecule and it is likely that TMs 1 and 11 are positioned on opposite sides of the dipyridamole binding site. In hENT1-L442I and hENT2-I33M/L442I, both residues evidently contribute simultaneously to dipyridamole binding, suggesting that, while far apart in the primary structure of the protein, these two residues are likely close to one another in the folded protein, as is the case for other membrane transporters. For example, in the *Escherichia coli* lactose transporter LacY, TM 11 is adjacent to TM 2 (41). In CeENT1, the conformations of TMs 1 and 11 may be subtly different such that these residues are too far apart to simultaneously contribute to dipyridamole binding.

Functional analysis of the TM 1 and 11 mutants of hENT1 and CeENT1 (i.e., determination of kinetic parameters for uridine transport) revealed that, for both proteins, an Ala residue at the TM 1 position resulted in a modestly higher K_m value and a reduced V_{max} value, yielding reduced V_{max}:K_m ratios, a measure of transporter efficiency (Table 5-2). A Thr at the TM 11 position resulted in greatly increased K_m values for both proteins (Table 5-2, Fig. 5-4). Combining the I429T and I49M mutations of CeENT1 resulted in a K_m value that was ~10-fold higher than that of wildtype, even though the I49M mutation alone decreased the K_m value for uridine. CeENT1-I49M/I429T represented the equivalent of hENT1-L442T, with a Met at the TM 1 position and a Thr at the TM 11 position, and for both proteins, the resulting K_m values of the mutants were ~10-fold

higher than those of the wildtype proteins. These results supported a common role for the TM 1 and 11 positions in uridine transport by hENT1 and CeENT1.

In conclusion, this work identified two residues, one in each of TMs 1 and 11 of hENT1 and CeENT1, that were functionally and conformationally linked with respect to dipyridamole binding and contributed similarly to uridine transport efficiency in both proteins. The role of these residues in dipyridamole interactions with ENT family proteins was further confirmed in mutational analysis of hENT2. It is unclear whether these residues line the permeant translocation channel and/or the dipyridamole binding sites without detailed structural data. This question could also be addressed in a follow-up substituted cysteine-accessibility study.

References

1. Vickers, M. F., Young, J. D., Baldwin, S. A., and Cass, C. E. (2000) *Emerging Therapeutic Targets* **4**, 515-539

2. Cass, C. E., Young, J. D., Baldwin, S. A., Cabrita, M. A., Graham, K. A., Griffiths, M., Jennings, L. L., Mackey, J. R., Ng, A. M. L., Ritzel, M. W. L., Vickers, M. F., and Yao, S. Y. M. (1999) in *Membrane Transporters as Drug Targets* (Amidon, G. L., and Sadee, W., eds) Vol. 12, 1 Ed., 12 vols., Kluwer Academic/Plenum Publishers

3. Griffith, D. A., and Jarvis, S. M. (1996) *Biochim Biophys Acta* **1286**, 153-181

4. Baldwin, S. A., Mackey, J. R., Cass, C. E., and Young, J. D. (1999) *Mol Med Today* **5**, 216-224

5. Cass, C. E. (1995) in *Drug Transport in Antimicrobial and Anticancer Chemotherapy* (Georgopapadakou, N. H., ed), pp. 403-451, Marcel Deker, New York, NY

6. Van Belle, H. (1993) *Cardiovasc Res* **27**, 68-76

7. Hyde, R. J., Cass, C. E., Young, J. D., Baldwin, S. A. (2001) *Mol Memb Biol* **18**, 53-63

8. Sundaram, M., Yao, S. Y., Ingram, J. C., Berry, Z. A., Abidi, F., Cass, C. E., Baldwin, S. A., and Young, J. D. (2001) *J Biol Chem* **2**, 2

9. Griffiths, M., Beaumont, N., Yao, S. Y., Sundaram, M., Boumah, C. E., Davies, A., Kwong, F. Y., Coe, I., Cass, C. E., Young, J. D., and Baldwin, S. A. (1997) *Nat Med* **3**, 89-93

10. Griffiths, M., Yao, S. Y., Abidi, F., Phillips, S. E., Cass, C. E., Young, J. D., and Baldwin, S. A. (1997) *Biochem J* **328**, 739-743

11. Crawford, C. R., Patel, D. H., Naeve, C., and Belt, J. A. (1998) *J Biol Chem* **273**, 5288-5293

12. Visser, F., Vickers, M. F., Ng, A. M., Baldwin, S. A., Young, J. D., and Cass, C. E. (2002) *J Biol Chem* **277**, 395-401.

13. Baldwin, S. A., Beal, P. R., Yao, S. Y., King, A. E., Cass, C. E., and Young, J. D. (2004) *Pflugers Arch* **447**, 735-743

14. Acimovic, Y., and Coe, I. R. (2002) *Mol Biol Evol* **19**, 2199-2210

15. Appleford, P. J., Griffiths, M., Yao, S. Y., Ng, A. M., Chomey, E. G., Isaac, R. E., Coates, D., Hope, I. A., Cass, C. E., Young, J. D., and Baldwin, S. A. (2004) *Mol Membr Biol* **21**, 247-260

16. Jarvis, S. M., McBride, D., and Young, J. D. (1982) *J Physiol (Lond)* **324**, 31-46

17. Jarvis, S. M., Janmohamed, S. N., and Young, J. D. (1983) *Biochem J* **216**, 661-667

18. Jarvis, S. M. (1986) *Mol Pharmacol* **30**, 659-665

19. Hammond, J. R. (1991) *Mol Pharmacol* **39**, 771-779

20. Dixon, M. (1953) *Biochem J* **55**, 170-171

21. Barclay, B. J., Kunz, B. A., Little, J. G., and Haynes, R. H. (1982) *Can J Biochem* **60**, 172-184

22. Grenson, M. (1969) *Eur J Biochem* **11**, 249-260

23. Hogue, D. L., Ellison, M. J., Young, J. D., and Cass, C. E. (1996) *J Biol Chem* **271**, 9801-9808

24. Hogue, D. L., Ellison, M. J., Vickers, M., and Cass, C. E. (1997) *Biochem Biophys Res Commun* **238**, 811-816

25. Vickers, M. F., Mani, R. S., Sundaram, M., Hogue, D. L., Young, J. D., Baldwin, S. A., and Cass, C. E. (1999) *Biochem J* **339**, 21-32

26. Yao, S. Y., Ng, A. M., Muzyka, W. R., Griffiths, M., Cass, C. E., Baldwin, S. A., and Young, J. D. (1997) *J Biol Chem* **272**, 28423-28430

27. Appleford, P. J., Griffiths, M., Yao, S. Y. M., Ng, A. M. L., Chomey, E. G., Isaac, R. E., Coates, D., Hope, I. A., Cass, C. E., Young, J. D., and Baldwin, S. A. (2004) *Mol Membr Biol* **In press**

28. Paterson, A. R., Lau, E. Y., Dahlig, E., and Cass, C. E. (1980) *Mol Pharmacol* **18**, 40-44

29. Smits, P. H., De Haan, M., Maat, C., and Grivell, L. A. (1994) *Yeast* **10 Suppl A**, S75-80

30. Ward, J. L., Sherali, A., Mo, Z. P., and Tse, C. M. (2000) *J Biol Chem* **275**, 8375-8381

31. Abramson, J., Smirnova, I., Kasho, V., Verner, G., Kaback, H. R., and Iwata, S. (2003) *Science* **301**, 610-615

Chapter 6: Identification and Characterization of Amino Acid Residues of Human Equilibrative Nucleoside Transporter 1 Involved in High-Affinity Interactions with Coronary Vasodilator Drugs

Introduction

Nucleosides are hydrophilic molecules that do not readily diffuse across biological membranes and act as the metabolic precursors of fundamental biological molecules such as DNA, RNA and ATP. Nucleoside analogs are antimetabolite agents used in the treatment of various cancers and viral diseases (1). Specialized integral membrane nucleoside transporter proteins mediate the cellular uptake and release of free nucleosides (2). The equilibrative nucleoside transporter (ENT) family has many members in eukaryotic organisms and most mediate facilitated diffusion of nucleosides according to their concentration gradients although some members are proton-coupled (3). ENTs appear to share a common membrane architecture consisting of 11 transmembrane segments (TMs), a large loop between TMs 1 and 2 and a large cytoplasmic loop between TMs 6 and 7 (4). In mammalian cells, hENT1 and hENT2 are responsible for the two major plasma membrane ENT processes, designated as equilibrative sensitive (*es*) or equilibrative insensitive (*ei*), respectively, in accordance with their sensitivities to the inhibitor nitrobenzylmercaptopurine ribonucleoside (NBMPR) (5-8). hENT1 and hENT2 both transport a broad range of physiological nucleosides and nucleoside analogs but differ functionally in that hENT2 is capable of transporting nucleobases and generally displays lower affinities for its permeants (9,10).

Adenosine is a signalling molecule that, when released from cells in response to ischemia or hypoxia-induced ATP depletion, binds to cell-surface adenosine receptors to induce a wide range of protective mechanisms, including vasodilation and prevention of platelet aggregation, excitatory neurotransmitter release and inflammatory responses (11). The primary mechanism by which the protective effects of adenosine are terminated is by its reuptake through ENTs that are present in high abundance on endothelial cells (12). Highly potent inhibitors of nucleoside transport, including draflazine, soluflazine, dilazep, dipyridamole and NBMPR, have been developed to block ENT-mediated adenosine uptake as a means to potentiate the protective effects of adenosine (5). These inhibitors do not share any structural similarities with each other, with the exception of draflazine and soluflazine, and only NBMPR is a nucleoside. All of the inhibitors are

capable of inhibiting hENT1 and hENT2-mediated nucleoside transport with nanomolar and micromolar affinities, respectively.

The mechanisms of inhibition of dipyridamole, dilazep, NBMPR and draflazine have been addressed in several studies. Dipyridamole was shown to be a competitive inhibitor when present at nanomolar concentrations and allosteric at micromolar concentrations whereas dilazep was shown to bind allosterically or competitively depending on pH due to two ionzable groups with pKa values of ~5 and 8 (13-19). Using random mutagenesis and screening by phenotypic complementation in yeast (Chapter 3), residue 33, the last residues in TMs 1 of hENT1 and hENT2, was identified as important for binding of dilazep and dipyridamole (20). The mechanism of NBMPR binding has been shown to be either competitive or allosterically linked to the binding site for nucleosides (13,14,19), although recent molecular evidence suggests that L92, G154 and G179 of hENT1 are involved in both the permeant translocation channel and NBMPR binding (21-23). Draflazine was shown to be a mixed inhibitor of permeant transport and NBMPR binding but the molecular determinants of draflazine and soluflazine binding have not been identified (24-28).

The aim of the work described in this chapter was to identify additional amino acid residues of hENT1 involved in binding of dilazep, dipyridamole and/or NBMPR as well as those involved in binding of draflazine and soluflazine. The random mutagenesis and functional complementation screening methods that were previously employed in the identification of M33 and L442 of hENT1 (see Chapters 3 and 5) were utilized to identify W29, F80, N338 and F334 of hENT1 as previously unrecognized residues involved in inhibitor binding (20). A series of mutants, largely based on their identities in other ENT family members, was generated at each residue and tested for adenosine transport activity and inhibitor sensitivities. Although M33 and L442 were characterized in detail in Chapters 3, 4 and 5, a series of mutants at each of these positions were also generated and tested for adenosine transport and inhibitor sensitivities for completeness and also because their roles in draflazine and soluflazine interactions are unknown. Quantitative immunofluorescence confocal microscopy was employed to assess the localization and levels of recombinant protein abundance for each mutant. The results of these studies were used to construct a preliminary model of inhibitor binding and are discussed in

relation to the early pharmacological studies regarding the mechanism of inhibitor binding.

Results

Random mutagenesis and screening

Growth of yeast cells in the presence of methotrexate and sulfanilamide results in the depletion of TTP pools and growth arrest (29). Although yeast cells lack endogenous thymidine transport systems (30), production of recombinant hENT1 allows for salvage from the external medium of thymidine, which is then phosphorylated to TMP by recombinant *Herpes simplex* thymidine kinase in KTK yeast cells (31). When a nucleoside transport inhibitor is added, thymidine salvage through hENT1 is blocked, providing a functional complementation assay for hENT1 mutants with a reduced affinity for inhibitors. The yeast expression plasmid pYPhENT1 was randomly mutated by propagation in the *E. coli* mutator strain XL-1 RED (Stratagene) and transformed into KTK yeast under complementation conditions in the presence of inhibitory concentrations of dilazep, dipyridamole or draflazine. Soluflazine was not tested because high concentrations were required to inhibit complementation and there were insufficient quantities available for screening. Positive clones with mutations resulting in the following amino acid residue changes (screening inhibitor is given in parentheses) were identified: W29G (dilazep), M33I (dilazep, dipyridamole), F80C (dipyridamole), F334S (dipyridamole) and N338S (draflazine). Although M33 was identified in a similar screen of a hydroxylamine-mutated pYPhENT1 library for dilazep resistance (Chapter 3) (20), the other four residues have not been identified previously. W29 and M33 are located in TM 1, F80 in TM 2, F334 and N338S in TM 8 and :L442 in TM 11 (Fig. 6-1) (4).

Multiple sequence alignment of TMs 1, 2, 8 and 11

To assess the identities of the corresponding residues in other ENT family members from a variety of different organisms, multiple sequence alignment analysis was performed for TMs 1, 2, 8 and 11 (Fig. 6-2). In TM 1, W29 is conserved in all ENTs from non-protozoan organisms and in PfENT1 from *Plasmodium falciparum*, suggesting that this residue may play a role in the structure or function of ENTs. M33 corresponds to large aliphatic or aromatic side chains in other ENTs with the exceptions of LdNT2

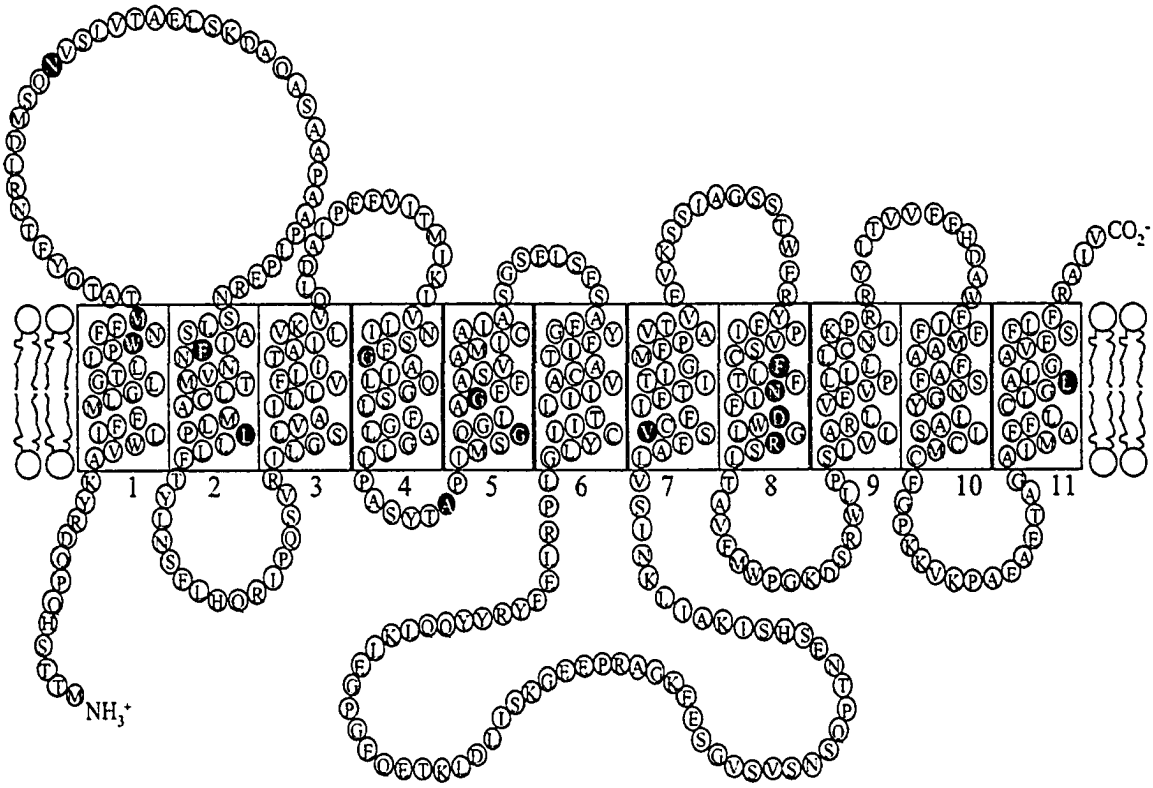

Figure 6-1. Toplogy model of hENT1.

The topology model of hENT1 contains 11 TMs (4). The location of the amino acid residues identified in the studies of this thesis are indicated by the shaded circles whereas those identified in other studies are indicated by the black-filled circles.

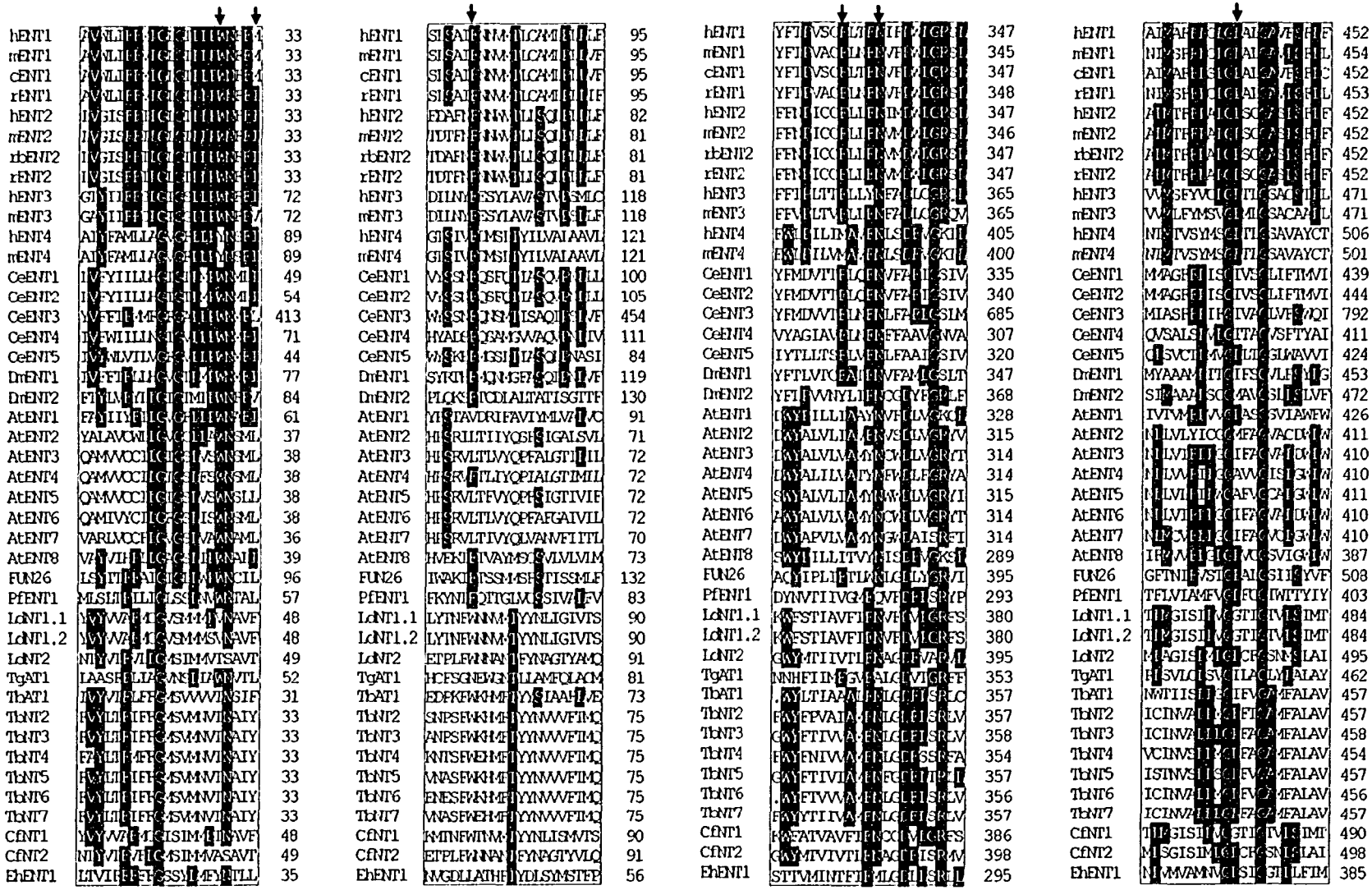

Figure 6-2. Multiple sequence alignment of the TMs 1, 2, 8 and 11 regions of ENT family proteins.

The protein sequences of 43 ENT family members were obtained from GenBank™ using the accession numbers AAC51103 (human; hENT1), AAF78452 (mouse; mENT1), AAS99848 (canine; cENT1), AAB88049 (rat; rENT1), AAC39526 (hENT2), AAF78477 (mENT2), AAK11605 (rabbit; rbENT2), AAB88050 (rENT2), AF326987 (hENT3), AF326986 (mENT3), NP_694979 (hENT4), AAH25599 (mENT4), AAM46663 (*Caenorhabditis elegans*; CeENT1), CAB01882 (CeENT2), CAB01223 (CeENT3), CAB62793 (CeENT4), AAA98003 (CeENT5), AAF52405 (*Drosophila melanogaster*; DmENT1), AAL28809 (DmENT2), NP_564987 (*Arabidopsis thaliana*; AtENT1), AAL25095 (AtENT2), AAL25096 (AtENT3), AAL25097 (AtENT4), NP_192423 (AtENT5) AAL25098 (AtENT6), AAL25094 (AtENT7), AAO31974 (AtENT8), P31381 (*Saccharomyces cerevisiae*; FUN26), AAG09713 (*Plasmodium falciparum*, PfENT1), AAC32597 (*Leishmania donovani*; LdNT1.1), AAC32315 (LdNT1.2), AAF74264 (LdNT2), AAF03246 (*Toxoplasma gondii*; TgAT1), AAD45278 (*Trypanosoma brucei*; TbAT1), AAQ16072 (TbNT2), AAQ16077 (TbNT3), AAQ16079 (TbNT4), AAQ16081 (TbNT5), AAQ16089 (TbNT6), AAQ16085 (TbNT7), AAG22610 (*Crithidia fasciculata*; (CfNT1), AAG22611 (CfNT2) and S49592 (*Entamoeba histolytica*; EhENT1) and subjected to multiple sequence alignment with DNAMAN version 4.03 software using the BLOSUM 62 substitution matrix. Residues that were identical in ≥ 33 % of sequences are shaded.

from *Leishmania donovani* and CfNT2 from *Crithidia fasciculata*, which contain Thr residues at this position.

In TM 2, F80 is highly conserved in mammalian, nematode and insect ENTs and corresponds to a Trp residue in many protozoan ENTs, suggesting that an aromatic side chain is preferred at this position. Several AtENTs from *Arabidopsis thaliana* and EhENT1 from *Entamoeba histolytica* contain Leu or Val at the residue corresponding to F80 whereas TgAT1 from *Toxoplasma gondii* contains a hydrophilic Asn side chain.

In TM 8, F334 is conserved in mammalian and nematode ENTs with the exception of hENT4 and mENT4, which contain a Met whereas many other ENTs from plants and protozoa contained aliphatic side chains of various sizes ranging from Ala to Ile at position 334 (or its equivalent). N338 is conserved in 40/43 of the sequences analyzed, with the exceptions being PfENT1 (Gln), TgAT1 (Ala) and EhENT1 (Met) suggesting that these residues play important roles in the structure and function of ENTs.

L442 in TM 11 of hENT1 is an important residue for dipyridamole interactions with hENT1 and CeENT1 from *Caenorhabditis elegans*, (Chapter 5). In TM 11, most ENTs contain a Leu or Ile at position 442, with the exceptions of AtENT4, 5 (Ala), DmENT2 and AtENT2 (Met), and LdNT1.1, 1.2 and CfNT2 (Gly), suggesting that these residues also play important roles in ENT structure and/or function.

Effects of mutations in hENT1 on the concentration dependence of adenosine transport

To determine the functional role of each of the six residues, a series of mutants at each position was generated based, in part, on the identities of corresponding residues in other ENT family members. Adenosine was selected as the permeant because it is transported by more ENT family members than other nucleosides and, in mammals, is the physiologically active molecule whose activity is affected by transport inhibitors (32). Furthermore, Fui1::TRP1 yeast cells do not possess endogenous adenosine transport systems, do not metabolize extracellular adenosine and, when producing recombinant ENTs, display robust initial rates of uptake of adenosine for time intervals of $\geq$ 60 min . Yeast cells producing recombinant hENT1, hENT2, rENT1 or one of the mutants were incubated in the presence of increasing concentrations of [^{3}H]-adenosine for 10 min in the absence (total uptake) or presence (background) of 10 mM uridine (see Fig. 6-3 for

representative results). The apparent K_m and V_{max} values and the V_{max}:K_m ratios (transport efficiencies) are presented in Table 6-1.

Wildtype transporters. hENT1 displayed K_m and V_{max} values of 18.6 ± 2.3 μM and 1280 ± 30 pmol/mg/min, respectively, whereas rENT1 displayed lower K_m and higher V_{max} values, 9.36 ± 1.18 μM and 527 ± 12 pmol/mg/min, respectively. hENT2 displayed higher K_m and V_{max} values than hENT1 and rENT1; these values were similar to the results reported for recombinant hENT1 and hENT2 produced in transfected mammalian cells (9).

W29 mutants. For the series of W29 mutants, substitution of residue 29 with the smaller side chains of Gly (Fig. 6-3A), Ala and Cys reduced apparent V_{max} values whereas substitution of Tyr increased the apparent K_m value 6.9-fold (Fig. 6-3B). The W29V mutant displayed a low V_{max}:K_m ratio with increased K_m and reduced V_{max} values whereas W29I was completely non-functional and thus was not included in the kinetic analysis. None of the mutants displayed transport activity similar to that of wildtype, suggesting that a Trp residue at position 29 is favored for efficient hENT1 function.

M33 mutants. The M33 series of mutants all displayed K_m values that were similar to that of wildtype hENT1 whereas substitution with the smaller side chains Ala (Fig. 6-3A) and Val reduced the apparent V_{max} to 17 and 33 % of the wildtype value, respectively. M33T was also generated, but was non-functional and thus was not included in the kinetic analyses. These results suggested that amino acid volume was important for transporter function at position 33.

F80 mutants. Substitution of any non-aromatic side chain for F80 caused a moderate increase in K_m values and the small side chain mutations (F80C, N) decreased V_{max} values. F80A was also generated but was non-functional and thus was not included in the kinetic analyses. Therefore, amino acid side chain volume appeared to also be an important factor at residue 80 of hENT1, althought the effects of these mutations were relatively minor.

F334 mutants. The apparent K_m values of the F334 mutants were similar to those of wildtype, whereas reduced V_{max} values were obtained for F334C, V and I. Substitution of Phe with Tyr resulted in a 4.8-fold higher apparent V_{max} value (Fig. 6-3A). The parallel mutation in rENT1 increased its apparent V_{max} value 3.4-fold

Table 6-1. Kinetic properties of adenosine transport by hENT1, rENT1, hENT2 and the hENT1 mutants.

Average K_m and V_{max} values (mean ± S.E., n=3) were determined by nonlinear regression analysis using GraphPad Prism version 4.0 software.

Protein	Mutation	Apparent K_m	Apparent V_{max}	V_{max}:K_m
		μM	*pmol/mg/min*	*pmol/mg/min/μM*
hENT1	wildtype	18.6 ± 2.3	1280 ± 30	69
	W29G	15.7 ± 2.5	513 ± 15	33
	W29A	31.5 ± 6.2	573 ± 26	18
	W29C	61.0 ± 14.7	301 ± 20	4.9
	W29T	65.9 ± 9.1	1220 ± 40	19
	W29Y	129 ± 13	1220 ± 40	9
	W29V	138 ± 14	555 ± 22	4
	M33A	20.6 ± 8.6	216 ± 19	11
	M33V	9.51 ± 1.38	212 ± 6	22
	M33L	13.9 ± 1.5	2650 ± 60	190
	M33I	16.3 ± 1.3	1450 ± 20	89
	M33F	25.0 ± 1.4	2500 ± 30	150
	M33Y	27.2 ± 1.6	1760 ± 20	64
	F80C	47.0 ± 4.3	697 ± 16	15
	F80N	43.8 ± 4.1	584 ± 13	13
	F80L	47.5 ± 2.4	2060 ± 30	83
	F80M	38.7 ± 2.4	1910 ± 40	49
	F80W	25.1 ± 3.5	2210 ± 60	88
	F334S	26.4 ± 2.4	1060 ± 20	40
	F334C	26.6 ± 1.5	375 ± 5	14
	F334V	16.7 ± 1.7	718 ± 14	43
	F334I	17.4 ± 1.7	680 ± 13	39
	F334Y	26.5 ± 1.9	6190 ± 100	240
	N338A	46.0 ± 3.9	1140 ± 20	25
	N338S	46.6 ± 3.0	1600 ± 30	34
	N338C	26.0 ± 2.6	853 ± 19	33
	N338D	30.1 ± 3.7	374 ± 10	12
	N338Q	22.7 ± 1.9	315 ± 5.7	14
	N338M	20.9 ± 2.6	785 ± 21	38
	L442I	180 ± 13	2260 ± 70	13
	L442T	>500	ND	ND
rENT1	wildtype	9.36 ± 1.18	527 ± 12	56
	F334Y	10.6 ± 0.8	1780 ± 23.6	170
hENT2	wildtype	125 ± 6	2020 ± 40	16

ND = not determined

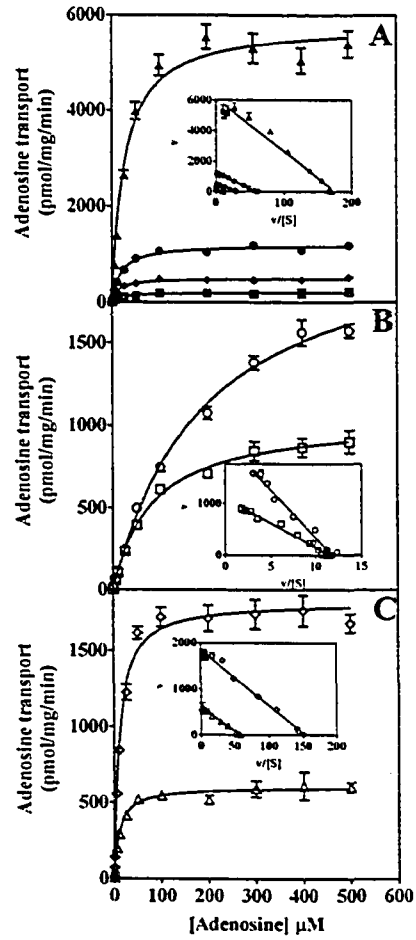

Figure 6-3. Concentration dependence of adenosine transport by recombinant hENT1, rENT1 and various mutants.

Yeast cells producing hENT1 (A, ●), hENT1-W29G (A, ◆), hENT1-M33A (A, ■), hENT1-F334Y (A, ▲), hENT1-W29Y (B, □), hENT1-L442I (B, ○), rENT1 (C, △) or rENT1-F334Y (C, ◇) were incubated for 10 min with increasing concentrations of [^{3}H]-adenosine. The Eadie-Hofstee plots are presented in the *insets*. The transport rates presented were derived from the difference between uptake observed in the absence and presence of 10 mM unlabeled uridine at each adenosine concentration. K_m and V_{max} values were obtained by nonlinear regression analysis using GraphPad Prism version 4.0 software, average values of which from 3 separate experiments are presented in Table 6-1. Each point is presented as the mean ± S.E. (n=4), and where the size of the point is larger than the S.E., it is not shown.

(Fig. 6-3C). Furthermore, the introduction of a hydrophilic residue in place of an aromatic residue (i.e., F334S) was suprisingly well tolerated, especially when compared to F334C, which displayed a 3.4-fold reduced V_{max} value. These results suggested that the hydroxyl groups of Ser and Tyr contributed to the transport capacity of these hENT1 mutants.

N338 mutants. The N338 series of mutants displayed modestly increased K_m values with the Ala, Ser or Asp substitutions, whereas the Asp and Gln substitutions decreased V_{max} values 3.4 and 4.1-fold, respectively. None of the mutants displayed V_{max}:K_m ratios that were comparable to wildtype, suggesting that residue 338 plays a role in transporter function. Despite its high level of conservation, both the bulky, hydrophobic side chain of Met and the hydrophilic side chain of Asp were tolerated at this position, suggesting that the extremely high level of conservation of N338 was not predictive of its importance in transporter function.

L442 mutants. Interestingly, Leu 442 was highly intolerant to mutation. L442A, G and M were all completely non-functional. L442I displayed a K_m value that was 9.7-fold higher than wildtype (Fig. 6-3B) and the K_m value of L442T could not be accurately determined even though functional transport was detected. In Chapter 5, L442I was shown to transport uridine with parameters that were not significantly different from wildtype whereas L442T displayed a significantly higher K_m value for uridine. These results suggested that L442 was a functionally critical residue with differential effects on, but important for both, adenosine and uridine transport by hENT1.

Immunofluorescence and quantitation of the abundance of recombinant hENT1 and hENT1 mutant proteins in yeast cells

To assess the localization and protein abundance of hENT1 and its various mutants, yeast cells producing recombinant transporters were stained using anti-hENT1 monoclonal primary antibodies which recognize the an epitope within residues 254-271 of the cytoplasmic loop connecting TMs 6 and 7 of hENT1 (33). Therefore, the cells were permeabilized to make the epitope accessible to the antibody.

Representative images are presented in Fig. 6-4. Yeast producing recombinant hENT1 displayed staining that varied >10-fold in intensity and was predominantly

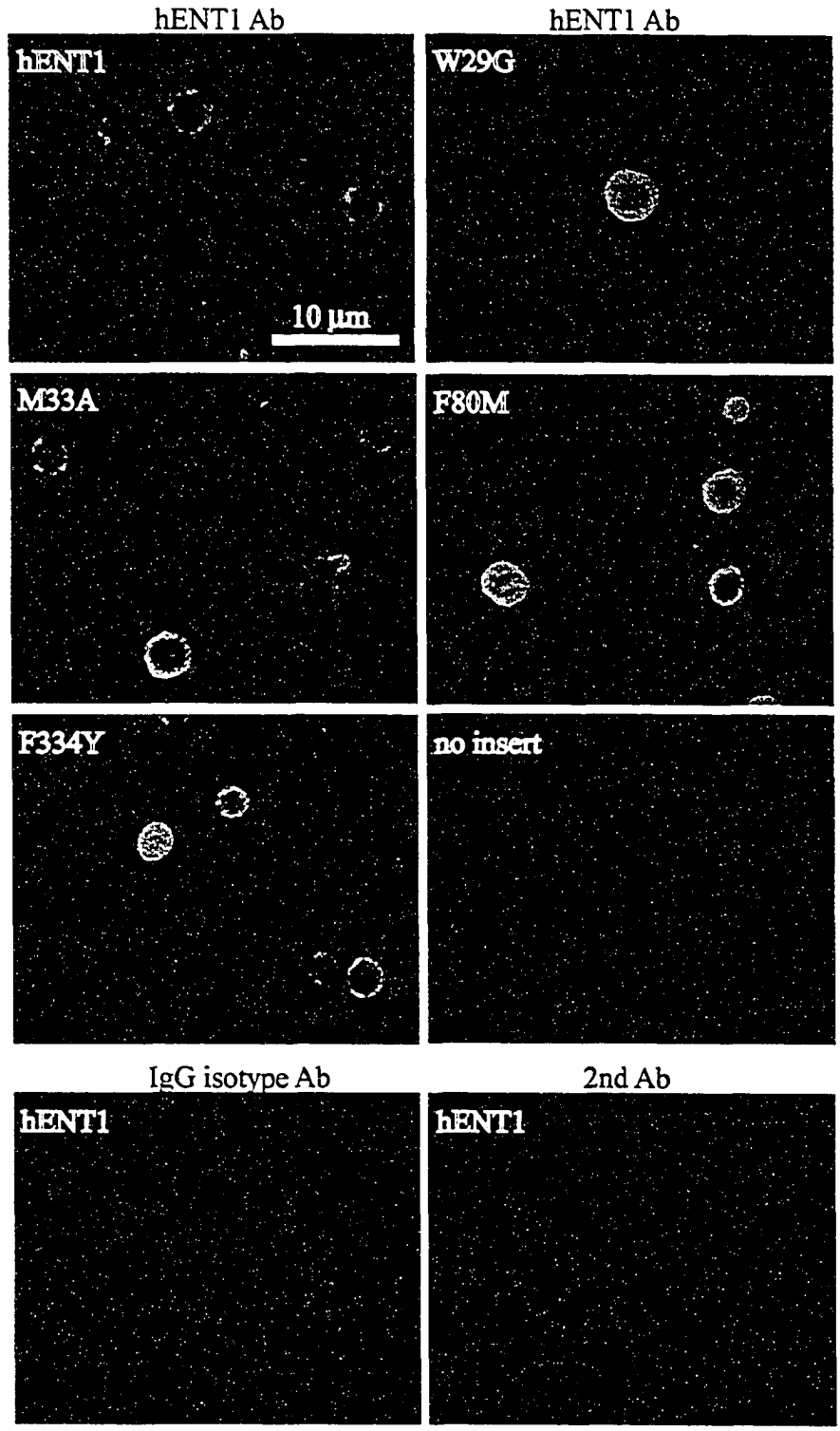

Figure 6-4. Immunostaining of yeast cells containing pYPhENT1, pYPGE15 or one the plasmid constructs encoding mutant hENT1.

Yeast cells producing hENT1, W29G, M33A, F80M, F334Y, N338S or L442I were stained with anti-hENT1 IgG (primary antibody) and Alexa Fluor 488 goat-anti mouse

IgG (secondary antibody). Antigen-negative control cells containing pYPGE15 (no insert) were stained with both the anti-hENT1 IgG and Alexa Fluor 488 IgG antibodies. Other controls included cells producing hENT1 stained with an IgG isotype primary antibody in place of the anti-hENT1 IgG or only with the secondary antibody (2^{nd} Ab). The cells were imaged using a 40X objective and the scale bar indicates a distance of 10 μm. The images presented are representative of 6-10 similar images recorded for hENT1 and each mutant.

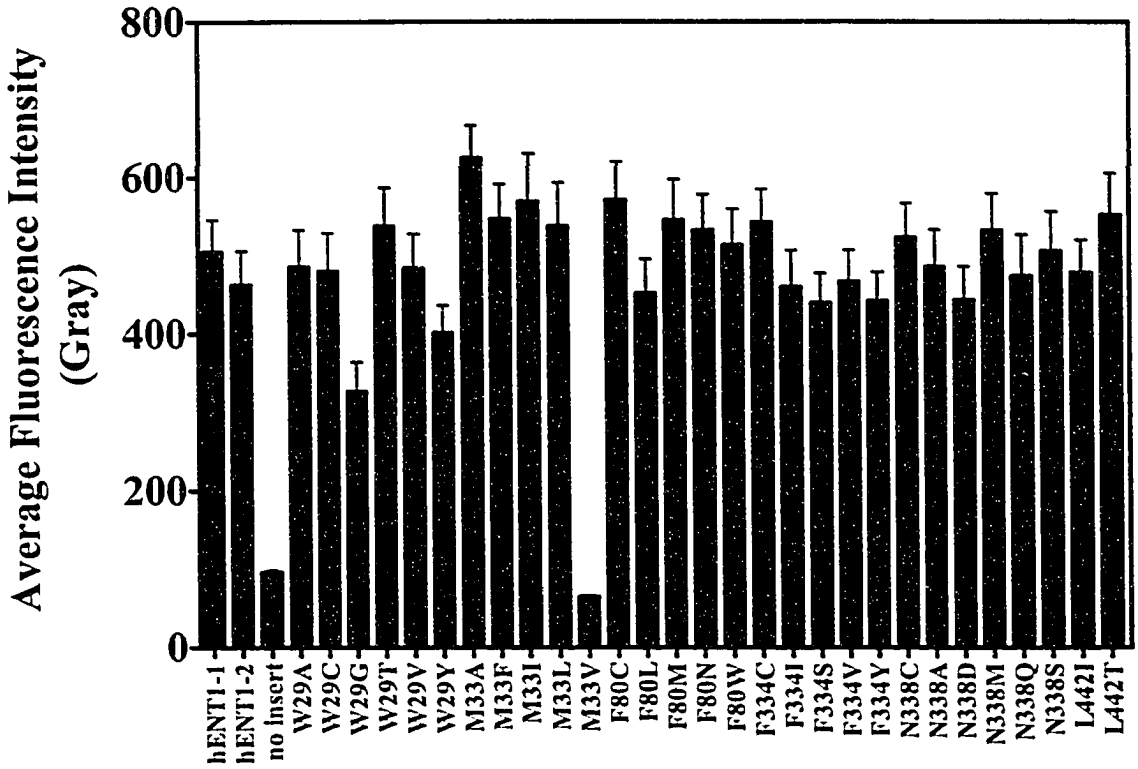

Figure 6-5. Average fluoresence intensity of immunostained yeast cells producing hENT1 or various mutants.

The fluoresence of 50 to 100 yeast cells producing hENT1 or one of the mutants from the immunostaining experiments was determined using Metamorph version 6.1 software. The mean ± S.E. fluoresence was plotted as a bar graph using GraphPad Prism version 4.0 software. Two different hENT1 cultures were independently immunostained and imaged to determine the reproducibility of the analysis (hENT1-1 and hENT1-2). As a negative control, yeast containing the expression vector without insert were included in the analysis and are labeled as "no insert" on the graph.

localized to the cell surface. Yeast cells containing pYPGE15 (vector with no insert) displayed staining that was considerably dimmer than that of yeast containing pYPhENT1. Yeast cells producing recombinant hENT1 that were stained with IgG isotype antibodies or only secondary antibodies did not display significant staining. Yeast cells producing recombinant hENT1 mutants displayed staining that was very similar in terms of intensity and localization to that of wildtype hENT1. Fig. 6-4 also shows representative images collected from yeast with the W29G, M33A, F80M, F334Y, N338S and L442I mutant proteins.

Several images were collected for hENT1 and each of the mutants. The fluorescence intensities of 50 to 100 cells producing either wildtype hENT1 or one of the mutants were recorded and averaged to determine the mean fluorescence intensity as a measure of protein abundance (Fig. 6-5). Cells with intact cell walls or poor structural integrity were excluded from these analyses. The results indicated that yeast cells containing pYPhENT1 displayed ~5-fold higher fluorescence intensities than yeast containing pYPGE15 (no insert). W29G and Y displayed modestly reduced fluorescence intensities compared to those of the two wildtype preparations, which may partially account for the reduced V_{max} value displayed by W29G. M33V displayed a fluorescence intensity that was comparable to that of the negative control, suggesting that the low activity of this mutant was due to low levels of mutant protein in the plasma membrane. Most of the hENT1 mutants displayed fluorescence intensities that were remarkably similar to those of wildtype hENT1. These results indicated that most of the mutant proteins displayed both similar localization and levels of protein abundance as the wildtype protein, suggesting that the changes in V_{max} values reflected effects on transporter activity rather than changes in cell-surface protein abundance.

Effects of mutations in hENT1 on sensitivity to transport inhibitors

To determine the contribution of the various residues to interactions of hENT1 with the transport inhibitors, concentration-effect relationships for inhibition of adenosine transport were determined with dipyridamole, dilazep, NBMPR, draflazine and soluflazine. The resulting IC_{50} values are presented in Tables 6-2 – 6-6. rENT1 was included in these analyses because it shares 78 % amino acid sequence identity with

hENT1 but, with the exception of NBMPR, is several orders of magnitude less sensitive to inhibitors. hENT2 was also included because it is relatively insensitive to inhibitors and the inhibitor sensitivities of these three wildtype transporters have not been addressed in parallel using identical genetic backgrounds.

Dipyridamole and dilazep (Tables 6-2 and 6-3). The trends in the data obtained for dipyridamole and dilazep were remarkably similar (compare Tables 6-2 and 6-3). rENT1 was 268 and 94-fold less sensitive to dipyridamole and dilazep, respectively, than hENT1 whereas hENT2 was 133 and 10,000-fold less sensitive to dipyridamole and dilazep, respectively. Mutations of W29 dramatically reduced sensitivity to these inhibitors with W29C being highly insensitive to dipyridamole and W29V being 300-fold less sensitive to dilazep than hENT1. M33V and M33A was the least sensitive mutant to both dipyridamole and dilazep, suggesting that amino acid volume is an important factor for sensitivity to these two inhibitors. M33L displayed an IC_{50} value for dipyridamole that was 33 % of the wildtype value. These results suggested that both the TM 1 residues were critical determinants of dipyridamole and dilazep sensitivity.

The F80 mutations modestly reduced sensitivity to dipyridamole and dilazep, with the exception of F80W which was somewhat more sensitive to dipyridamole than wildtype, suggesting that this residue was of relatively minor importance to interactions with these inhibitors. F334 mutations also modestly reduced sensitivity to these inhibitors, with large-volume side chains being preferred. The most notable effects were observed for F334S, which was 77 and 26-fold less sensitive to dipyridamole and dilazep, respectively. F334Y was well tolerated for dipyridamole interactions and favored for dilazep interactions, displaying an IC_{50} value that was 25 % of that of wildtype. N338 mutations decreased sensitivity to dipyridamole and dilazep with N338A, N338Q and N338D displaying ≥10-fold higher IC_{50} values. N338C displayed an IC_{50} value for dipyridamole that was similar to that of wildtype and was the most sensitive to dilazep within the N338 mutant series. F80, F334 and N338 were significant contributors to dipyridamole and dilazep sensitivity, although to a lesser extent than W29 and M33.

Consistent with what was shown in Chapter 5, L442I displayed increased sensitivity to dipyridamole, and the results of Table 6-3 indicated that this mutant also

Table 6-2. Inhibition of hENT1, rENT1, hENT2 and the hENT1 mutants by dipyridamole.

IC_{50} values (mean ± S.E., n=3) were determined by nonlinear regression analysis using GraphPad Prism version 4.0 software.

Protein	Mutation	IC_{50}	Ratio with wildtype
		nM	
hENT1	wildtype	19.2 ± 1.2	1.0
	W29G	196 ± 21	10
	W29T	217 ± 13	11
	W29V	385 ± 40	20
	W29Y	389 ± 49	20
	W29A	527 ± 161	28
	W29C	>30000	>>>
	M33L	6.37 ± 0.25	0.33
	M33F	207 ± 16	11
	M33Y	219 ± 19	11
	M33I	266 ± 22	14
	M33V	963 ± 124	50
	M33A	>30000	>>>
	F80W	13.1 ± 0.3	0.69
	F80L	29.7 ± 2.3	1.6
	F80M	41.8 ± 4.0	2.2
	F80N	50.5 ± 6.0	2.6
	F80C	238 ± 18	12
	F334Y	30.5 ± 1.5	1.6
	F334V	149 ± 6	7.8
	F334I	153 ± 8	8.0
	F334C	187 ± 26	9.8
	F334S	1470 ± 210	77
	N338C	16.1 ± 1.1	0.84
	N338M	102 ± 6	5.3
	N338S	177 ± 11	9.25
	N338A	251 ± 29	13
	N338Q	371 ± 41	19
	N338D	420 ± 44	22
	L442I	4.12 ± 0.25	0.22
	L442T	17.9 ± 2.1	0.94
rENT1	wildtype	5150 ± 280	1.0
	I33L	208 ± 13	0.040
	I33M	434 ± 35	0.084
	F80W	3330 ± 190	0.65
	N339C	275 ± 33	0.053
	L443I	779 ± 147	0.15
hENT2	wildtype	2550 ± 130	1.0

Table 6-3. Inhibition of hENT1, rENT1, hENT2 and the hENT1 mutants by dilazep.

IC_{50} values (mean ± S.E., n=3) were determined by nonlinear regression analysis using GraphPad Prism version 4.0 software.

Protein	Mutation	IC_{50}	Ratio with wildtype
		nM	
hENT1	wildtype	15.4 ± 0.7	1.0
	W29T	336 ± 24	22
	W29G	463 ± 19	30
	W29A	643 ± 35	42
	W29Y	759 ± 49	49
	W29C	836 ± 61	54
	W29V	4680 ± 1090	300
	M33L	152 ± 6	9.9
	M33I	173 ± 8	11
	M33F	625 ± 25	41
	M33Y	1030 ± 30	67
	M33V	ND	ND
	M33A	4960 ± 520	320
	F80M	24.0 ± 1.2	1.6
	F80L	30.7 ± 1.0	2.0
	F80C	41.1 ± 2.6	2.7
	F80W	41.7 ± 3.0	2.7
	F80N	49.3 ± 1.7	3.2
	F334Y	3.87 ± 0.27	0.25
	F334I	70.5 ± 3.7	4.6
	F334V	130 ± 8	8.4
	F334C	155 ± 19	10
	F334S	408 ± 16	26
	N338C	56.4 ± 2.9	3.7
	N338S	94.9 ± 3.9	6.2
	N338M	122 ± 5	7.9
	N338A	151 ± 9	9.8
	N338D	203 ± 9	13
	N338Q	356 ± 49	23
	L442I	7.18 ± 0.41	0.47
	L442T	13.2 ± 0.7	0.85
rENT1	wildtype	1450 ± 50	1.0
	I33M	20.7 ± 1.6	0.014
	F334Y	158 ± 98	0.11
	L443I	258 ± 13	0.18
hENT2	wildtype	158000 ± 25000	1.0

displayed increased sensitivity to dilazep. Due to the intolerance of this residue to mutation, further analysis of this residue was not possible.

Several mutants displayed increased sensitivity to dipyridamole and/or dilazep. Parallel mutations of the corresponding rENT1 residues were generated and tested for sensitivity to dipyridamole and dilazep (Tables 6-2 and 6-3). The I33L, I33M, F80W, N339C and L443I rENT1 mutants all displayed increased sensitivity to dipyridamole, with I33L and N339C have the greatest effects. Similarly, the I33M, F334Y and L443I rENT1 mutants displayed increased sensitivity to dilazep, with I33M displaying a similar IC_{50} value to hENT1. This observation suggested that residue 33 is the major determinant of the relative insensitivity of rENT1 to dilazep. Overall, these results suggested these residues shared common roles in dipyridamole and dilazep binding that were conserved between hENT1 and rENT1.

NBMPR (Table 6-4). hENT1 displayed an IC_{50} value of 2.13 ± 0.08 nM, which was similar to the value observed for rENT1 (2.26 ± 0.18 nM) and several orders of magnitude lower than that of hENT2 (7830 ± 1140 nM). M33I, F80C and L442I did not display significant differences in their IC_{50} values for NBMPR compared to wildtype and were not pursued further whereas W29G, F334S and N338S displayed altered sensitivity warranting further investigation.

The W29 series of mutants displayed a wide range of IC_{50} values for NBMPR, with aromatic residues being highly preferred, followed by Val, Thr, Ala and Cys. W29G displayed an IC_{50} value that was 120-fold higher than that of wildtype, suggesting that amino acid volume at this position was critical for high-affinity NBMPR interactions. Small and hydrophilic substitutions for F334 yielded modest increases in sensitivity to NBMPR. Aromatic and aliphatic residues yielded IC_{50} values that were very similar to wildtype. However, the magnitude of the observed changes associated with mutating this residue was very small, indicating that this residue did not play a major role in NBMPR interactions. Mutations of N338 yielded decreases in sensitivity ranging from 2.8 to 10-fold, suggesting that this residue was of intermediate importance to NBMPR sensitivity relative to W29 and F334. Overall, substitution of small-side chain residues for W29 had the greatest effects on NBMPR sensitivity, suggesting that this residue was a major contributor to NBMPR binding.

Table 6-4. Inhibition of hENT1, rENT1, hENT2 and the hENT1 mutants by NBMPR.

IC_{50} values (mean ± S.E., n=3) were determined by nonlinear regression analysis using GraphPad Prism version 4.0 software.

Protein	Mutation	IC_{50}	Ratio with wildtype
		nM	
hENT1	wildtype	2.13 ± 0.08	1.0
	M33I	2.36 ± 0.11	1.1
	F80C	1.89 ± 0.42	0.89
	L442I	1.70 ± 0.29	0.80
	W29Y	8.53 ± 0.65	4.0
	W29V	44.6 ± 3.8	21
	W29T	46.2 ± 4.2	22
	W29A	103 ± 11	49
	W29C	141 ± 19	66
	W29G	261 ± 29	120
	F334S	0.882 ± 0.02	0.41
	F334C	0.901 ± 0.03	0.42
	F334V	1.27 ± 0.04	0.60
	F334I	2.08 ± 0.07	0.98
	F334Y	2.73 ± 0.07	1.3
	N338A	6.03 ± 0.46	2.8
	N338D	9.54 ± 1.06	4.5
	N338M	9.93 ± 0.67	4.7
	N338S	10.2 ± 0.6	4.8
	N338C	13.3 ± 1.1	6.3
	N338Q	21.9 ± 3.9	10
rENT1	wildtype	2.26 ± 0.18	1.0
hENT2	wildtype	7830 ± 1140	1.0

Although modest increases in sensitivity to NBMPR were observed for hENT1-F334S and C, parallel mutations of hENT2 did not significantly alter the NBMPR sensitivity of this protein (data not shown).

Draflazine and soluflazine (Tables 6-5 and 6-6). Like dipyridamole and dilazep, the trends observed for draflazine and soluflazine were similar (compare Tables 6-5 and 6-6). Both hENT1 and hENT2 were inhibited by nanomolar concentrations of draflazine whereas rENT1 was 230 and 5.8-fold less sensitive, respectively. Both rENT1 and hENT2 were highly resistant to soluflazine, being 216 and 83-fold less sensitive than hENT1, respectively. Both W29G and N338S displayed reduced sensitivity to draflazine and soluflazine whereas F80C was modestly less sensitive to draflazine and M33I was modestly less sensitive to soluflazine.

W29 mutations reduced sensitivity to draflazine and soluflazine with larger effects observed for soluflazine and W29G and C being the least sensitive to both inhibitors. Similar to what was observed for the other inhibitors, F80 mutations had relatively small effects of draflazine sensitivity (Table 6-5). M33 mutations reduced sensitivity to soluflazine but not draflazine, indicating a difference between the two inhibitors. N338 mutations had dramatic effects on the sensitivity to both inhibitors, with N338M being the least sensitive mutant at 180 and 93-fold less sensitive to draflazine and soluflazine, respectively. Small and hydrophilic side chains of Cys, Asp and Ser were favored at position 338 with the wildtype Asn residue yielding the highest sensitivity.

As was observed for dipyridamole, a Leu or Met at position 33 was indicative of high sensitivity to soluflazine. The corresponding rENT1 mutants yielded IC_{50} values for soluflazine that were 24 % and 21 % of wildtype, respectively. These results suggested that W29 and N338 were important determinants of draflazine and soluflazine binding whereas M33 was only important for soluflazine interactions.

Table 6-5. Inhibition of hENT1, rENT1, hENT2 and the hENT1 mutants by draflazine.

IC_{50} values (mean ± S.E., n=3) were determined by nonlinear regression analysis using GraphPad Prism version 4.0 software.

Protein	Mutation	IC_{50}	Ratio with wildtype
		nM	
hENT1	wildtype	9.94 ± 0.50	1.0
	M33I	9.34 ± 1.10	0.94
	F334S	9.51 ± 1.61	0.96
	L442I	7.40 ± 0.72	0.75
	W29Y	55.4 ± 4.3	5.6
	W29A	58.5 ± 4.6	5.9
	W29V	61.3 ± 7.6	6.2
	W29T	62.8 ± 6.1	6.3
	W29G	78.6 ± 6.3	7.9
	W29C	144 ± 19	15
	F80W	13.6 ± 0.4	1.3
	F80M	13.9 ± 0.4	1.4
	F80L	15.0 ± 0.4	1.5
	F80N	26.9 ± 0.8	2.7
	F80C	40.7 ± 1.0	4.1
	N338C	55.7 ± 4.6	5.6
	N338D	78.1 ± 5.8	7.9
	N338S	312 ± 25	31
	N338Q	444 ± 62	45
	N338A	546 ± 49	55
	N338M	1810 ± 230	180
rENT1		2290 ± 190	1.0
hENT2		392 ± 19	1.0

Table 6-6. Inhibition of hENT1, rENT1, hENT2 and the hENT1 mutants by soluflazine.

IC_{50} values (mean ± S.E., n=3) were determined by nonlinear regression analysis using GraphPad Prism version 4.0 software.

Protein	Mutation	IC_{50}	Ratio with wildtype
		nM	
hENT1	Wildtype	92.3 ± 6.4	1.0
	F80C	127 ± 28	1.4
	F334S	109 ± 34	1.2
	L442I	86.0 ± 8.2	0.93
	W29Y	407 ± 39	4.4
	W29V	1170 ± 174	13
	W29T	2270 ± 240	25
	W29A	2300 ± 270	25
	W29C	4730 ± 910	51
	W29G	13420 ± 1300	150
	M33L	45.6 ± 2.0	0.49
	M33I	244 ± 30	2.6
	M33V	350 ± 37	3.8
	M33Y	482 ± 31	5.2
	M33F	986 ± 82	11
	M33A	1140 ± 170	12
	N338S	733 ± 49	7.9
	N338D	893 ± 88	9.7
	N338C	1540 ± 110	17
	N338A	1600 ± 120	17
	N338Q	6310 ± 780	68
	N338M	8580 ± 650	93
rENT1	wildtype	19900 ± 1600	1.0
	I33L	4720 ± 470	0.24
	I33M	4150 ± 290	0.21
hENT2	wildtype	7630 ± 527	1.0

Discussion

Screening by random mutagenesis for residues of hENT1 involved in inhibitor interactions led to the identification of four novel residues: W29, F80, F334 and N338. In the work described in this chapter, these residues, together with the previously identified M33 and L442 (Chapters 3 and 5), were subjected to detailed analyses. Multiple sequence alignments of the TMs that contain these residues revealed that N338 and W29 were the most highly conserved and the character of the other residues was conserved, tending to be large and hydrophobic (Fig. 6-2). Furthermore, the residues in TMs 1 and 8 were within regions previously identified as being highly conserved in the ENT family suggesting that they form part of important structural regions on the protein (3).

The experiments of Table 6-1 and Figs. 6-3 to 6-5 indicated that all the identified residues were important determinants of adenosine transport efficiency with reduced apparent V_{max} values reported for many mutants that could be attributed to changes in the activity of the transporter rather than reduced protein abundance. These experiments suggested that all of the residues were important for protein function. The most notable effects were observed for W29 and L442 mutations. The conservative mutations W29Y and L442I increased the apparent K_m values for adenosine by 6.9 and 9.7-fold. In Chapter 5, L442I displayed kinetic parameters for uridine transport that were similar to wildtype, suggesting that this residue may play a role in permeant selectivity. The increased V_{max} values observed for the F334 mutants (F334Y vs wildtype and F334S vs F334C) suggested that the hydroxyl group-containing side residues contributed hydrogen bonds to yield the observed effects, which were reproducible in both hENT1 and rENT1 (Fig. 6-3). These results implicated all six residues as important for adenosine transport but it was unclear whether or not they directly participated in permeant recognition or translocation.

Comprehensive parallel analysis of the inhibitor sensitivities of hENT1, hENT2 and rENT1 were performed (Tables 6-2 to 6-6). Many early studies have investigated the inhibitor sensitivities of *es* versus *ei* transporters and human versus rat *es* transporters but

these studies have been difficult to interpret because results obtained from different research groups using cells of different origins and containing multiple transport systems were directly compared (5,34). This study circumvented these problems by studying the transporters in isolation, using an identical genetic background and conditions of assay. The rank orders of inhibitor sensitivity were as follows: dipyridamole (hENT1>>hENT2>rENT1), dilazep (hENT1>rENT1>>hENT2), NBMPR (hENT1~rENT1>>hENT2), draflazine (hENT1>hENT2>>rENT1) and soluflazine (hENT1>>hENT2>rENT1) (Tables 6-2 to 6-6). The results obtained for soluflazine, which were inconsistent with studies performed in rat erythroyctes and Ehrlich ascites cells, both of which are of rodent origin, suggested that soluflazine has selectivity for the *ei* transporter (ENT2) (24,28). It is possible that a similar study conducted in a different model system, such as *Xenopus laevis* oocytes or transfected cell lines, may yield slightly different results due to differences in membrane environments and/or post translational modifications.

All six residues affected sensitivity to dipyridamole and dilazep and the trends were remarkably similar, suggesting that these two structurally unrelated inhibitors bind to the same site (compare Tables 6-2 and 6-3). Furthermore, that increased sensitivity to dipyridamole and dilazep could be engineered into rENT1, suggested that the roles of the six residues in the binding of these inhibitors were conserved. Although residue 33 was analyzed in detail previously (Chapters 3, 4 and 5), this study established that a Leu residue at this position was a determinant of high sensitivity to dipyridamole. The L442I mutation was also previously shown to increase sensitivity to dipyridamole (Chapter 5) and in this study, it was shown to also increase sensitivity to dilazep (Table 6-3). In general, bulky, hydrophobic residues were preferred for high-affinity inhibitor interactions, suggesting that hENT1 binds dipyridamole and dilazep via hydrophobic interactions.

Early studies suggested that dipyridamole was a competitive inhibitor of the *es* transporter's outward-facing permeant binding site whereas the mechanism of dilazep inhibition was implicated to be allosteric (13-17,19,35). A preliminary model depicted in Chapter 7 (Fig. 7-1) suggests that W29, M33, F334, N338 and L443 could line the permeant translocation channel and that all of these residues, with the exception of N338,

lie towards the extracellular aspect of the transporter. These results, in combination with the functional significance and high level of conservation of these residues (Fig. 6-2, Table 6-1), suggested that dipyridamole and dilazep share a common binding site that overlaps with the outward-facing permeant binding site.

The trends observed for the W29 and N338 series of mutants for draflazine and soluflazine were also remarkably similar, suggesting that these two inhibitors shared a common mechanism of inhibition (compare Tables 6-5, 6-6). Hydrophilic residues were highly preferred at N338, suggesting that this residue forms hydrogen bonds with draflazine and soluflazine. The trends observed for the W29 series of mutants for draflazine and soluflazine were also similar to that observed for NBMPR, with aromatic residues being highly preferred at this position (Table 6-4). A common structural feature between draflazine, soluflazine and NBMPR is the presence of fluorophenyl (draflazine, soluflazine) or nitrobenzyl (NBMPR) groups, which for NBMPR, have been shown to be critical for high-affinity binding (36). It is possible that W29 interacts with these moieties via aromatic ring stacking interactions.

Soluflazine inhibition displayed a common characteristic with dipyridamole and dilazep in being affected by M33 mutations, with a Leu residue at this position yielding increased sensitivity to both soluflazine and dipyridamole (Tables 6-2, 6-6). These results suggested that soluflazine binding shares molecular determinants with both dipyridamole and draflazine.

Draflazine has been shown to be a mixed-type inhibitor of transport and NBMPR binding whereas some its analogs were purely competitive inhibitors (24-26,37). The results of Table 6-5 suggested that N338 was the major determinant of draflazine sensitivity, which is on the intracellular end of TM 8 (Fig. 6-1). Although N338 may be accessible from the extracellular side, it is possible that draflazine could access its binding site from either side of the membrane with differing affinities, providing an explanation for its mixed-type inhibition behavior (24). Although N338 mutations decreased adenosine transport efficiencies, it was surprisingly tolerant of both charged (Asp) and hydrophobic (Met) substitutions despite its high level of conservation. Its location on the cytoplasmic end of TM 8 as part a highly conserved hydrophilic patch including D341 and R345, indicated that it may be involved in the efflux activity of

hENT1. Efflux and equilibrium exchange experiments using non-metabolized permeants may be able to address the role of N338 is this regard.

The inhibitor sensitivities of the hENT1 mutants, which in many cases were verified in parallel studies with the corresponding rENT1 mutants, suggested that the most favorable residue combinations for inhibitor binding were: Trp at 29, Met or Leu at 33, Phe at 80, Phe or Tyr at 334, Asn at 338 and Ile at 442. Using this information and the sequence alignments presented in Fig. 6-2, moderate sensitivities to dilazep, dipyridamole and soluflazine would be predicted for AtENT3, 6 and 7 because they contain the inhibitor-preferred Leu, Asn and Ile residues at the positions corresponding to M33, N338 and L442, respectively, but also contain less favorable aliphatic residues at the positions corresponding to F80 and F334. This prediction is consistent with published results, which demonstrated inhibition of AtENT3 by dilazep and dipyridamole and AtENT6 and 7 by dilazep (dipyridamole was not tested) (38,39). TgAT1 also contains four of the five most favorable residues at the corresponding positions for dipyridamole and soluflazine interactions, with the exception of an Asn at the position corresponding to F80. TgAT1 has been shown to be completely inhibited by 1 μM dipyridamole (40). Lastly, the primary residue responsible for the relative insensitivity of rENT1 to dilazep was I33 (Table 6-3). Thus the findings of the current study can be applied to both closely and distantly related transporters in the ENT family, providing evidence for common inhibitor binding sites. However, CeENT1 and 2, which contain four of the five preferred residues for inhibitor binding, have been characterized and found to be sensitive to nanomolar concentrations of dipyridamole but insensitive to NBMPR, dilazep and draflazine, indicting that additional determinants of inhibitor binding have yet to be identified (41).

In conclusion, this work identified four novel residues involved in inhibitor binding, the roles of which, in addition to the two residues identified in Chapters 3 and 5, were characterized with respect to adenosine transport, cellular localization and inhibitor sensitivity. The determinants of high-affinity inhibitor interactions were verified by assessing the results of published studies on other ENT family members with limited sequence identity to hENT1. The functional characteristics of the identified mutants revealed that W29 and L442 are critical for transporter function and that substitution of

amino acid residues containing hydroxyl groups for F334 increased transporter activity. These results provided support for the proposed model in which dipyridamole, dilazep, NBMPR and soluflazine compete with permeants for binding to the outward-facing conformation of hENT1 (5). Four of the five residues identified were large and hydrophobic and, if involved in directly binding the inhibitor molecules, are likely to contribute hydrophobic and/or aromatic stacking interactions whereas N338 would likely participate in hydrogen bonding interactions. Future studies that will test the validity of this model will include comprehensive SCAM using a functional Cys-less hENT1 mutant.

References

1. Cass, C. E. (1995) in *Drug Transport in Antimicrobial and Anticancer Chemotherapy* (Georgopapadakou, N. H., ed), pp. 403-451, Marcel Deker, New York, NY
2. Cass, C. E., Young, J. D., Baldwin, S. A., Cabrita, M. A., Graham, K. A., Griffiths, M., Jennings, L. L., Mackey, J. R., Ng, A. M. L., Ritzel, M. W. L., Vickers, M. F., and Yao, S. Y. M. (1999) in *Membrane Transporters as Drug Targets* (Amidon, G. L., and Sadee, W., eds) Vol. 12, 1 Ed., 12 vols., Kluwer Academic/Plenum Publishers
3. Acimovic, Y., and Coe, I. R. (2002) *Mol Biol Evol* **19**, 2199-2210
4. Sundaram, M., Yao, S. Y., Ingram, J. C., Berry, Z. A., Abidi, F., Cass, C. E., Baldwin, S. A., and Young, J. D. (2001) *J Biol Chem* **2**, 2
5. Griffith, D. A., and Jarvis, S. M. (1996) *Biochim Biophys Acta* **1286**, 153-181
6. Griffiths, M., Beaumont, N., Yao, S. Y., Sundaram, M., Boumah, C. E., Davies, A., Kwong, F. Y., Coe, I., Cass, C. E., Young, J. D., and Baldwin, S. A. (1997) *Nat Med* **3**, 89-93
7. Griffiths, M., Yao, S. Y., Abidi, F., Phillips, S. E., Cass, C. E., Young, J. D., and Baldwin, S. A. (1997) *Biochem J* **328**, 739-743
8. Crawford, C. R., Patel, D. H., Naeve, C., and Belt, J. A. (1998) *J Biol Chem* **273**, 5288-5293
9. Ward, J. L., Sherali, A., Mo, Z. P., and Tse, C. M. (2000) *J Biol Chem* **275**, 8375-8381
10. Yao, S. Y., Ng, A. M., Vickers, M. F., Sundaram, M., Cass, C. E., Baldwin, S. A., and Young, J. D. (2002) *J Biol Chem* **277**, 24938-24948
11. Van Belle, H. (1993) *Cardiovasc Res* **27**, 68-76
12. Jennings, L. L., Cass, C. E., Ritzel, M. W. L., Yao, S. Y. M., Young, J. D., Griffiths, M., Baldwin, S. A. (1998) *Drug Dev Res* **45**, 277-287
13. Koren, R., Cass, C. E., and Paterson, A. R. (1983) *Biochem J* **216**, 299-308.
14. Jarvis, S. M., Janmohamed, S. N., and Young, J. D. (1983) *Biochem J* **216**, 661-667

15. Jarvis, S. M., McBride, D., and Young, J. D. (1982) *J Physiol (Lond)* **324**, 31-46
16. Jarvis, S. M. (1986) *Mol Pharmacol* **30**, 659-665
17. Gati, W. P., Paterson, A. R. P. (1989) *Mol Pharm* **36**, 134-141
18. IJzerman, A. P., and Voorschuur, A. H. (1990) *Naunyn Schmiedebergs Arch Pharmacol* **342**, 336-341
19. Hammond, J. R. (1991) *Mol Pharmacol* **39**, 771-779
20. Visser, F., Vickers, M. F., Ng, A. M., Baldwin, S. A., Young, J. D., and Cass, C. E. (2002) *J Biol Chem* **277**, 395-401.
21. Endres, C. J., SenGupta, D. J., and Unadkat, J. D. (2004) *Biochem J* **Pt**
22. SenGupta, D. J., Lum, P. Y., Lai, Y., Shubochkina, E., Bakken, A. H., Schneider, G., and Unadkat, J. D. (2002) *Biochemistry* **41**, 1512-1519
23. SenGupta, D. J., and Unadkat, J. D. (2004) *Biochem Pharmacol* **67**, 453-458
24. Hammond, J. R. (2000) *Nauyn Schmiedebergs Arch Pharmacol* **361**, 373-382
25. IJzerman, A. P., Kruidering, M., van Weert, A., van Belle, H., and Janssen, C. (1992) *Naunyn Schmiedebergs Arch Pharmacol* **345**, 558-563
26. Ijzerman, A. P., Thedinga, K. H., Custers, A. F., Hoos, B., and Van Belle, H. (1989) *Eur J Pharmacol* **172**, 273-281
27. Jones, K. W., and Hammond, J. R. (1993) *Eur J Pharmacol* **246**, 97-104
28. Griffith, D. A., Conant, A. R., and Jarvis, S. M. (1990) *Biochem Pharmacol* **40**, 2297-2303
29. Barclay, B. J., Kunz, B. A., Little, J. G., and Haynes, R. H. (1982) *Can J Biochem* **60**, 172-184
30. Grenson, M. (1969) *Eur J Biochem* **11**, 249-260
31. Vickers, M. F., Mani, R. S., Sundaram, M., Hogue, D. L., Young, J. D., Baldwin, S. A., and Cass, C. E. (1999) *Biochem J* **339**, 21-32
32. Hyde, R. J., Cass, C. E., Young, J. D., Baldwin, S. A. (2001) *Mol Memb Biol* **18**, 53-63
33. Jennings, L. L., Hao, C., Cabrita, M. A., Vickers, M. F., Baldwin, S. A., Young, J. D., and Cass, C. E. (2001) *Neuropharmacology* **40**, 722-731.
34. Plagemann, P. G. W., Wohlhueter, R. M., Woffendin, C. (1988) *Biochim Biophys Acta* **947**, 405-443

35. Shi, M., Young, J. D. (1986) *Biochem J* **240**, 879-883

36. Paul, B., Chen, M. F., and Paterson, A. R. (1975) *J Med Chem* **18**, 968-973

37. Jones, K. W., and Hammond, J. R. (1992) *J Neurochem* **59**, 1363-1371

38. Wormit, A., Traub, M., Florchinger, M., Neuhaus, H. E., and Mohlmann, T. (2004) *Biochem J* **Pt**

39. Li, G., Liu, K., Baldwin, S. A., and Wang, D. (2003) *J Biol Chem* **278**, 35732-35742

40. Chiang, C. W., Carter, N., Sullivan, W. J., Jr., Donald, R. G., Roos, D. S., Naguib, F. N., el Kouni, M. H., Ullman, B., and Wilson, C. M. (1999) *J Biol Chem* **274**, 35255-35261

41. Appleford, P. J., Griffiths, M., Yao, S. Y., Ng, A. M., Chomey, E. G., Isaac, R. E., Coates, D., Hope, I. A., Cass, C. E., Young, J. D., and Baldwin, S. A. (2004) *Mol Membr Biol* **21**, 247-260

Chapter 7: General Discussion

Molecular modeling

To determine the structural locations of each of the six residues identified in the studies of this thesis, helical wheel projections of TMs 1, 2, 8 and 11 were generated (Fig. 7-1). All of the TMs display amphipathic characteristics to varying degrees, and contribute to inhibitor interactions and permeant transport, suggesting that they could be close together in the folded protein and line the permeant translocation channel and/or inhibitor-binding site. Although residues in TMs 4 and 5 have been implicated in inhibitor or permeant binding (1-4), they were not included because their roles were not addressed in the current study. Furthermore, it is not the intention of this model to exclude the possibility of the contribution of other TMs and/or residues to inhibitor or permeant binding, or to imply that TMs 1, 2, 8 and 11 are immediately adjacent to one another. Furthermore, although depicted as ideal alpha helices, TMs 1, 2 and 8 contain proline residues which could induce "kinks" in the structures of these TMs.

In TM 1, W29 and M33 are on the same helical face along with three relatively hydrophilic residues: G22, T25 and N30. G22 and N30 are conserved in all the ENTs analyzed in Fig. 6-1 (with two exceptions N30 where corresponds to a Ser), whereas T25 corresponds to a Thr or Ser residue in 17 of the 43 sequences, indicating that M33 and W29 likely face the permeant translocation channel.

TM 2 contains many hydrophilic residues including S75, N82, T85, N81 and S77. F80 is on a relatively hydrophobic face of TM 2 suggesting that it does not line the permeant translocation channel whereas L92, a residue previously shown to be specifically involved in hENT1 affinity for NBMPR, inosine and guanosine is on the hydrophilic face of TM 2 (5).

F334 and N338 are in close proximity to the highly conserved hydrophilic residues D341 and R345, the corresponding residues of which in LdNT2 have been shown to be critical for transporter function and targeting (6). G344 and F337 are also highly conserved and on the same helical face as F334 and N338 (Fig. 6-2). N338, D341, G344 and R345 form a hydrophilic patch on the intracellular end of TM8, suggesting that this region may form part of the endofacial nucleoside binding site. Several hydrophilic residues, including T336 and S332 are also found on the opposite side of TM 8 from

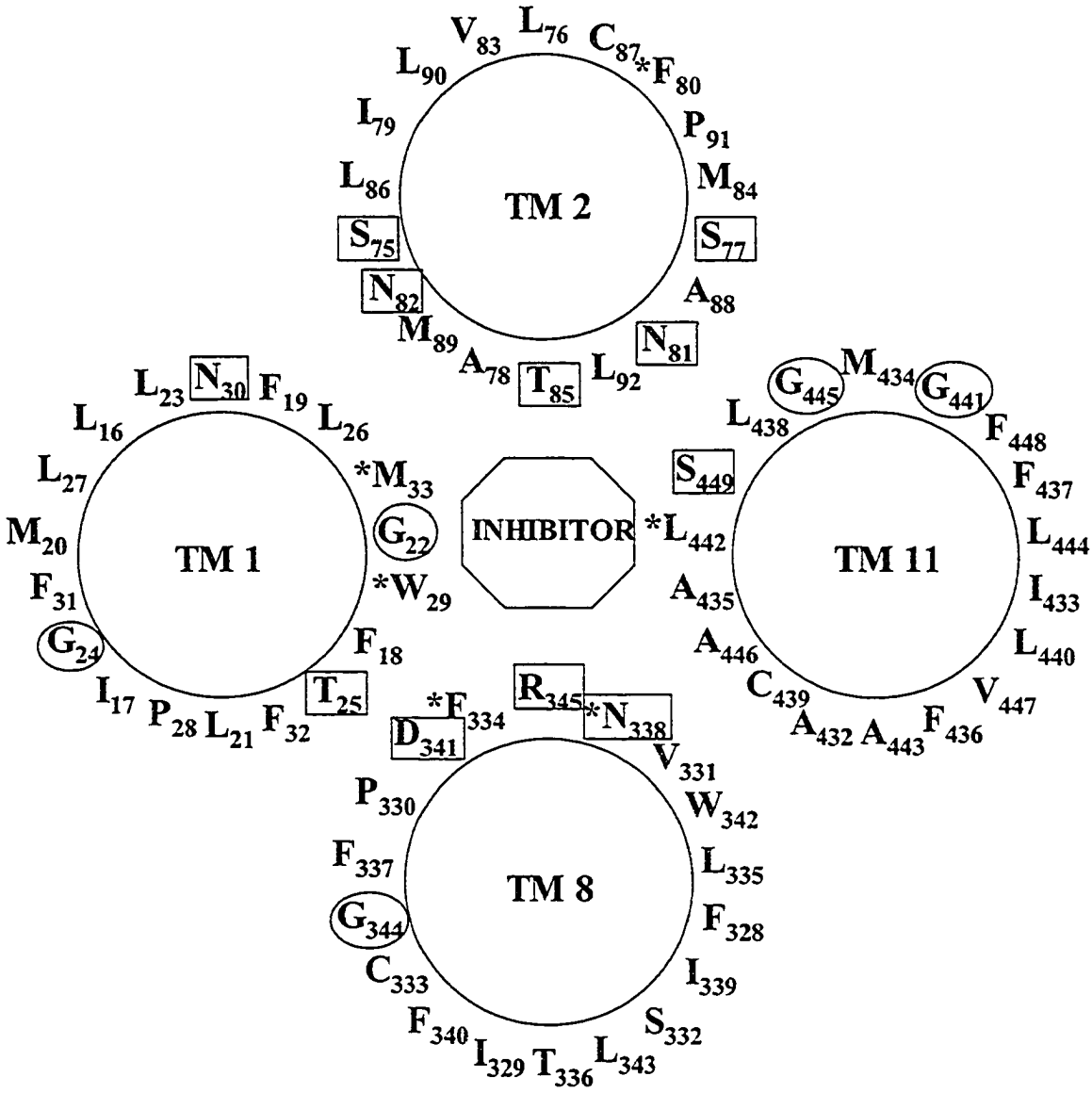

Figure 7-1. Helical wheel projections of TMs 1, 2, 8 and 11 of hENT1.

Helical wheel projections, viewed from the extracellular side of the membrane, were generated using the HelixWheel program on the EXPASY molecular biology server and transposed onto a high-resolution helical wheel template. The residues in question in this study are marked with a *. Highly conserved glycine residues are circled and residues that are hydrophilic in >40% of the ENTs in Fig. 6-2 are boxed.

F334 and N338 but these residues are not conserved in the ENT family and could form hydrogen-bonds with the main chain of the helix and therefore face the lipid bilayer.

TM 11 is very hydrophobic, with L442 on a face containing several smaller Ala side chains, C439, S449 and G445, suggesting a structural role for this TM. L442 is also the second residue of a highly conserved GXXXG helix-helix interaction motif involving G441 and G445 (Fig. 7-1) (7,8). Given the intolerance of L442 to mutation and the effects of L442I on substrate selectivity (uridine versus adenosine transport, compare Tables 5-2 and 6-1), it could form part of the permeant translocation channel or stabilize the helix-helix packing interface involving G441 and G445. S449, although not highly conserved, corresponds to hydrophilic, residues (Ser, Thr, Asp, Gly) in 25 of the 43 sequences being otherwise Ala, Gly or Tyr in Fig. 6-2 and could therefore line the permeant translocation channel and participate in hydrogen bond interactions.

NBMPR

The nature of NBMPR interactions with the mammalian *es* transporter has been a topic of intensive investigation, especially because of the debate as to whether NBMPR binds to the same, or overlapping, sites with nucleoside permeants (9-11). The molecular cloning and characterization of ENT1 and ENT2 from humans and rats led to the identification of TMs 3-6 of rENT1 as a region important for NBMPR interactions, and subsequently G154 in TM 4 and L92 in TM 2 of hENT1 as important determinants of NBMPR sensitivity (2,5,12). TMs 3-6 were also implicated in the unique abilities of hENT2 and rENT2 to transport 2', 3'-deoxy nucleosides and nucleobases, implying that this region is involved in permeant recognition (13,14). Furthermore, mutation of L92 affected the apparent affinities for inosine and guanosine and the corresponding residue of G154 in rENT2, C140, was shown to form part of the exofacial uridine-binding site (5,15). All of these studies strongly suggest that NBMPR competes with nucleoside permeants for binding to the exofacial permeant binding site.

In the studies of Chapter 6, additional residues of hENT1 that, when mutated, reduced the affinity for NBMPR were identified. These included W29, F334 and N338

although the effects resulting from mutation of F334 were very small (Table 6-4). Both W29 and N338 are highly conserved in the ENT protein family, suggesting that they may play important roles in permeant recognition and translocation. The experiments of Table 6-1 suggested that W29 was functionally important for adenosine transport, with various mutations of this residue causing either reduced V_{max} values (W29G, A, C), increased K_m values (W29Y), or both (W29V). It was also observed that W29T lacked the ability to transport uridine whereas the kinetic parameters for adenosine transport were not severely compromised (Fig. 7-1, Table 6-1). Multiple sequence alignment analysis revealed that LdNT2 and the TbNTs 1-7, all of which lack the ability to transport uridine and other pyrimidine nucleosides, contain a Thr residue at the position that corresponds to W29 of hENT1 (Fig. 7-2). The experiments of Table 6-4 indicated that residues with small side chain volumes (Ala, Cys and Gly), when substituted for W29, resulted in notably reduced affinities for NBMPR, with W29G being 120-fold less sensitive. It was proposed in Chapter 6 that the aromatic moiety of NBMPR interacts with W29 since aromatic residues were highly preferred at this position; this conclusion is consistent with results of earlier structure-activity relationship studies that identified hydrophobicity of the subsituent at the purine 6 position as a critical determinant for high-affinity binding of derivatives of thioinosine to the transport inhibitory site (16). W29 was an important functional determinant of permeant transport efficiency and selectivity and of NBMPR binding, providing evidence that the NBMPR-binding site overlaps with that of permeants.

Asn 338, although highly conserved in the ENT family, displayed high tolerance for hydrophilic (N338D, S) and large hydrophobic residues (N338M). It is currently unclear why N338 is so highly conserved in the ENT family since this residue appeared to be an inactive component of the permeant binding site. SCAM approaches on a functional Cys-less mutant of hENT1 will be able to address this question. The role of N338 in NBMPR intreractions is also not clear since there was no apparent relationship with amino acid properties in Table 6-4. The effects of mutating this residue on NBMPR sensitivity may be due to nonspecific changes in the conformation of the protein.

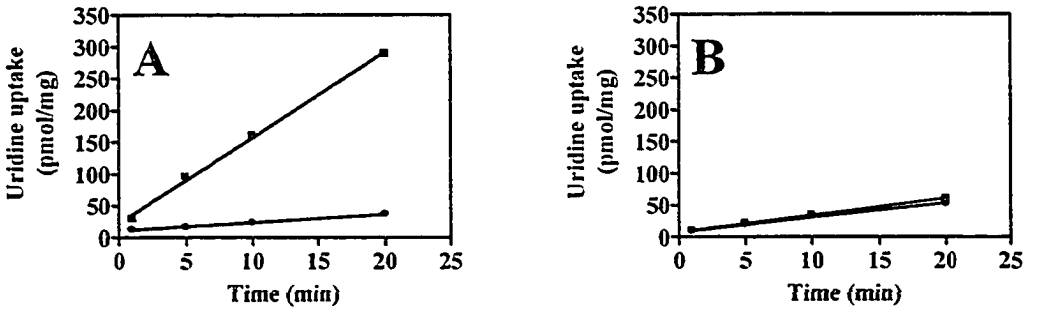

Figure. 7-2. Time course for uridine uptake by yeast producing hENT1 or hENT1-W29T.

Yeast cells producing recombinant hENT1 (A) or hENT1-W29T (B) were incubated in the presence of 1 μM [^{3}H]-uridine for various time points up to 20 min in the absence (■) or presence (●) of 10 μM NBMPR. Each point represents the mean ± S.E. of six separate determinations, and where the point is larger than the S.E., it is not shown. The data was analyzed by linear regression using GraphPad Prism version 4.0 software. Three separate experiments yielded similar results.

Dipyridamole and Dilazep

As for NBMPR, the nature of dipyridamole and dilazep binding to the *es* transporter has been postulated by some authors to be either allosteric or competitive (10,11,17-21). The early observations that rat *es* transporters were ~100-fold less sensitive to dipyridamole and dilazep than those of humans, pigs and rabbits (Table 1-1) were later exploited in a chimera study involving hENT1 and rENT1 that identified TMs 3-6 as a major region involved in inhibitor interactions (22,23). The chimera study suggested that dilazep and dipyridamole competed with nucleoside permeants for binding to hENT1. However, the individual amino acid residues responsible for the effects observed in the chimera study have yet to be identified.

In the experiments of this thesis, an alternative approach involving random mutagenesis and screening for mutants with reduced sensitivities to inhibitors identified six residues of hENT1 that, when mutated, similarly alter sensitivity to dipyridamole and dilazep. In Chapter 3, residue 33 of hENT1 and hENT2 was identified as a determinant responsible for ~10-fold of the dipyridamole and dilazep sensitivity differences between hENT1 and hENT2 (Fig. 3-4, Table 3-2). In Chapter 4, it was demonstrated that residue 33 in hENT2, when mutated to Met, Cys or Ser, increased transporter affinity for nucleosides and capacity for transport of purine nucleosides (Figs. 4-2, 4-3 and Table 4-2). Met and Cys, but not Ser, at residue 33 also increased dipyridamole sensitivity (Fig. 4-4, Table 4-3), suggesting hydrogen-bond formation between Met, Cys or Ser and nucleosides. In contrast, Met and Cys interacted with aromatic moieties on dipyridamole.

hENT2-I33C was sensitive to modification by the membrane-impermeant sulfhydryl reagent pCMBS in a permeant and dipyridamole-protectable manner (Figs.4-5, 4-6). These studies provided direct evidence that dipyridamole and nucleosides interacted with the same residue on the extracellular aspect of hENT2, providing evidence in favor of the competitive model of dipyridamole binding. Mutational analysis of residue 33 of hENT1 in Chapters 5 and 6 suggested that residues with small side chains affected the transport capacity and severely affected the affinity for dipyridamole and dilazep, with hENT1-M33A being insensitive to 30 μM dipyridamole (Fig. 5-3 and

Tables 5-1, 6-2). Chapter 6 also demonstrated that a Leu residue at position 33 was favored over the wildtype Met residue of hENT1, indicating that several other ENT family members, including AtENT2-7 and TgAT1, might interact with dipyridamole. Each Chapter revealed new information about the role of residue 33 in permeant and inhibitor interactions was obtained. There is strong evidence that residue 33 is functionally important in both hENT1 and hENT2 and that it is directly involved in permeant and dipyridamole binding. It could not be shown that residue 33 directly participates in dilazep binding (Fig. 4-6), but the similarities in the trends observed for dilazep and dipyridamole in the mutational analyses of Chapter 6 (compare Tables 6-2 and 6-3) suggested that dilazep interacts in a way that does not occlude this residue.

It should also be noted that in the experiments of Chapters 3, 5 and 6, residue 33 mutations of hENT1 were observed in >95% of clones isolated from screens of independent hydroxylamine or XL1-RED-generated mutant libraries for either dilazep or dipyridamole resistance. These results suggested that residue 33 is the single greatest determinant of the sensitivity differences between hENT1 and either hENT2 or rENT1 and that several other residues with smaller contributions may be responsible for the remainder of these differences. This statement is further confirmed by the observation that rENT1-I33M displayed an IC_{50} value for dilazep that was comparable to that of hENT1 (Table 6-3).

Random mutagenesis and screening of CeENT1 for mutants with reduced sensitivity to dipyridamole led to the identification of I429, which corresponded to L442 of hENT1 (Fig. 5-2). The results of Chapter 5 suggested a functional and conformational interaction between TM 1 and 11 residues and that, despite being far apart in the primary sequence, these residues are close together in the folded protein. Furthermore, this study indicated that both residues were involved in dipyridamole interactions with hENT1, CeENT1 and hENT2. The subsequent experiments of Chapter 6 indicated that both residues contributed similarly to rENT1 dipyridamole and dilazep sensitivity (Tables 6-2, 6-3). Interestingly, although hENT1-L442I displayed wildtype kinetic parameters for uridine transport, this mutant displayed severely impaired adenosine transport (Tables 5-2, 6-1). Both uridine and adenosine transport were severely affected by the L442T mutation and other mutations generated at this position (L442G, A, M) rendered hENT1

non-functional (Tables 5-2, 6-1). It is currently unclear whether the intolerance of L442 to mutation is due its location as the second residue in a highly conserved GXXXG helix-helix interaction motif or to effects on the permeant translocation channel. L442 of hENT1 is a critical residue for permeant, dipyridamole and dilazep interactions, and if this residue participates in interactions with all three molecules, then it would support the competitive inhibition model for binding of the two inhibitors.

The other four residues that were identified as important for dilazep and dipyridamole interactions were W29, F80, F334 and N338 (Fig. 6-1). Dipyridamole and dilazep were the only two inhibitors whose interactions were affected by mutation of all six residues and the observed trends in Tables 6-2 and 6-3 were remarkably similar, once again suggesting that dipyridamole and dilazep bind to the same site.

It was shown in Chapter 6 that the F334Y mutation was capable of increasing the apparent V_{max} for adenosine, a result that was also observed for uridine transport. F334S also displayed a higher apparent V_{max} than F334C, suggesting that H-bond interactions were responsible for the increased V_{max} values (Table 6-1, Fig. 6-2). It should be noted that, Cys and Met residues at position 33 were implicated in H-bond interactions (Chapter 4), whereas this was not the case for F334C (Chapter 6). Sulfur has a modest electronegativity value (2.58) compared to that of oxygen (3.44). H-bond interactions involving sulfur-containing side chains, although rare, have been observed in the crystal structures of proteins whereas interactions with aromatic moieties are much more common (24). The ability of the sulfur atom of Cys and Met to form H-bonds is likely to be dependent on the conformation and microenvironment of the side chain.

The functional importance of the identified residues and the predicted extracellular location of five of the six residues (Fig. 6-1) suggested that dipyridamole and dilazep compete with permeants for binding to overlapping binding sites on the extracellular side of the protein. This conclusion is inconsistent an earlier study of [^{3}H]-dilazep binding that suggested that at neutral pH dilazep bound allosterically with permeants for binding to the transporter (17). The reason for this discrepancy is currently unclear and it is surprising that these two inhibitors, which share no structural relationships, appear to bind to identical sites. It is also not clear why no residues within TMs 3-6 were identified in the various screens, as would have been predicted by the

chimera study (23). It is possible that several residues in this region, which are individually minor contributors to dipyridamole and dilazep interactions, additively produced the effects observed in the chimera study. Therefore, mutating combinations of residues that differ between hENT1 and rENT1 within this region may identify the remainder of the determinants of the inhibitor sensitivity differences between these two proteins. Alternatively, transplanting large regions between hENT1 and rENT1 may have nonspecifically altered the tertiary structure of the protein to produce the observed effect. The observation that the hENT1 chimera that contained TMs 3-6 of rENT1, which was insensitive to dipyridamole and dilazep, also displayed ~30-fold reduced functional activity compared to wildtype hENT1 is evidence for the latter scenario (23).

Draflazine and soluflazine

Although several pharmacological studies involving draflazine, soluflazine and their analogs have been performed, no molecular studies of their interactions with nucleoside transporter proteins have been published. Draflazine interactions with the *es* transporter have been reported as complex, and studies of its effects on NBMPR binding yielded a pattern of mixed inhibition (25,26). However, other inhibitors in this chemical family, appear to be purely competitive inhibitors of NBMPR binding (25). The studies of Chapter 6 provide insights into the mechanism of binding of these inhibitors.

It was proposed that draflazine and soluflazine form hydrogen bonds with N338 and interact with W29 via aromatic stacking interactions with the fluorophenyl groups in a similar fashion as NBMPR. Notable differences between these two inhibitors were the observations that soluflazine sensitivity was affected by M33 mutations and, like dipyridamole, a Leu at this position was the most favorable for binding (Table 6-6). These results suggested that the soluflazine binding site shares common characteristics with the binding sites of dipyridamole and draflazine.

A mechanism for draflazine binding was proposed in Chapter 6 in which draflazine could access its binding site from either side of the membrane with differing affinities, given the location of N338 on the intracellular end of TM 8. This mechanism is consistent with the observation that draflazine is a mixed-type inhibitor of nucleoside transport and NBMPR binding to mammalian *es* transporter (25,26).

Studies that suggested that solulfazine is a selective inhibitor of *ei* transporters of rat and mouse origin were not supported by the results obtained in Table 6-6 for hENT1 and hENT2 (25,27). When rENT2 was produced in yeast, it displayed uridine transport activity that was resistant to 10 μM soluflazine, suggesting that the yeast membrane environment slightly altered the soluflazine binding pockets of *ei* transporters.

The studies of Chapter 6 provided insights into the molecular determinants of draflazine and soluflazine sensitivities. Because draflazine appears to bind via a unique mechanism, it should be informative to exploit the 230-fold difference in sensitivity between hENT1 and rENT1 via chimera approaches. Instead of swapping large regions

between hENT1 and rENT1 as was done previously, swapping of individual TMs might better define the involved TMs, leading to identification of individual residues responsible for the sensitivity differences. One would hypothesize that different regions would be identified for draflazine interactions than were for dipyridamole (23).

Conclusions and future directions

The results of the studies in this thesis led to the construction of a preliminary model of inhibitor binding by TMs 1, 2, 8 and 11, in which W29, M33, F334, N338 and L442, but not F80, of hENT1 appear form to part of the permeant translocation pathway and/or inhibitor binding site (Fig. 7-1). Five of the six residues, with N338 being the exception, are in a relatively extracellular location in their respective TMs (28). These observations support the notion that NBMPR, dipyridamole and dilazep bind to the outward-facing permeant binding site of hENT1 whereas draflazine binds to the transporter on either side of the protein.

Although the experiments outlined in this thesis identified and characterized six important residues involved in inhibitor interactions with hENT1, the molecular determinants of the species differences in sensitivity to these agents have been only partially addressed. Furthermore, residue 33 of hENT2 was the only residue for which direct evidence of interactions with dipyridamole was provided for this transporter. Both of these issues could be addressed by systematic SCAM studies using a Cys-less mutant of hENT1.

Fui1::TRP1 yeast cells producing hENT1 were unable to grow in the presence of 100 μM 5-fluorouridine unless an inhibitor of hENT1-mediated transport is added whereas yeast producing rENT1 were not protected by dilazep, dipyridamole or draflazine. Screening of a randomly mutated rENT1 library for functional clones that are protected by dilazep, dipyridamole or draflazine may reveal additional residues involved in inhibitor interactions with rENT1.

As outlined in Chapter 1, the interpretation of data obtained from cells and tissues from different origins is difficult due to variations in the membrane environment and post

translational modifications, and the presence of multiple transport systems. Chapter 6 contains a parallel analysis of the inhibitor sensitivities of hENT1, hENT2 and rENT1. With the sequences of many ENTs from non-mammalian organisms available, a comprehensive species inhibitor sensitivity study could be performed using high throughput methods, such as that developed for the yeast expression system used in Chapters 4-6 (29,30).

Another important avenue for future research would involve a systematic study of inhibitor analogs for structure-activity relationship studies to determine the structural determinants for high-affinity binding of inhibitor molecules. Novel inhibitors could also be identified using high-throughput screens of compound libraries for those with specificity for each of mammalian ENT and CNT isoforms, providing useful tools as specific probes each transporter. Collectively, these approaches would serve to clearly define the structural mechanisms and molecular determinants of high-affinity inhibitor interactions.

References

1. Valdes, R., Vasudevan, G., Conklin, D., and Landfear, S. M. (2004) *Biochemistry* **43**, 6793-6802
2. SenGupta, D. J., and Unadkat, J. D. (2004) *Biochem Pharmacol* **67**, 453-458
3. SenGupta, D. J., Lum, P. Y., Lai, Y., Shubochkina, E., Bakken, A. H., Schneider, G., and Unadkat, J. D. (2002) *Biochemistry* **41**, 1512-1519
4. Vasudevan, G., Ullman, B., and Landfear, S. M. (2001) *Proc Natl Acad Sci U S A* **98**, 6092-6097
5. Endres, C. J., SenGupta, D. J., and Unadkat, J. D. (2004) *Biochem J* **Pt**
6. Arastu-Kapur, S., Ford, E., Ullman, B., and Carter, N. S. (2003) *J Biol Chem* **278**, 33327-33333
7. Lemmon, M. A., Flanagan, J. M., Hunt, J. F., Adair, B. D., Bormann, B. J., Dempsey, C. E., and Engelman, D. M. (1992) *J Biol Chem* **267**, 7683-7689
8. Russ, W. P., and Engelman, D. M. (2000) *J Mol Biol* **296**, 911-919
9. Griffith, D. A., and Jarvis, S. M. (1996) *Biochim Biophys Acta* **1286**, 153-181
10. Koren, R., Cass, C. E., and Paterson, A. R. (1983) *Biochem J* **216**, 299-308.
11. Jarvis, S. M., Janmohamed, S. N., and Young, J. D. (1983) *Biochem J* **216**, 661-667
12. Sundaram, M., Yao, S. Y. M., Ng, A. M. L., Cass, C. E., Baldwin, S. A., Young, J.D. (2001) *Biochemistry* **40**, 8146-8151
13. Yao, S. Y., Ng, A. M., Vickers, M. F., Sundaram, M., Cass, C. E., Baldwin, S. A., and Young, J. D. (2002) *J Biol Chem* **277**, 24938-24948
14. Yao, S. Y., Ng, A. M., Sundaram, M., Cass, C. E., Baldwin, S. A., and Young, J. D. (2001) *Mol Membr Biol* **18**, 161-167.
15. Yao, S. M., Sundaram, M., Chomey, E. G., Cass, C. E., Baldwin, S. A., Young, J. D. (2001) *Biochem J* **353**, 387-393
16. Paul, B., Chen, M. F., and Paterson, A. R. (1975) *J Med Chem* **18**, 968-973
17. Gati, W. P., Paterson, A. R. P. (1989) *Mol Pharm* **36**, 134-141
18. Jarvis, S. M., and Young, J. D. (1986) *J Membr Biol* **93**, 1-10
19. Hammond, J. R. (1991) *Mol Pharmacol* **39**, 771-779

20. Shi, M., Young, J. D. (1986) *Biochem J* **240**, 879-883
21. Jones, K. W., and Hammond, J. R. (1992) *J Neurochem* **59**, 1363-1371
22. Plagemann, P. G. W., Woffendin, C. (1988) *Biochim Biophys Acta* **969**, 1-8
23. Sundaram, M., Yao, S. Y. M., Ng, A. M. L., Griffiths, M., Cass, C. E., Baldwin, S. A., and Young, J. D. (1998) *J Biol Chem* **273**, 21519-21525
24. Pal, D., and Chakrabarti, P. (2001) *J Biomol Struct Dyn* **19**, 115-128
25. Hammond, J. R. (2000) *Nauyn Schmiedebergs Arch Pharmacol* **361**, 373-382
26. Ijzerman, A. P., Thedinga, K. H., Custers, A. F., Hoos, B., and Van Belle, H. (1989) *Eur J Pharmacol* **172**, 273-281
27. Griffith, D. A., Conant, A. R., and Jarvis, S. M. (1990) *Biochem Pharmacol* **40**, 2297-2303
28. Sundaram, M., Yao, S. Y., Ingram, J. C., Berry, Z. A., Abidi, F., Cass, C. E., Baldwin, S. A., and Young, J. D. (2001) *J Biol Chem* **2**, 2
29. Zhang, J., Visser, F., Vickers, M. F., Lang, T., Robins, M. J., Nielsen, L. P. C., Nowak, I., Baldwin, S. A., Young, J. D., and Cass, C. E. (2003) *Mol Pharm* **64**, 1512-1520
30. Vickers, M. F., Zhang, J., Visser, F., Tackaberry, T., Robins, M. J., Nielsen, L. P., Nowak, I., Baldwin, S. A., Young, J. D., and Cass, C. E. (2004) *Nucleosides Nucleotides Nucleic Acids* **23**, 361-373